Mechanisms and Novel Therapeutic Approaches for KRAS-Mediated Resistance to Anti-EGFR Therapy in Colorectal Cancer Cells

by

Kyle James Knickelbein

B.S. in Bioengineering, Pennsylvania State University, 2011

Submitted to the Graduate Faculty of

the School of Medicine in partial fulfillment

of the requirements for the degree of

Doctor of Philosophy

University of Pittsburgh

2016

UNIVERSITY OF PITTSBURGH

SCHOOL OF MEDICINE

This dissertation was presented

by

Kyle James Knickelbein

It was defended on

August 18, 2016

and approved by

Robert W. Sobol, Ph.D., Department of Pharmacology and Chemical Biology

Patricia L. Opresko, Ph.D., Department of Environmental and Occupational Health

Guillermo G. Romero, Ph.D., Department of Pharmacology and Chemical Biology

Ferruccio E. Galbiati, Ph.D., Department of Pharmacology and Chemical Biology

Dissertation Advisor: Lin Zhang, Ph.D., Department of Pharmacology and Chemical Biology

Mechanisms and Novel Therapeutic Approaches for KRAS-Mediated Resistance to Anti-EGFR Therapy in Colorectal Cancer Cells

Kyle James Knickelbein, Ph.D.

University of Pittsburgh, 2016

Colorectal cancer (CRC) is the third-leading cause of cancer-related deaths in the United States. The treatment of metastatic disease remains a significant clinical challenge, with nearly 90% of patients dying within five years after diagnosis. The successful treatment of CRC is heavily dependent upon the genetic makeup of the tumors. Mutations in the *KRAS* oncogene, which occur in 35-40% of CRCs, generally exhibit lack of response to anti-epidermal growth factor receptor (EGFR) antibody targeted therapy, a front-line treatment option that improves the efficacy of standard chemotherapy regimens. Unfortunately, despite intensive efforts, direct therapeutic targeting of mutant KRAS has been largely unsuccessful. As a result, it is necessary to further elucidate the underlying mechanisms of sensitivity and resistance to anti-EGFR therapy in CRC cells in order to uncover novel therapeutic strategies. In this study, we found that clinically-utilized anti-EGFR antibodies kill CRC cells by upregulating the pro-apoptotic B cell CLL/lymphoma-2 (Bcl-2) family protein p53-upregulated modulator of apoptosis (PUMA) through the p53 homologue p73. In CRC cells with acquired resistance to anti-EGFR antibodies due to *KRAS* mutations or genetic amplification, PUMA expression was strongly suppressed when compared to parental cells after antibody treatment. To overcome resistance to anti-EGFR therapy, we first conducted a compound screen which revealed that Aurora kinase inhibition can preferentially kill isogenic CRC cells with *KRAS* mutations. Aurora kinase inhibition was found to enhance the induction of apoptosis in combination with anti-EGFR antibody treatment in

resistant CRC cells with *KRAS* amplification in cell culture. We also found that the combination treatment completely suppressed tumor growth and promoted apoptosis in resistant cell tumors in nude mice. Collectively, our data indicate that PUMA and other Bcl-2 family proteins play a critical role in mediating the sensitivity and resistance to anti-EGFR antibodies. Furthermore, our results indicate that targeting apoptotic pathways can be utilized to overcome KRAS-mediated resistance to targeted therapies.

TABLE OF CONTENTS

LIST OF TABLES

LIST OF FIGURES

PREFACE

"Your work is going to fill a large part of your life, and the only way to be truly satisfied is to do what you believe is great work. And the only way to do great work is to love what you do. If you haven't found it yet, keep looking. Don't settle. As with all matters of the heart, you'll know when you find it." —Steve Jobs, Apple Inc. Co-Founder

The above quote summarizes my path into the medical sciences well. I know that after some exploration I have found an area that I truly enjoy. I am very grateful that I can be a part of this amazing field.

During my time as a graduate student, there were many people who supported me along the way and whom I'd greatly like to thank. I want to thank the Department of Pharmacology and Chemical Biology, and also my thesis committee, for maintaining a supportive environment here at the University of Pittsburgh. Their support has meant a lot to me, and they have guided my way through all of the major milestones of the program. I also want to thank my mentor, Dr. Zhang, and his wife, Dr. Yu, for providing a collaborative and welcoming environment in the lab. His mentorship has taught me how to be a better scientist and how to more effectively manage problems. This experience has taught me so much, especially by experiencing the successes and learning to deal with failures along the way.

I also want to greatly thank my family and friends for encouraging me, especially when times were difficult. My mother, Barbara, and my step-father, Richard, deserve a lot for listening to me and providing guidance when I needed it the most. I have sincerely appreciated their support along this entire journey. My close friends from college, Matt, Gina, and Jim, as well as great friends that I have met here as a student, Andrea and Rochelle, have also been pivotal for always being there for me and providing an outlet from the lab. This work is also dedicated to my grandmother, Mimi, whom our family lost after a short battle with cancer when I was young. I wish that she were here with us now, but I know that she would have been proud with the path that I have taken.

The work we have performed here in Chapters II and III is currently being organized into a manuscript. Several members of the lab have been very helpful during the completion of these experiments. I first want to give credit to Dr. Jingshan Tong, the second author of my manuscript, for assisting with the completion of the xenograft experiments. Dr. Dongshi Chen, the third author, assisted with the virus-mediated overexpression experiment. Dr. Yi-Jun Wang provided critical reading and helpful comments during the final drafting process. Finally, Dr. Alberto Bardelli and his laboratory generously supplied us with the parental and resistant colorectal cancer cell lines and also gave helpful experimental insight when we first started to use these models for this project. Dr. Sandra Misale from Dr. Bardelli's lab was particularly helpful with answering any questions we had along the way.

The material in Chapter I has been published as a review in the journal Genes and Diseases with myself as the first author (reference number 24 in the Bibliography). Dr. Zhang, the corresponding author, provided me with key revisions and helpful comments during our drafting. This review paper in its entirety, along with any other figures not original to this

dissertation, has been reproduced here with permission. The appropriate citations are found below the corresponding tables and figures. All artwork contained within the schematic figures is original artwork done by myself.

1.0 INTRODUCTION

Cancer is defined as an abnormal or uncontrolled growth of cells within the body. While growth and division is a regular part of normal cellular physiology, unrestricted growth can lead to the formation of solid masses (tumors) within the body. Additionally, this uncontrolled cellular proliferation can lead to the presence of lesions at secondary sites (metastasis). Left unchecked, the continued proliferation of a malignant cancer can result in patient mortality [1].

In total, there exist more than 100 different types of cancer, which are classified according to the organ site from which the cancer cells arise [2]. In the year 2016 alone, statistics reported by the National Cancer Institute estimate that nearly 1.7 million people in the United States will be diagnosed with cancer, and about 700,000 are estimated to succumb to the disease [2]. Although the trends indicate that overall cancer mortality is declining in the United States, cancer is still a significant healthcare concern. Projected for the year 2016, some of the most prevalent cancers include: lung, breast, skin, renal, and colorectal cancer (CRC) [2].

1.1 COLORECTAL CANCER

1.1.1 Colorectal Cancer Background and Genetics

Although numerous advances have been made in both detection and treatment of CRC, it remains as one of the most fatal cancers in the United States [3]. According to the American Cancer Society (ACS), nearly 137,000 people were predicted to be diagnosed and 50,000 were predicted to succumb to CRC in the year 2014 [4]. Metastatic disease typically presents with the poorest prognosis with a five-year survival estimate around 11% [5].

The initiation of tumor formation in epithelial cells lining the colon is known to correspond with a number of genetic changes. A model of CRC progression from a normal epithelium to a metastatic lesion was proposed by Bert Vogelstein and Eric Fearon, which illustrates an accumulation of events driving cancer progression (Fig. 1).

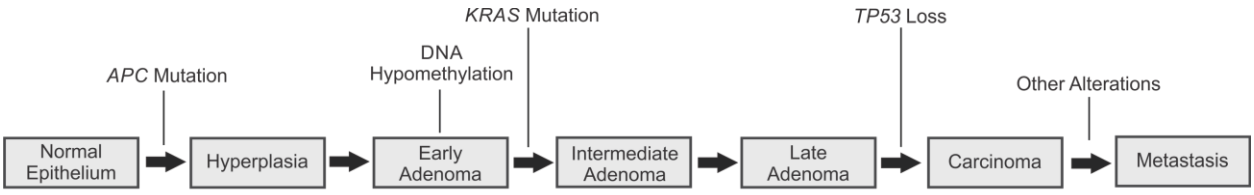

Figure 1. Genetic Model of Colorectal Cancer Progression. This model of colorectal cancer progression is adapted with permission from Fearon et al. Cell 1990 [6].

Various forms of genetic and epigenetic instability are known to occur in CRC. It is estimated that around 80% of CRC cases possess chromosomal instability (CIN), which encompasses genetic mutations and amplification [7]. For example, the loss of the *APC* tumor suppressor gene is a frequent early event in CRC pathogenesis that occurs in approximately 80%

of cases of sporadic CRC, which leads to deregulated β-catenin signaling [8, 9]. Additionally, deletions of or mutations in the *TP53* tumor suppressor gene are also highly prevalent in CRC. Estimates establish the mutation rate of *TP53* at around 50% [10, 11]. While the aforementioned genes play a heavy role in CRC progression, a number of oncogenes also play a crucial role not only in the progression of the disease, but also in the response to therapy.

Mutations in the *KRAS* oncogene have been reported in more than one-third of CRC cases [12, 13]. *KRAS* mutations, although not a significant prognostic factor, have been shown to play a critical role in CRC treatment. Recently, activation of this oncogene has been linked to resistance to the agents utilized in front-line therapy for CRC [14, 15]. Intensive efforts have been devoted to understanding how *KRAS* mutations affect CRC therapy, in particular targeted therapy, and how to overcome mutant-KRAS-mediated therapeutic resistance. The National Cancer Institute (NCI) has also recently established the RAS Program to explore innovative ways to attack the proteins encoded by mutant *RAS* genes or other vulnerabilities as a way to treat key types of cancer such as CRC, highlighting the critical importance of this oncogene in cancer treatment.

1.1.1.1 KRAS Biology. RAS proteins represent prototypical members of a large family of small GTP-binding proteins [16]. The human RAS superfamily consists of more than 100 members divided into six subfamilies [17]. Three prototypical RAS proteins include HRAS, NRAS, and KRAS [18]. While they are highly homologous in amino acid sequence and are ubiquitously expressed, KRAS is the only one that is essential for normal development as shown by mouse genetic studies [19-21]. KRAS can be expressed as two different splice variants, referred to as 4A and 4B, through alternative splicing within exon 4 [18]. The 4B variant is the dominant form commonly known as KRAS [13].

KRAS is a membrane-bound GTPase that cycles between an active GTP-bound form and an inactive GDP-bound form as a result of GTP hydrolysis (Fig. 2) [17, 22]. The switches between these two states are controlled by two classes of proteins: guanosine nucleotide exchange factors (GEFs) and GTPase-activating proteins (GAPs). As their names suggest, GEFs assist with the exchange of bound GDP with GTP, whereas GAPs stimulate the hydrolytic ability of RAS to convert bound GTP to GDP [16].

The proper membrane localization and function of the RAS proteins are regulated by several post-translational modifications in the C-terminal "CAAX" motif. Three key modifications include: farnesylation of the cysteine residue, proteolytic removal of the terminal three residues (AAX), and methylation of the cysteine residue [18, 22]. In addition, the plasma membrane localization of KRAS also requires a basic poly-lysine region located immediately upstream of the C-terminus [22, 23].

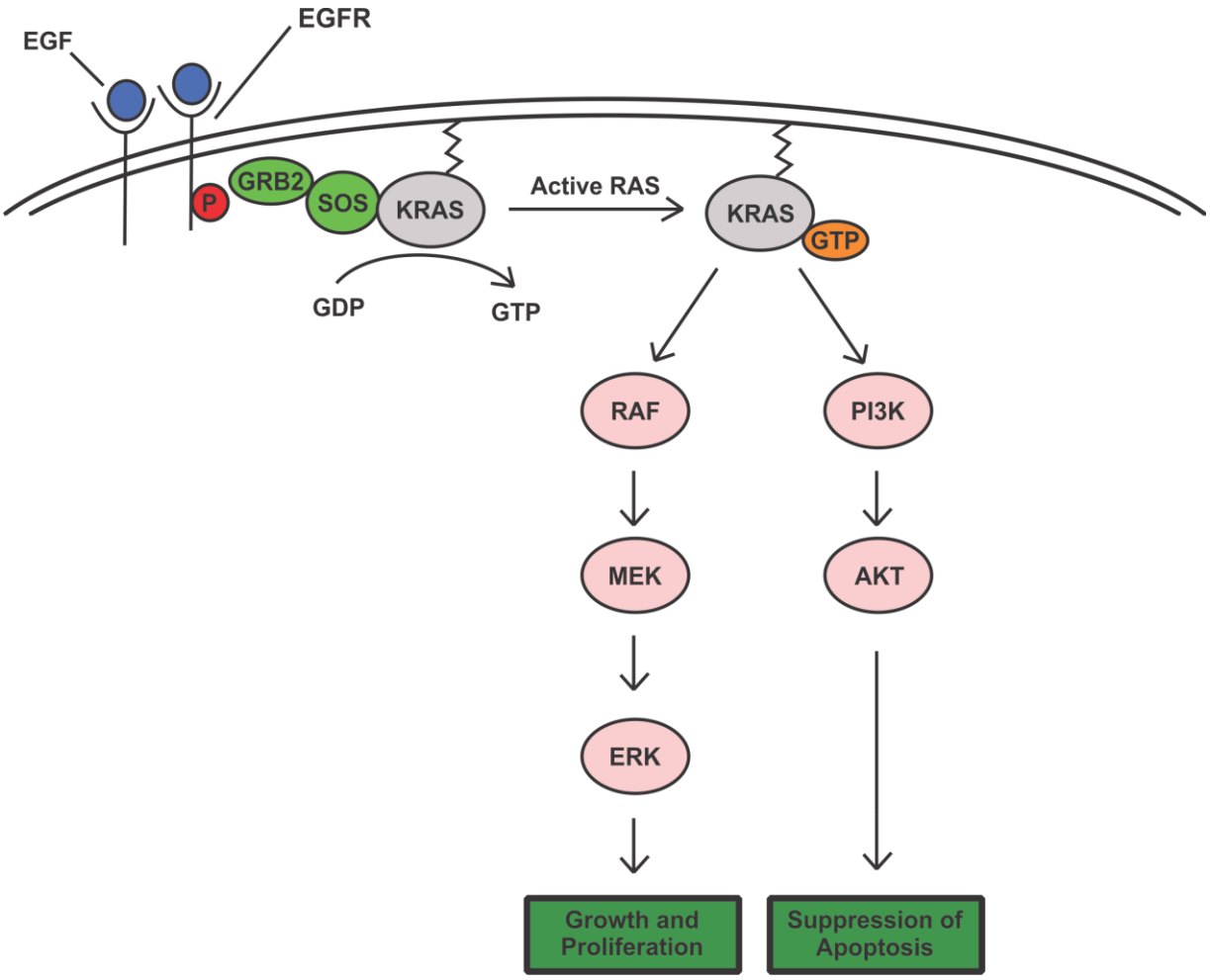

Figure 2. EGFR-Induced and KRAS-Mediated Signaling Pathways. Receptor tyrosine kinase signaling is a well-studied model of RAS activation. Here, activation of EGFR upon ligand binding and its subsequent auto-phosphorylation create a docking site for the SOS/GRB2 complex, resulting in nucleotide exchange by SOS and the GTP-bound form of KRAS. KRAS then signals through the RAF/MEK/ERK and PI3K/AKT cascades to promote cell growth and suppress apoptosis. This figure is adapted from Knickelbein et al. Genes and Diseases 2015 [24].

Once properly activated, KRAS mediates a myriad of intracellular signaling events through its numerous effector pathways. Signaling by receptor tyrosine kinases (RTKs), in particular the epidermal growth factor receptor (EGFR), is a widely-utilized and well-understood model for studying KRAS activation (Fig. 2) [19, 25]. In brief, the activation of EGFR upon ligand binding and its subsequent auto-phosphorylation create a docking site for the adaptor protein growth factor receptor-bound protein 2 (GRB2), which binds to the GEF Son of Sevenless (SOS) in the cytosol. The recruitment of this protein complex to the phosphorylated receptor enables SOS to function as the exchange factor for KRAS, which swaps the bound GDP for GTP and places KRAS in the active state (Fig. 2) [19, 25, 26].

Among numerous downstream effectors of KRAS, the best characterized include the kinases RAF and phosphoinositide-3 kinase (PI3K), as well as the GEFs for the RAS-like (Ral) small GTPases (RalGEFs) [27, 28]. The major signaling axes of RAS proceed through the RAF/MEK/ERK and PI3K/AKT kinase cascades and ultimately control processes such as cell growth and survival (Fig. 2) [19]. This is accomplished in part by ERK-regulated activation of transcription factors that promote cell cycle progression and by AKT-mediated inactivation of pro-apoptotic proteins that result in the suppression of apoptosis [19, 29]. In addition, a number of alternate effectors of KRAS have been described in an extensive body of literature, which regulate processes such as cell migration, endocytosis, alterations in the cytoskeleton, and calcium signaling [22, 27, 29, 30].

1.1.1.2 Role of KRAS in Colorectal Cancer. Nearly 30% of human cancers possess activating *RAS* mutations [31], 85% of which are *KRAS* mutations [32]. In CRCs, *KRAS* mutations are found in approximately 35-40% of cases, and those of *HRAS* and *NRAS* are observed in <5% [5, 33]. The overwhelming majority of *KRAS* mutations are found within codons 12 and 13, and the

remainder in codons 61, 146, and other residues [33, 34]. While the hotspot codon 12 and 13 mutations of *KRAS* do not interfere with its ability to associate with GAPs, they alter the position of a catalytic glutamate residue at codon 61 [16, 18]. While these mutations do not result in a complete ablation of KRAS GTPase ability, it does however decrease the rate of GTP hydrolysis by 3-9 fold compared to wild-type (WT) KRAS [18]. Using isogenic knock-out and knock-in CRC cell lines with either WT *KRAS* or activating mutations, recent studies have illustrated that these mutations play a significant role in tumor cell survival and tumor progression [35-38]. The functional consequences of *KRAS* mutations include increased cellular proliferation, suppression of apoptosis, altered cell metabolism, as well as changes in the tumor microenvironment [16]. For example, GTP-bound KRAS enables the upregulation of growth factors and transcription factors known to promote cell cycle progression, such as c-Jun and c-Fos [16]. Recent studies identified the Yes-associated protein 1 (YAP1) transcriptional co-activator as a key mediator of the oncogenic effect of KRAS [39, 40]. From a therapeutic standpoint, suppression of apoptosis is probably one of the most important consequences of *KRAS* mutations [31]. Activated KRAS can inhibit the apoptotic signaling cascade through its key effector PI3K, which in turn activates AKT, a potent pro-survival kinase [29, 31]. The action of the AKT kinase inhibits apoptosis through several mechanisms, including the phosphorylation and subsequent inactivation of the pro-apoptotic B cell CLL/lymphoma-2 (Bcl-2) family protein Bad, and the inhibitory phosphorylation of the initiator caspase-9 [29].

1.1.2 Current Treatment Strategies and Targeted Therapies

1.1.2.1 Conventional Chemotherapy. CRC patients are often treated with conventional cytotoxic chemotherapy and recently-developed targeted therapy. Cytotoxic chemotherapy

typically entails the use of pyrimidine analogs such as 5-fluorouracil (5-FU) [41], which inhibits thymidylate synthase required for nucleotide synthesis [42]. Other cytotoxic drugs commonly used for CRC treatment include the topoisomerase I inhibitor irinotecan, the platinum drug oxaliplatin, and the oral pro-drug capecitabine (metabolized into fluorouracil) [42, 43]. Front-line treatment involves combinations of these agents, such as FOLFOX (fluorouracil, leucovorin (folinic acid, which further increases thymidylate synthase inhibition), and oxaliplatin) and FOLFIRI (fluorouracil, leucovorin, and irinotecan) [15, 42, 44], which have been shown to improve response rates and overall survival of CRC patients over fluorouracil and leucovorin-based treatments alone [43].

1.1.2.2 Targeted Therapy. Targeted therapies are treatments that aim to inhibit the processes that cancer cells rely on for survival and proliferation, and these agents have recently moved to the forefront for CRC treatment [45]. Several targeted therapies have been approved by the US Food and Drug Administration (FDA) for CRC treatment, including the anti-vascular endothelial growth factor (VEGF) antibody bevacizumab, which suppresses tumor angiogenesis, the anti-EGFR antibodies cetuximab and panitumumab, and more recently, the multi-kinase inhibitor Regorafenib, which targets RTKs involved in angiogenesis and mitogenic signaling [46, 47]. The utilization of targeted therapies has been highly prevalent for CRC treatment. For example, it was estimated that roughly 44% of all CRC patients treated in the US received anti-EGFR antibody therapy in 2008 [48]. When compared with best supportive care, both cetuximab and panitumumab as single agents have been shown to increase both progression-free survival and overall response in randomized Phase III clinical trials [15].

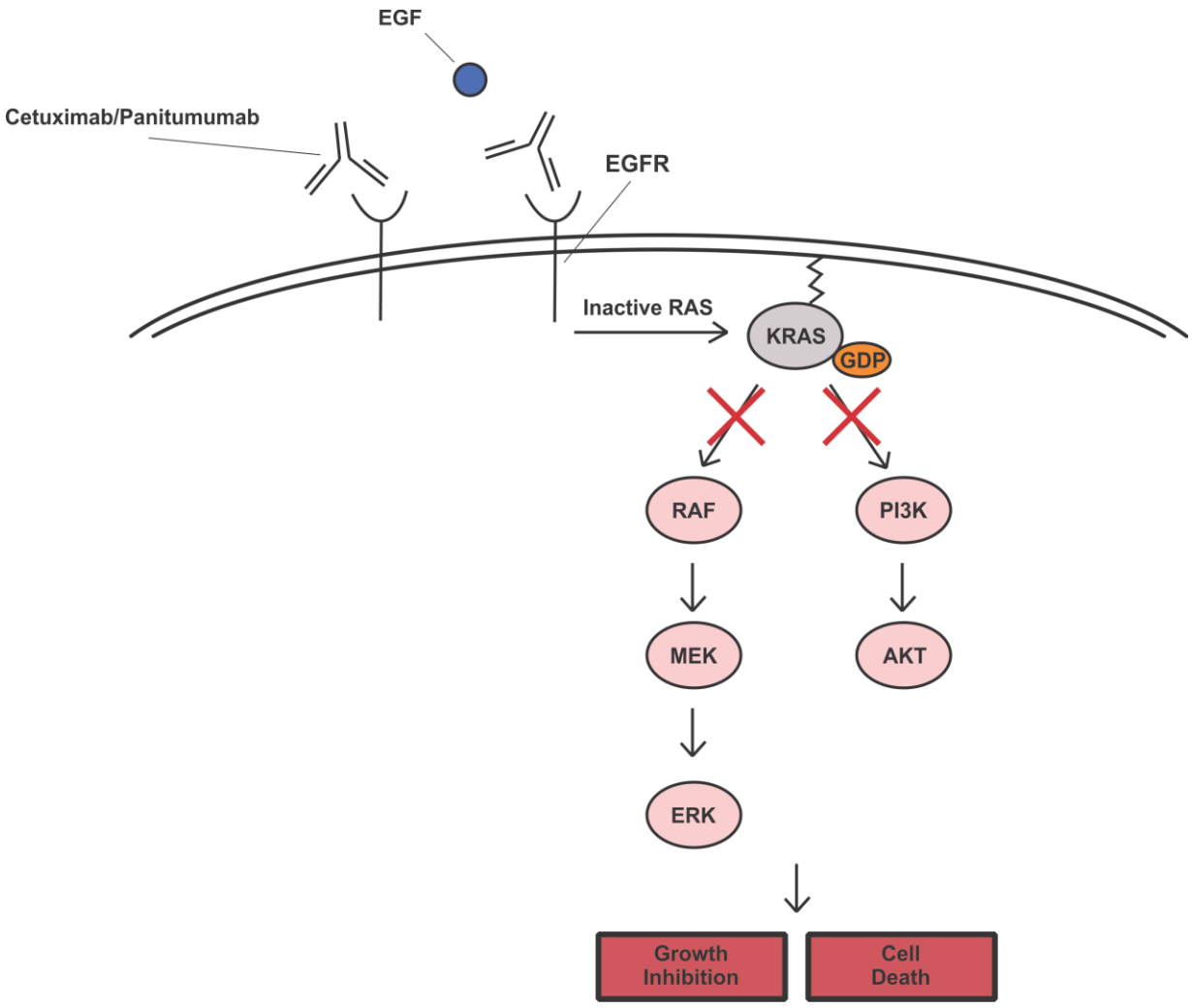

Figure 3. EGFR Blockade Silences Downstream KRAS Effector Signaling. Anti-EGFR antibodies, including cetuximab and panitumumab, bind to EGFR and prevent ligand binding and subsequent KRAS activation, leading to growth suppression and cell death due to the inhibition of the RAF/MEK/ERK and PI3K/AKT pathways. Mutant KRAS can override the effect of anti-EGFR antibodies leading to cell growth and survival. This figure is adapted from Knickelbein et al. Genes and Diseases 2015 [24].

EGFR is a member of the ERBB family of RTKs that is frequently overexpressed in CRC [49]. Much akin to KRAS signaling, EGFR transduces signals from extracellular stimuli through key intracellular pathways, such as the RAS/RAF/MEK/ERK and PI3K/AKT cascades [50]. The anti-EGFR antibodies used for CRC treatment, including cetuximab and panitumumab, both can inhibit ligand binding and EGFR homo-dimerization or hetero-dimerization with other ERBB family members (Fig. 3), which are necessary for its subsequent auto-phosphorylation and full activation [47, 51]. Cetuximab is a chimeric human-murine antibody of the IgG1 isotype, whereas panitumumab is a humanized antibody of the IgG2 isotype [52, 53]. In addition to their effect on ligand binding, cetuximab and panitumumab can promote EGFR internalization and subsequent degradation, which in turn decreases the cell surface level expression of EGFR [53]. Interestingly, cetuximab can also block EGFR nuclear translocation whereby it can act as a transcription factor [47]. Both cetuximab and panitumumab have become part of first-, second-, and third-line therapy for CRC [15, 53, 54]. Data from clinical trials have shown the therapeutic benefit of anti-EGFR antibody therapy either as a stand-alone agent or in combination with chemotherapy regimens [55-57]. However, primary and secondary resistance to this therapy has become a significant issue in the clinic.

1.1.2.3 Alterations of *KRAS* Status and the Response to Targeted Therapy. The emergence of drug resistance is a major challenge in anti-cancer therapy, and the utilization of newer targeted therapies encounters the same dilemma. This has been exemplified by the finding that alterations in the *KRAS* gene render anti-EGFR antibodies ineffective for CRC treatment. An initial study published in 2006 showed the lack of response to cetuximab in patients with *KRAS*-mutant metastatic CRCs [58]. An additional study confirmed the causal role of *KRAS* mutations in promoting resistance to anti-EGFR antibody therapy [59]. A host of subsequent studies,

including further clinical trials and retrospective analyses of tumor samples, verified the notion that *KRAS* mutations underlie the lack of response to anti-EGFR therapy [60-63]. These findings led to the issuance of a provisional clinical opinion by the American Society of Clinical Oncology (ASCO) in 2009, stating that metastatic CRC patients eligible to receive an anti-EGFR antibody therapy should have their *KRAS* mutational status profiled, and those with a codon 12 or 13 mutation in *KRAS* should be excluded from this treatment [64]. Collectively, these studies have established *KRAS* status as a key factor in deciding treatment options for patients diagnosed with metastatic CRC, as well as defining *KRAS* status as a major biomarker of resistance to anti-EGFR antibody therapy [65].

A critical question that remains is how resistance to anti-EGFR therapy emerges. Several recent studies have characterized the mechanism of secondary resistance to anti-EGFR therapy by assessing the temporal alterations of *KRAS* mutational status. Cell culture studies using CRC cells that are exquisitely sensitive to anti-EGFR antibodies have shown that prolonged treatment with anti-EGFR antibodies selects for resistant clones that harbor *KRAS* mutations [66, 67]. The results of these studies led to the conclusions that not only can *KRAS* mutations pre-exist in a small proportion of a population of cancer cells, but they can also be continuously generated *de novo* due to genomic instability. The end result is a state of acquired resistance brought about by the selection pressure of anti-EGFR antibody treatment which selects for cell populations harboring *KRAS* mutations [68]. Furthermore, *KRAS* mutations were detected in serum samples and metastases from treated patients, with the levels of these mutations correlating with relapse and disease progression [67, 69, 70]. In addition to point mutations, amplification of *KRAS*, although an extremely rare event in CRC, can also lead to resistance to anti-EGFR therapy [71].

Given the role of KRAS as a key downstream effector of EGFR signaling, it is perhaps not surprising that constitutive activation of KRAS by mutations bypasses the upstream effect of EGFR inhibition. However, the exact players that are responsible for circumventing the response to anti-EGFR therapy in a *KRAS*-mutant background remain elusive [72]. Recent studies indicate that *KRAS*-mutant cells heavily rely on the RAF/MEK/ERK cascade for survival, which provides a clue for dissecting the precise signaling pathways underlying the resistance phenotype [66]. Analysis of cell line models and CRC samples indicates that oncogenic KRAS plays a role in the maintenance of high expression levels of Bcl-2-related gene long isoform (Bcl-xL), an anti-apoptotic Bcl-2 family protein, whose overexpression alone is sufficient to confer resistance to anti-EGFR antibodies in CRC cells [73]. This study suggests that suppression of apoptosis is a mechanism of mutant-KRAS-mediated resistance to anti-EGFR therapy.

1.2 STRATEGIES TO OVERCOME *KRAS*-MEDIATED THERAPEUTIC RESISTANCE

1.2.1 Direct and Indirect Targeting Agents

The high mutation frequency and its role in therapeutic resistance make KRAS an ideal target for anti-cancer therapy. The proof-of-principle for targeting KRAS has been demonstrated by the profound phenotypes of KRAS ablation in mice and human cancer cells [50, 74]. A variety of strategies have been designed to target mutant RAS, including more direct targeting by

attempting to promote RAS' GTPase ability and indirect targeting by suppressing its post-translational modifications or downstream effectors (Table 1) [75].

Despite numerous attempts, developing small-molecule inhibitors of KRAS has proven to be extremely challenging. Several recent reports have described novel small molecules that interfere with GEF binding to lock KRAS in an inactive state [76]. For example, *in silico* and NMR-based screens were used to identify small molecules that bind to a distinct pocket on KRAS and inhibit SOS-mediated nucleotide exchange to prevent the activation of WT or mutant KRAS [77-79]. More specific approaches have been utilized to identify small-molecule inhibitors that covalently bind to mutant KRAS. A disulphide-fragment-based screening approach was used to identify electrophilic compounds that can form a disulfide bond with the cysteine residue in the G12C mutant of KRAS [80]. While these compounds do not affect WT KRAS, they can preferentially bind to the G12C mutant, disrupt SOS binding, and increase its affinity for GDP to prevent the activation of mutant KRAS. A similar approach identified a GDP analog as a covalent inhibitor of the G12C mutant [81].

Another approach for targeting KRAS is to inhibit its post-translational modifications using farnesyltransferase (FTase) inhibitors (FTIs), which inhibit the prenylation of KRAS that is required for proper plasma membrane attachment [82]. FTIs were shown to suppress cancer cell growth in pre-clinical studies, but unfortunately, they did not exhibit clinical efficacy as single agents [83, 84]. The lack of clinical response to FTIs was explained by the prenylation of KRAS through alternative mechanisms, such as those involving geranylgeranyltransferase I (GGTase I) [83, 85]. Dual inhibitors of GGTase and FTase, such as L778,123, were therefore developed. However, its toxicities in clinical trials prohibited further clinical development [86]. Another strategy illustrated by a recent study is to inhibit the interaction between KRAS and cyclic GMP

phosphodiesterase δ (PDEδ), which mediates correct localization and signaling by farnesylated KRAS [87].

Table 1. Recently-Developed Agents for Targeting Mutant KRAS

	Target	Mechanism of Action	References
Direct-Targeting Agents			
Small molecules from fragment-based screen	KRAS; WT, G12V, G12D; HRAS	Inhibition of SOS binding	[78]
4,6-dichloro-2-methyl-3-aminoethylindole (DCAI)	KRAS; G12D	Inhibition of SOS binding	[79]
Hits from fragment-based screen	KRAS; G12C	Inhibition of SOS binding	[80]
SML-8-73-1	KRAS; G12C	GDP Analog	[81]
Indirect-Targeting Agents			
Farnesyltransferase inhibitors	Farnesyltransferase; post-translational modification	Inhibition of prenylation by farnesyl group	[82, 85]
Geranylgeranyl-transferase I inhibitors	Geranylgeranyltransferase I; post-translational modification	Inhibition of prenylation by geranylgeranyl group	[83]
Inhibitors of KRAS and PDEδ interaction	KRAS and PDEδ interaction	Inhibition of prenylation	[87]
Inhibitors of RAF, MEK, and PI3K	RAF, MEK, and PI3K	Inhibition of KRAS effector pathways	[46, 88, 89]
Cetuximab and Pimasertib	EGFR and MEK; upstream and downstream KRAS pathway components	Dual inhibition of EGFR and MEK signaling	[66]
NVP-BEZ235-AN and AZD6244	PI3K and MEK; upstream and downstream KRAS pathway components	Dual inhibition of PI3K and MEK signaling	[90]
siRNA	Human and mouse KRAS pathway genes	Inhibition of protein expression	[91]
RAF265 and Selumetinib	RAF1/BRAF and MEK	Dual inhibition of RAF and MEK signaling	[92]

This table is adapted from Knickelbein et al. Genes and Diseases 2015 [24].

Additional anti-cancer strategies that target KRAS-mutant cells rely on the inhibition of its downstream effector proteins. This can be accomplished through the use of either single or combination treatments. For example, the RAF inhibitor Regorafenib has been recently approved by the FDA for the treatment of metastatic CRCs [46]. A number of PI3K and MEK pathway inhibitors have been developed and tested in clinical trials [88, 89]. A small interfering RNA (siRNA) library against RAS pathway genes has also been created, and transfection of this library into CRC cells could suppress cell growth both *in vitro* and *in vivo* [91]. Utilizing CRC cell lines that were selected for resistance to anti-EGFR antibodies, a recent study revealed that dual inhibition of both EGFR and MEK resulted in a pronounced reduction of cell viability in resistant cell populations [66]. Concomitant blockade of RAF1 and MEK in CRC cells with activating *KRAS* mutations was also shown to drastically reduce cell viability [92]. Furthermore, the combination of PI3K and MEK inhibitors suppressed KRAS G12D-mutant murine lung tumors [90].

Despite the promises, targeting KRAS-driven cancers remains one of the most difficult challenges in anti-cancer therapy due to several obstacles, including limited understanding of RAS-mediated signaling transduction feedback loops, pathway redundancy, tumor heterogeneity, unclear mechanisms of how RAS proteins activate their downstream targets, as well as unresolved structures of protein complexes formed by RAS oncoproteins [93]. It is essential to fill in these knowledge gaps in order to develop more effective agents for targeting KRAS-mutant cancers.

1.2.2 Synthetic Lethality

An emerging theme for targeting oncogenic mutations, including those of *KRAS*, exploits the concept of synthetic lethality, a genetic term referring to loss of viability resulting from a combination of two separate non-lethal mutations [94]. While synthetic lethality has been extensively studied in lower organisms such as yeast, its applications have only recently been extended into anti-cancer therapy. In the case of mutant KRAS, synthetic lethality has been used loosely to indicate selective or preferential killing of KRAS-mutant cells as the result of another mutation, treatment with a pharmacological agent, a change in gene expression, or other perturbations (Fig. 4). A good example of a genetic mutation that elicits drug sensitivity is that of *BRCA1*- or *BRCA2*-mutant breast tumors to poly (ADP-ribose) polymerase (PARP) inhibitors [95]. It is attractive to use this approach to target oncogenic mutations because pharmacologically more tractable targets can be explored, and normal cells not possessing the sensitizing mutations would in theory be spared during drug treatment.

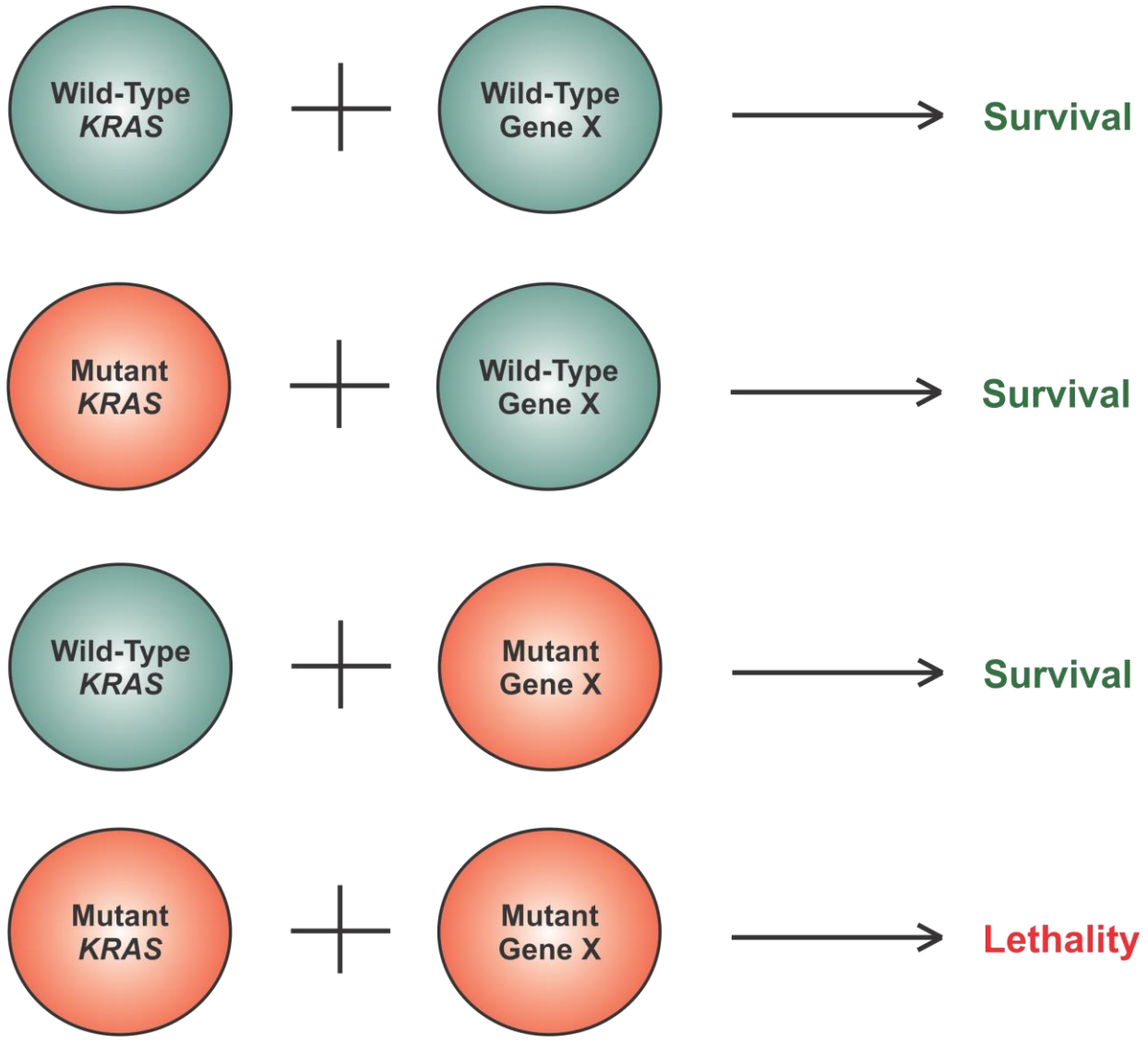

Figure 4. Mutant-*KRAS*-Mediated Synthetic Lethality. While a mutation in *KRAS* or gene X alone is insufficient to kill cells, a combination of mutations in these two genes can lead to cell death, resulting in synthetic lethality. Therefore, specific targeting of mutant *KRAS* can be achieved indirectly by targeting gene X. This figure is adapted from Knickelbein et al. Genes and Diseases 2015 [24].

A powerful approach for uncovering synthetic lethal interactions is large-scale screening based on RNA interference (RNAi) [96]. For *KRAS*-mutant cancers, a host of synthetic lethal interactions have been uncovered and characterized (Table 2). A recent study employing a small hairpin RNA (shRNA) library screen on isogenic WT and *KRAS*-mutant CRC cells identified several synthetic lethal interactions with mutant KRAS, including depletions of the mitotic protein polo-like kinase-1 (PLK1), anaphase-promoting complex/cyclosome (APC/C) subunits, as well as components of the proteasome [97]. An RNAi-based screen was also used to identify the depletion of TANK-binding kinase 1 (TBK1), a kinase involved in NF-κB signaling, to be synthetically lethal with mutant KRAS [98]. This finding also provided a mechanistic link between suppression of TBK1 expression with the downregulation of Bcl-xL through NF-κB signaling [98]. Other synthetic lethal partners with mutant KRAS that have been identified include the transforming growth factor beta-activated kinase 1 (TAK1), the Snail2 transcriptional repressor, the serine/threonine protein kinase STK33, the GATA-2 transcription factor, and the dual inhibition of Bcl-xL and MEK [99-103]. These examples illustrate the usefulness of genetic approaches for uncovering novel synthetic lethal interactions, which can potentially be translated into new therapeutic agents to selectively target *KRAS*-mutant cancers.

Table 2. Synthetic Lethal Interactions in *KRAS*-Mutant Cancers

Genes or Proteins	Cancer Type	Method of Discovery	References
PLK1	Colorectal	shRNA screen	[97]
Anaphase-Promoting Complex/Cyclosome (APC/C)	Colorectal	shRNA screen	[97]
Proteasome	Colorectal	shRNA screen	[97]
TBK1	Lung	shRNA screen	[98]
STK33	Colorectal, Breast, and Leukemia	shRNA screen	[99]
SNAI2	Colorectal	shRNA screen	[100]
TAK1	Colorectal	Gene expression profiling and knockdown	[101]
GATA2	Lung	shRNA screen	[102]
Bcl-xL/MEK	Colorectal, Pancreatic, and Lung	shRNA screen	[103]

This table is adapted from Knickelbein et al. Genes and Diseases 2015 [24].

1.3 MECHANISMS OF CELL DEATH

Several well-characterized cell death pathways have been implicated in colorectal cancer cell death. Autophagy, a process by which intracellular organelles and proteins are recycled via a lysosomal compartment, has been associated with the induction of cell death in colorectal cancer cells following treatment with pharmacological agents [104]. Additionally, necroptosis, a programmed form of necrosis, can also be initiated in colorectal cancer cells leading to cell death upon exposure to tumor necrosis factor-related apoptosis-inducing ligand (TRAIL) or tumor necrosis factor-α (TNF-α) [104, 105]. A third major form of cell death is apoptosis, or programmed cell death. Apoptosis is a conserved process that functions in normal cellular physiology, but is also of paramount importance in cancer, whereby cancer cells can evade the induction of apoptosis leading to therapeutic resistance [106].

1.3.1 Apoptosis

Apoptotic cell death proceeds via several distinct intracellular pathways. Two of the major apoptotic pathways have been well-characterized and are known as the intrinsic and extrinsic apoptotic pathways [107]. Furthermore, apoptosis is heavily regulated by the function of the various Bcl-2 family proteins, particularly within the intrinsic apoptotic pathway, which ultimately regulate the induction of apoptosis [106].

1.3.1.1 Extrinsic and Intrinsic Pathways. A classic mechanism for extrinsic apoptosis, or death-receptor-mediated apoptosis, occurs via a clustering of extracellular receptors, known as death receptors, as a trimeric complex and ligand binding. This enables adapter protein recruitment, followed by association with pro-caspase-8. At this point, pro-caspase-8 is converted into its active form, allowing for the initiation of apoptosis. Well-characterized players involved in extrinsic apoptosis include Fas ligand/Fas receptor and TNF ligand/TNF receptor pairs [107].

The second arm of apoptosis induction occurs via the intrinsic, or mitochondrial-mediated pathway [107]. Both anti-cancer agents as well as environmental stressors such as hypoxia can activate intrinsic apoptosis, which ultimately leads to mitochondrial membrane dysfunction and subsequent release of cytochrome *c* into the cytosol. The release of cytochrome *c* is necessary for the formation of the apoptosome, which induces the activation of pro-caspase-9 leading to cleavage of the executioner caspase-3 [107]. The ability of the mitochondrial-mediated apoptosis pathway to induce cell death is heavily dependent upon the function of the various pro- and anti-apoptotic Bcl-2 family proteins [106, 108].

1.3.1.2 Bcl-2 Family Proteins. Within the intrinsic pathway, the Bcl-2 family proteins function to regulate the integrity of the outer mitochondrial membrane. The Bcl-2 proteins can be divided into two distinct classes: pro-apoptotic and anti-apoptotic [109]. The relative balance between pro-apoptotic and anti-apoptotic Bcl-2 proteins can ultimately determine whether or not a cell will undergo apoptosis. Some of the key anti-apoptotic proteins include myeloid cell leukemia-1 (Mcl-1), Bcl-xL, and Bcl-2, while some of the notable pro-apoptotic proteins include Bcl-2-interacting mediator of cell death (Bim), Bcl-2-interacting domain death agonist (Bid), Noxa, and the p53-upregulated modulator of apoptosis (PUMA) [106, 109]. Interestingly, Bid is notable as it is able to promote cross-talk between the intrinsic and extrinsic pathways; caspase-8-mediated Bid cleavage allows for the truncated form of Bid (tBid) to promote mitochondrial apoptosis [107, 110]. Bcl-2-associated x protein (Bax) and Bcl-2 antagonist killer 1 (Bak) are also pro-apoptotic Bcl-2 family proteins, but are further classified as effector proteins that are ultimately responsible for outer mitochondrial membrane permeability [109].

The Bcl-2 family proteins share amongst them unique protein domains known as Bcl-2 homology (BH) domains. Notably, the anti-apoptotic Bcl-2 family protein repertoire in addition to the effector proteins Bax and Bak share the domains BH1-4 [109]. On the other hand, the second division of the pro-apoptotic Bcl-2 proteins is known as the BH3-only proteins, which function to sensitize cells to apoptosis by either promoting activation of Bax and Bak or relieving their inhibition by binding to anti-apoptotic Bcl-2 family proteins [109]. This action allows for homo-oligomerization of both Bax and Bak, which promotes mitochondrial outer membrane permeabilization (MOMP) leading to activation of the caspase cascade (Fig. 5) [109]. The BH3-only proteins possess varying degrees of inhibition of the anti-apoptotic Bcl-2 proteins. For example, the BH3-only protein Noxa binds preferentially to the anti-apoptotic proteins Mcl-1

and A1 [111]. However, Bim and PUMA are able to antagonize Mcl-1 and A1 as well as Bcl-2 and Bcl-xL [106, 111].

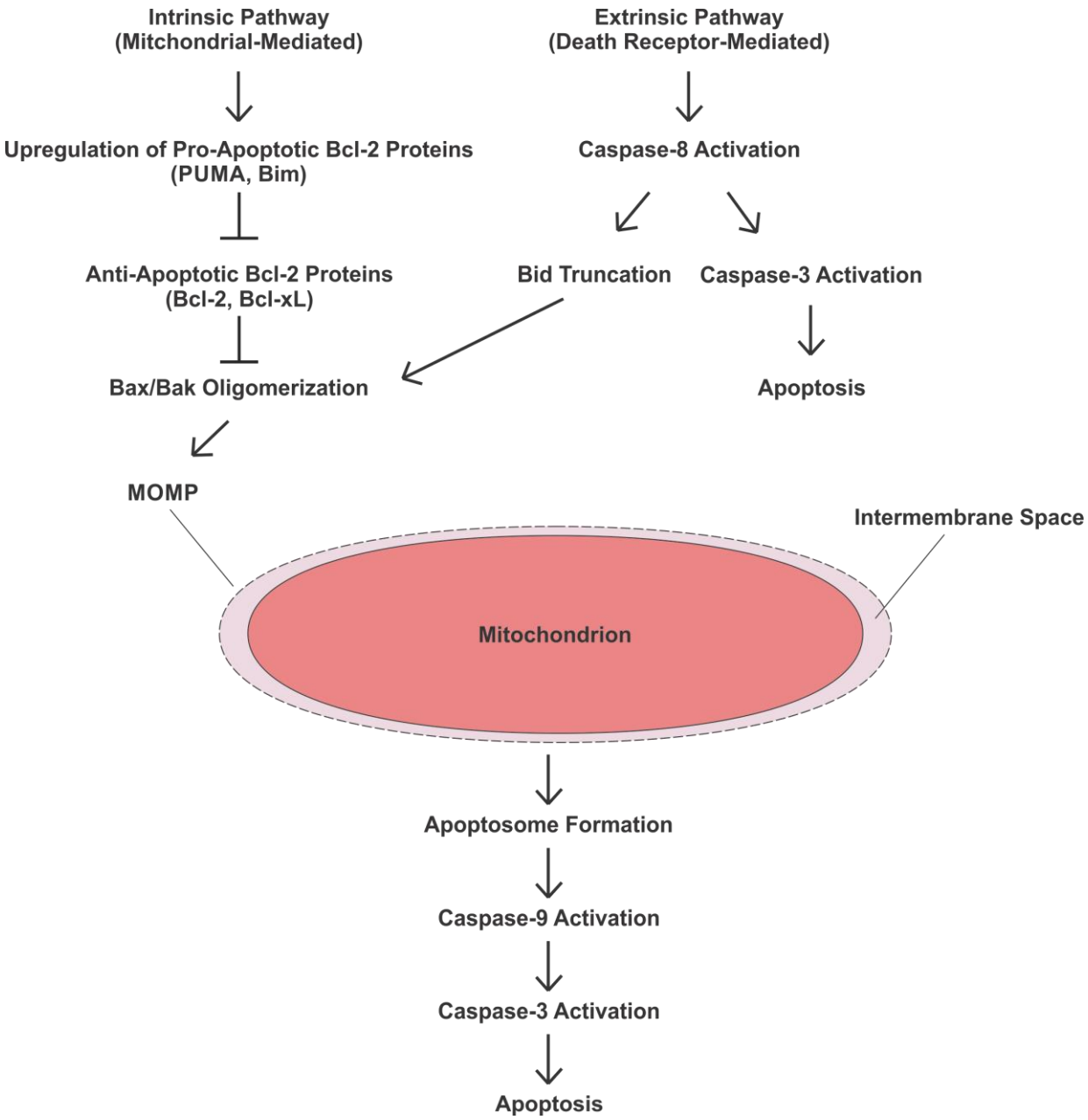

Figure 5. Intrinsic and Extrinsic Apoptosis Pathways. This schematic depicts two of the major pathways contributing to the initiation of apoptosis. This figure is original artwork created in part from information within the publication Tait et al. Journal of Cell Science 2012 [108]. DOI: 10.1242/jcs.099234

1.3.1.3 PUMA Expression and Transcriptional Regulation. PUMA is classified as a BH3-only protein within the Bcl-2 family. Identified as a target of p53 transcription, PUMA has been shown to induce apoptosis in colorectal cancer cells upon its overexpression alone [112]. However, much work has demonstrated that PUMA can be induced by additional transcription factors and that PUMA expression mediates the apoptotic chemotherapeutic response. For example, PUMA has been shown to be induced by the p65 subunit of NF-κB and mediates the sensitivity to chemical inhibitors of the Aurora kinases [113]. Furthermore, PUMA expression also mediates the chemotherapeutic response in colorectal cancer cells to the FDA-approved agent Regorafenib through the action of NF-κB [114]. The results of such studies suggest that decreased PUMA expression is detrimental in cancer cells by promoting resistance to chemotherapy.

2.0 MECHANISMS OF SENSITIVITY AND RESISTANCE TO ANTI-EGFR ANTIBODY THERAPY IN COLORECTAL CANCER CELLS

2.1 INTRODUCTION

Colorectal cancer (CRC) is currently the third-leading cause of cancer related deaths amongst both men and women in the United States [4]. Additionally, nearly half of all patients diagnosed ultimately present with a metastatic lesion, and the five-year survival rate of metastatic disease is estimated at only 11% [5]. Current treatment efforts include surgical intervention, radiotherapy, conventional chemotherapy, and also the use of newer targeted therapies [45]. The utilization of targeted therapy encompasses monoclonal antibodies against VEGF-A, such as bevacizumab, and the use of monoclonal antibodies against EGFR, notably cetuximab and panitumumab [52, 54]. Interestingly, apoptosis induction in colorectal cancer cells has been previously reported; however, the mechanisms of how anti-EGFR antibody therapy induces cell death in colorectal cancer cells are not well characterized [115]. Furthermore, while anti-EGFR antibodies have produced a higher rate of response when combined with conventional chemotherapy, resistance can ultimately occur due to mutations in the *KRAS* oncogene [60].

KRAS is a small GTPase that connects signaling from growth factor receptors through major intracellular signaling pathways such as PI3K/AKT and RAF/MEK/ERK [16, 22]. In normal cellular physiology, KRAS cycles between an inactive GDP-bound and an active GTP-

bound form [16]. When mutated, principally at codons 12 and 13, the GTPase ability of KRAS is profoundly hindered, resulting in a state of constitutive activation and signaling through its downstream effector pathways [16, 22]. Clinically, KRAS mutations have since been found to correlate with a lack of response to anti-EGFR antibody therapy [72]. Furthermore, it has been shown that continuous culturing of cell lines sensitive to anti-EGFR therapy leads to the emergence of alterations in the *KRAS* oncogene, conferring resistance [67]. While these resistant derivatives are insensitive to the induction of cell death, the exact mechanisms governing this phenomenon have not been studied.

In this study, we investigated the mechanisms of cell death upon treatment with anti-EGFR antibodies in colorectal cancer cells. We observed that both cetuximab and panitumumab induce apoptosis, which is dependent upon the expression of the pro-apoptotic Bcl-2 family PUMA. PUMA expression was found to be dependent upon the activity of the p73 transcription factor. PUMA expression was suppressed in anti-EGFR antibody-resistant cells, and interestingly, the activation of p73 was also found to be strongly suppressed. Our results suggest that resistance to anti-EGFR antibodies is mediated in part through decreased activation of p73 and decreased induction of PUMA expression.

2.2 MATERIALS AND METHODS

2.2.1 Cell Culture and Drug Treatment

Human parental CRC cell lines, including DiFi, CCK-81, HCA-46, and OXCO-2, and the anti-EGFR antibody resistant derivatives, including DiFi cetuximab-resistant (R1 clone) and HCA-46

panitumumab-resistant cells, were generously donated by the laboratory of Dr. Alberto Bardelli at the University of Turin. DiFi, CCK-81, HCA-46, and OXCO-2 cells were tested for the absence of mycoplasma approximately every 6 months. Unless otherwise specified, all CRC cell lines were maintained in McCoy's 5A modified media (Invitrogen, Carlsbad, CA) supplemented with 10% FBS (HyClone, Logan, UT, USA) and 1% penicillin-streptomycin consisting of 100 units/mL penicillin and 100 µg/mL streptomycin (Invitrogen). Cells were kept in a non-humidified incubator at 37°C with the addition of 5% CO_2.

Unless otherwise specified, cells were plated at 20-30% density in 12-well plates for drug treatment. Chemicals utilized include cetuximab (Eli Lilly and Company, NY/NJ), panitumumab (Amgen; supplied through UPCI Pharmacy), carbobenzoxy-valyl-alanyl-aspartyl-[O-methyl]-fluoromethylketone (zVAD-fmk) (R&D Systems), and ABT-737 (Selleck Chemicals, LLC). All agents except antibody treatments were first diluted in DMSO (Sigma) to establish a stock solution.

2.2.2 Analysis of Cell Viability and Cell Death

To analyze cellular viability, CellTiter AQueous One Solution (MTS assay; Promega) was utilized according to the manufacturer's instructions with a minor modification in clear 96-well plates. Following aspiration of the existing media, a 1:5 mix of MTS solution and medium (120 µL total) were added to each well. Absorbance measurements were carried out at 490 nm using a Wallac Victor 1420 Multilabel Counter (PerkinElmer) following incubation at 37°C for approximately 2 hours. Background readings containing the MTS-medium mix with no cells were subtracted from all measurements, and unless otherwise specified, all absorbances were normalized to untreated controls.

To measure ATP levels, the CellTiter-Glo Luminescent Cell Viability Assay (Promega) was utilized in clear-bottom black 96-well plates (Corning). Existing cell culture medium was aspirated, followed by addition of 50 µL of a 1:1 mix of CellTiter-Glo and medium. Plates were placed in the dark on a rotary shaker for 3 minutes followed by a 20-minute incubation at room temperature away from light. Luminescence was measured on the Multilabel Counter. Background readings containing the CellTiter-Glo-medium mix with no cells were subtracted from all measurements, and all absorbances were normalized to untreated controls.

For crystal violet staining, attached cells were washed with HBSS and stained by incubating cells at room temperature with a 0.05% crystal violet solution containing 3.7% paraformaldehyde prepared in distilled water.

Cell death was analyzed by staining floating and attached cells with Hoechst 33258 (Invitrogen) and by counting condensed and fragmented nuclei, which were divided by the total number of cells counted to obtain the final percentages. Each condition was analyzed in duplicate per experiment counting at least 300 cells per sample.

Analysis of cell death by flow cytometry was performed by collecting floating and attached cells and diluting in 100 µL of Annexin-V binding buffer (10 mM HEPES, 140 mM NaCl, and 2.5 mM $CaCl_2$). Each sample diluted in buffer additionally contains an equivalent of 2 µL of Annexin-V Alexa Fluor 488 conjugate and 2 µL of propidium iodide (PI; Invitrogen), the latter at a stock concentration of 50 µg/mL. After incubation at room temperature away from light for at least 15 minutes, 300 µL of Annexin-V binding buffer without the Annexin-V conjugate or PI were added to each sample. Cells were immediately analyzed by flow cytometry (BD Accuri C6). 10,000 events were analyzed per sample per experiment.

Caspase-3/-7 activity was measured using the Homogeneous AMC Capase-3/-7 Assay Kit (SensoLyte) according to the manufacturer's instructions using clear-bottom black 96-well plates (Corning). Fluorescence readings were taken using a Wallac Victor 1420 Multilabel Counter (PerkinElmer). Background readings containing the reagent-medium mix with no cells were subtracted from all measurements, and all absorbances were normalized to untreated controls.

2.2.3 Cell Transfection and Transduction

Cells were plated at 20-30% density 24 hours prior to transfection of either plasmids or siRNA. Cells were transfected utilizing Lipofectamine 2000 according to the manufacturer's instructions with modifications. Briefly, siRNAs were transfected in 1X Opti-MEM (Gibco) with 200 or 400 pmol of siRNA per well of a 12-well plate, or, if specified, the equivalent amount if a larger area of cells was used for transfection. Transfections were carried out for 4 hours before the addition of McCoy's 5A medium. Drug treatments were performed approximately 24 hours following the start of transfection. The sequences utilized for each siRNA are found in Table 5. For overexpression experiments, the equivalent of 0.2 µg of plasmid per well of a 12-well plate was utilized. Plasmids included N-terminal HA-tagged pcDNA3.1 empty vector (control plasmid), HA-tagged p73α in a pcDNA3 vector [116], and N-terminal-myristolated, constitutively-active AKT1 in a pUSEamp (+) vector (#21-151, Upstate).

For adenovirus infection, cells were infected at both 20 and 40 MOI for 24 hours utilizing a GFP-tagged PUMA-expressing adenovirus which was described previously [117].

2.2.4 Western Blotting

For protein expression analysis, all samples were collected in 2X Laemmli buffer and were subsequently used for Western blotting. Briefly, samples were loaded onto 10% Bis-Tris gels and ran at approximately 175V for 45 minutes. Gels were transferred on a TransBlot SD semi-dry transfer cell (Biorad) using PVDF membranes. Following the transfer, membranes were blocked in a 5% milk solution containing TBS and 0.05% Tween-20 (TBS-T) for 1 hour prior to overnight incubation in primary antibody at 4°C. After primary incubation, membranes were washed three times with TBS-T, followed by secondary antibody incubation for 1 hour at room temperature with either goat anti-mouse (Pierce #31432) or goat anti-rabbit (Pierce #31462). Membranes were washed again with TBS-T prior to developing by chemiluminescence detection using Western Lighting-Plus ECL according to the manufacturer's directions (Perkin-Elmer).

Antibodies utilized included: β-Actin (Sigma #A5441), cleaved caspase-3 (Cell Signaling #9661), Mcl-1 (BD #559027), Bax (BD #610983), Bid (Cell Signaling #2002), Bcl-xL (BD #610212), Bim (Cell Signaling #2819), Bcl-2 (DAKO #M0887), PUMA (QCB #3795), p73 (Bethyl A300-126A), p-AKT (Cell Signaling #4058), total AKT (Cell Signaling #9272), p-ERK1/2 (Cell Signaling #4376), total ERK1/2 (Cell Signaling #9102), p-FoxO3A (Cell Signaling #9464), total FoxO3A (MI 07702), p53 (Santa Cruz #126), p-EGFR (Cell Signaling #2234), total EGFR (BD 610016), KRAS (Santa Cruz #30), and HA (Roche #12CA5).

2.2.5 Reverse Transcription and Quantitative PCR

RNA extracts were prepared from cells using the Quick-RNA MiniPrep kit (Zymo Research) according to the manufacturer's instructions. From the extracted RNA, cDNA was prepared

using SuperScript III Reverse Transcriptase (Invitrogen). Following reverse transcription, quantitative PCR was performed using a profile consisting of 95°C for 2 minutes (Stage I), 95°C for 20 seconds, 58°C for 30 seconds, and 70°C for 30 seconds (Stage II), and 65°C for 5 seconds (Stage III). Fold changes were determined by subtracting Cq values of the loading control from the Cq values of the gene of interest. From here, taking 2 raised to the negative differential and normalizing to untreated controls was done to obtain the relative level of expression. Primers utilized are listed in Table 4.

2.2.6 Protein Immunoprecipitation

Cells were lysed in buffer consisting of 50 mM Tris, 150 mM NaCl, 1% NP-40, 1 mM EDTA, and 10% glycerol prepared in distilled water. The final pH was adjusted to 7.5. Protease-inhibitor tablets (Roche) were also added to the buffer prior to lysis. Cell lysates were incubated with EZview Red Protein G Affinity Gel (Sigma) beads utilizing an antibody against p-p73 (Cell Signaling #4665). Cell lysates were incubated overnight at 4°C. Following the overnight incubation, the bead-protein complex was washed, lysed in 2X Laemmli buffer and analyzed by Western blot.

2.2.7 Chromatin Immunoprecipitation

Chromatin immunoprecipitation (ChIP) experiments were carried out with the ChIP Assay Kit (Millipore). Each time point was collected by first crosslinking the DNA in 1% formaldehyde and scraping to collect all cells. Following cell lysis, samples were sonicated to shear DNA and were centrifuged at 13,000 rpm for 10 minutes at 4°C to separate cell debris. The supernatant

was then diluted 10-fold in ChIP dilution buffer and 20 µL from each sample were saved as an input fraction. Lysates were pre-cleared by addition of 75 µL of Salmon Sperm DNA/Protein A for 30 minutes on a rotor at 4°C.

After pre-clearing, supernatant fractions were collected and incubated overnight at 4°C with 1-2 µg of the appropriate antibody. Antibodies used included rabbit IgG (R&D Systems) for a negative control, HA (Roche #12CA5), and total p53 (Santa Cruz #126). The histone complexes were then collected by adding 60 µL of Salmon Sperm DNA/Protein A to each sample for 1 hour at 4°C on a rotor. Histone complexes were then washed with Low-Salt Wash Buffer (1 wash), High-Salt Wash Buffer (1 wash), LiCl Wash Buffer (1 wash), and TE Buffer (2 washes).

To elute the samples, 250 µL of a 1% SDS, 0.1M $NaHCO_3$ were added to the histone complexes and incubated for 15 minutes at room temperature with rotation (done twice), and all eluates were collected in a new tube. Crosslink reversal was initiated by adding 10 µL of 5M NaCl to each experimental sample and 1 µL to each input sample with incubation at 65°C for at least 4 hours. Subsequently, 5 µL of 0.5M EDTA, 10 µL of 1M Tris-HCl pH 6.5, and 0.02 mg of Proteinase K were added to all samples and incubated at 45°C for 1 hour. DNA was recovered by extraction with PC8 and precipitated with ethanol. Products were diluted in distilled water and analyzed by PCR using primers directed against the *PUMA* promoter region as indicated in Table 4.

2.2.8 MitoTracker Red CMXRos Mitochondrial Staining

Cells were treated in 12-well plates, and cell pellets were collected and stained with 100 nM CMXRos (Invitrogen) suspended in 400 µL medium per sample. After 15-30 minutes

incubation at 37°C, samples were analyzed by flow cytometry counting 30,000 events per sample.

2.2.9 Statistical Analysis

All statistical analyses were carried out with GraphPad Prism IV software. Two-sample Student's *t*-test analyses were performed to calculate all *P*-values and were considered statistically significant if *P* was found to be less than 0.05 in a two-tailed test. Bars representing the standard error of the means were reported with the means.

2.3 RESULTS

2.3.1 Anti-EGFR Antibodies Induce Apoptosis in a Subset of Colorectal Cancer Cells

Several colorectal cancer cell lines are inherently sensitive to anti-EGFR antibody therapy; therefore, these serve as ideal model systems to study targeted therapy-induced cell death. To elucidate the mechanisms of anti-EGFR antibody-induced cell death, we first confirmed the phenotype after antibody treatment in both DiFi and CCK-81 CRC cells. Both DiFi and CCK-81 cells were very sensitive to low doses of both cetuximab and panitumumab, correlating with previous studies (Fig. 6A) [67]. Previous reports have also indicated that DiFi cells undergo apoptosis when treated with anti-EGFR antibodies [115]. We therefore analyzed the expression level of the active form of the executioner caspase-3 in addition to the activity of executioner caspases 3 and 7 in both DiFi and CCK-81 cells (Fig. 6B-C). We observed that both the

expression and activity of the executioner caspases were elevated following both cetuximab and panitumumab treatment.

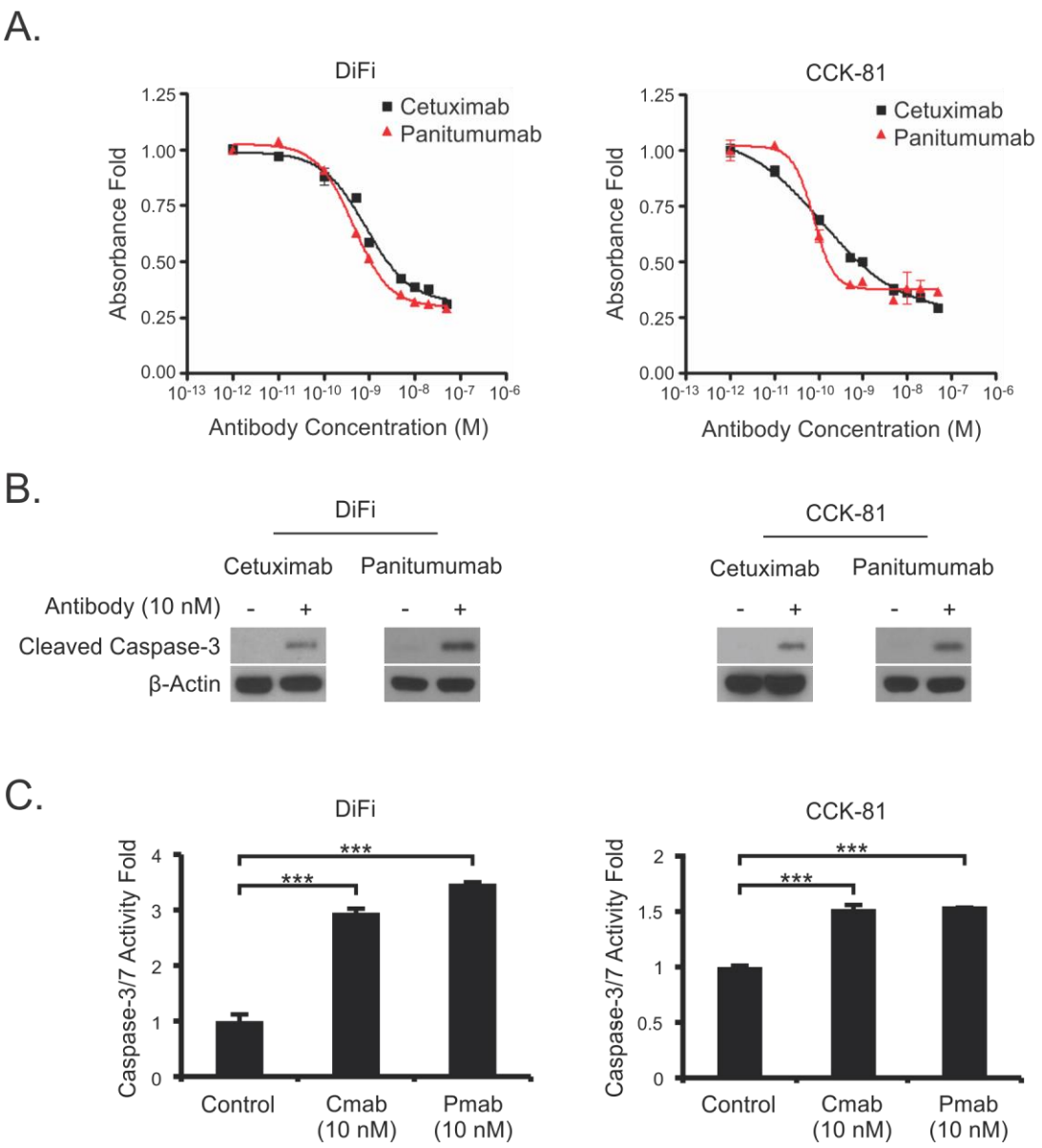

Figure 6. Colorectal Cancer Cells Sensitive to Anti-EGFR Antibodies Induce Caspase Activation Following Treatment. **(A)** DiFi parental cells were seeded at a density of 10,000 cells per well (left) and CCK-81 parental cells (right) were seeded at a density of 5,000 cells per well and were treated with the indicated doses of cetuximab or panitumumab for 72 hours. Cell metabolism was assessed by the MTS assay. Absorbances were normalized to the sample with the lowest treatment dose. **(B)** DiFi (left) and CCK-81 parental cells (right) were treated for 24 hours with 10 nM antibody. Cleaved caspase-3 was assessed by Western blot. **(C)** DiFi parental

cells (left) and CCK-81 parental cells (right) were seeded in 96-well plates at a density of 10,000 and 5,000 cells per well, respectively. Cells were treated 24 hours after plating at the indicated doses for 24 hours. Caspase activity was measured using the Caspase-3/-7 Activation kit. ***P<0.001.

To further confirm that apoptosis is induced following anti-EGFR antibody treatment, we performed Hoechst staining to observe the levels of fragmented nuclei and Annexin V/PI staining, of which Annexin V binding to the cell surface is indicative of apoptosis. We noted a strong increase in the amount of fragmented nuclei following anti-EGFR antibody treatment, as well as a significant increase in Annexin V-positive cells after treatment (Fig. 7A-B). The low levels of Annexin V-negative and PI-positive cells allowed us to rule out a significant contribution of cell death to necrosis (Fig. 7B). Furthermore, we demonstrated that the apoptotic cell death is caspase dependent, as pre-treatment with the pan-caspase inhibitor zVAD-fmk reduced the number of condensed and fragmented nuclei observed compared to cetuximab treatment alone (Fig. 7C).

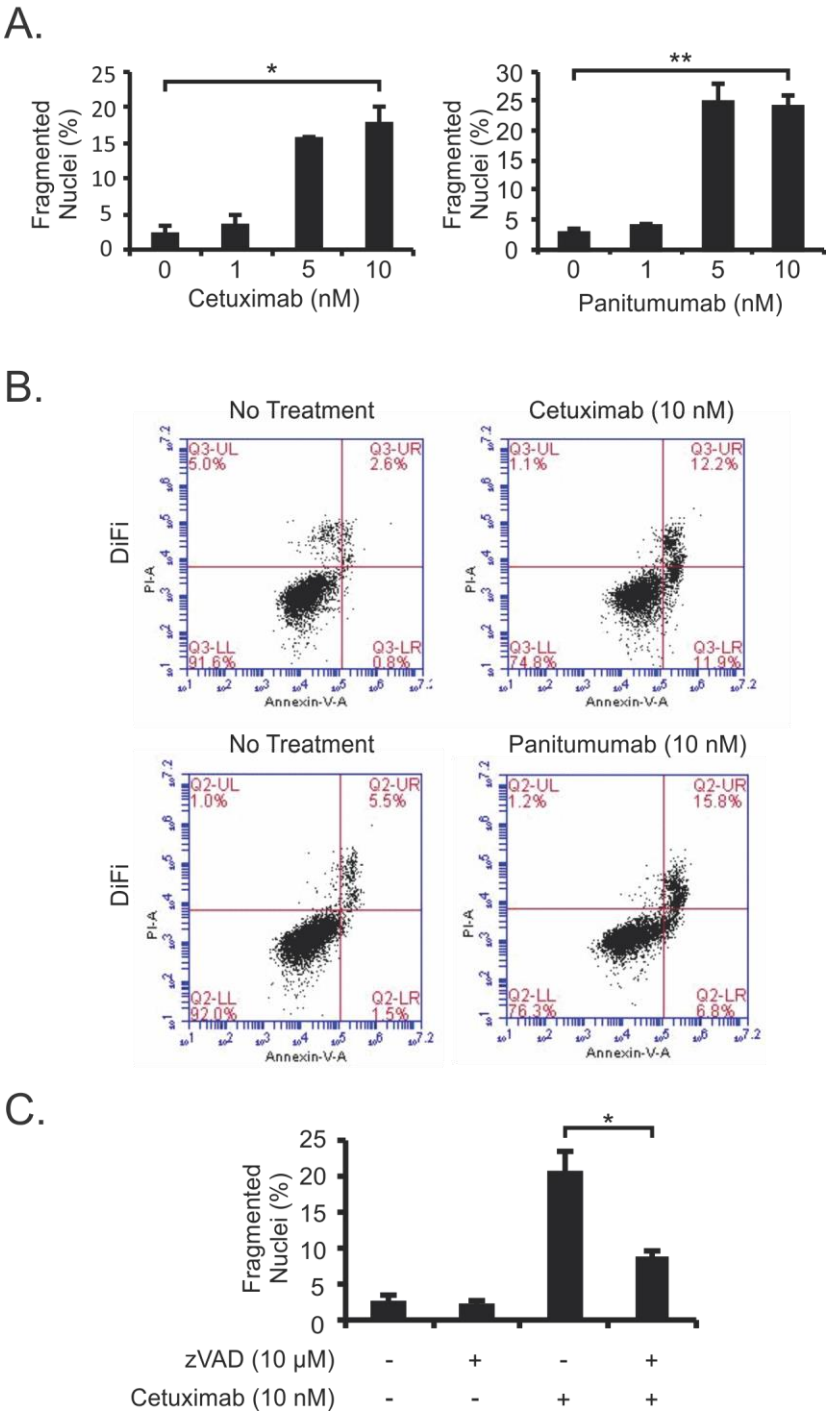

Figure 7. Anti-EGFR Antibodies Induce Apoptosis in Colorectal Cancer Cells. (A) DiFi parental cells were treated for 72 hours with indicated concentrations of antibodies and stained with Hoechst 33258. The numbers of condensed and fragmented nuclei were counted as a percentage of total cells. *P<0.05, **P<0.01. **(B)** DiFi parental cells were treated for 72 hours

as indicated. Results were analyzed by flow cytometry following Annexin V/PI staining. **(C)** DiFi parental cells were treated with zVAD, cetuximab, or their combination for 72 hours. Cells treated with the zVAD and cetuximab combination were pre-treated for 1 hour with 10 μM zVAD. Following treatment, cells were stained with Hoechst 33258 and the numbers of condensed and fragmented nuclei were counted as a percentage of the total cells counted. *$P<0.05$.

The mitochondria play a key role in the execution of apoptosis, specifically through activation of the intrinsic pathway which leads to loss of mitochondrial membrane potential [107]. Additionally, this indirectly results in the activation of the initiator caspase-9, which in turn activates the executioner caspase-3 [107]. Following anti-EGFR antibody treatment, we observed both the loss of mitochondrial membrane potential as well as increased protein levels of the active fragments of caspase-9 (Fig. 8A-B).

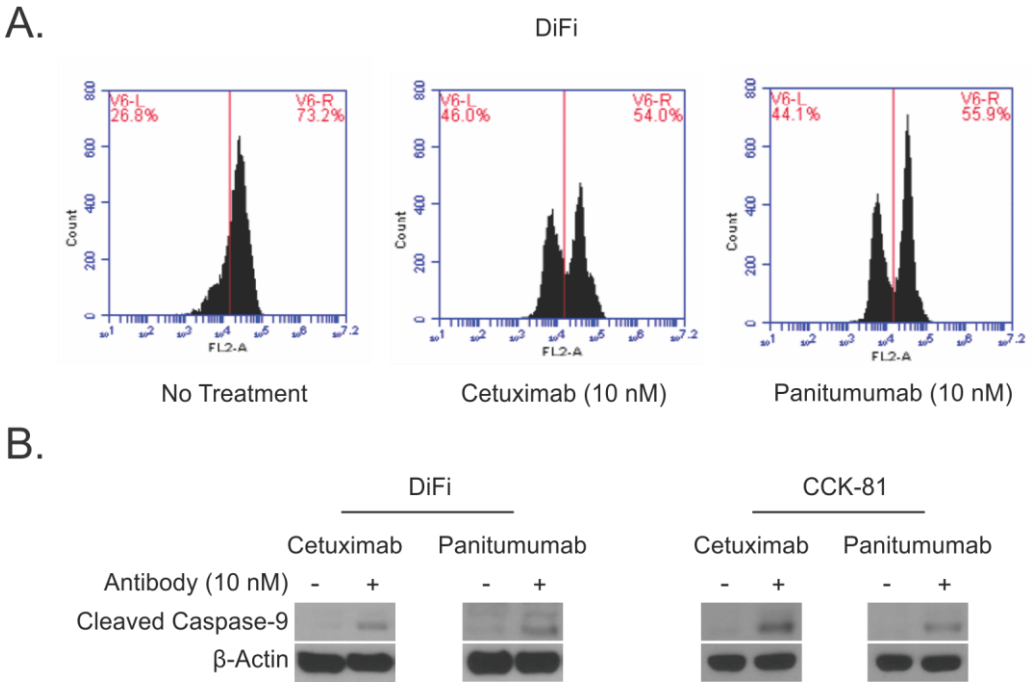

Figure 8. Mitochondrial-Mediated Apoptosis is Induced Following Anti-EGFR Antibody Treatment in Colorectal Cancer Cells. (A) DiFi parental cells were treated for 72 hours at the indicated doses. Mitochondrial membrane integrity was assessed by CMXRos staining analyzed by flow cytometry. **(B)** DiFi parental cells (left) and CCK-81 parental cells (right) were treated with the indicated concentrations of antibodies for 24 hours. Protein expression was determined by Western blot.

2.3.2 PUMA Expression is Induced by Anti-EGFR Antibodies and is Required for the Apoptotic Response

The Bcl-2 family proteins are central regulators of the intrinsic apoptotic pathway, and the initiation of apoptosis is ultimately governed by the balance of pro-survival and pro-apoptotic Bcl-2 proteins [118]. To determine how the Bcl-2 family proteins are being modulated in

response to anti-EGFR antibodies, we treated DiFi cells in a time-course experiment and assessed protein level expression. Interestingly, we observed a marked increase in the expression of PUMA at both the protein and mRNA levels (Fig. 9A). PUMA was also induced in a concentration-dependent manner (Fig. 9B). In additional cell models, although other Bcl-2 family proteins were modulated, PUMA expression was consistently increased upon anti-EGFR antibody treatment (Fig. 9C-D).

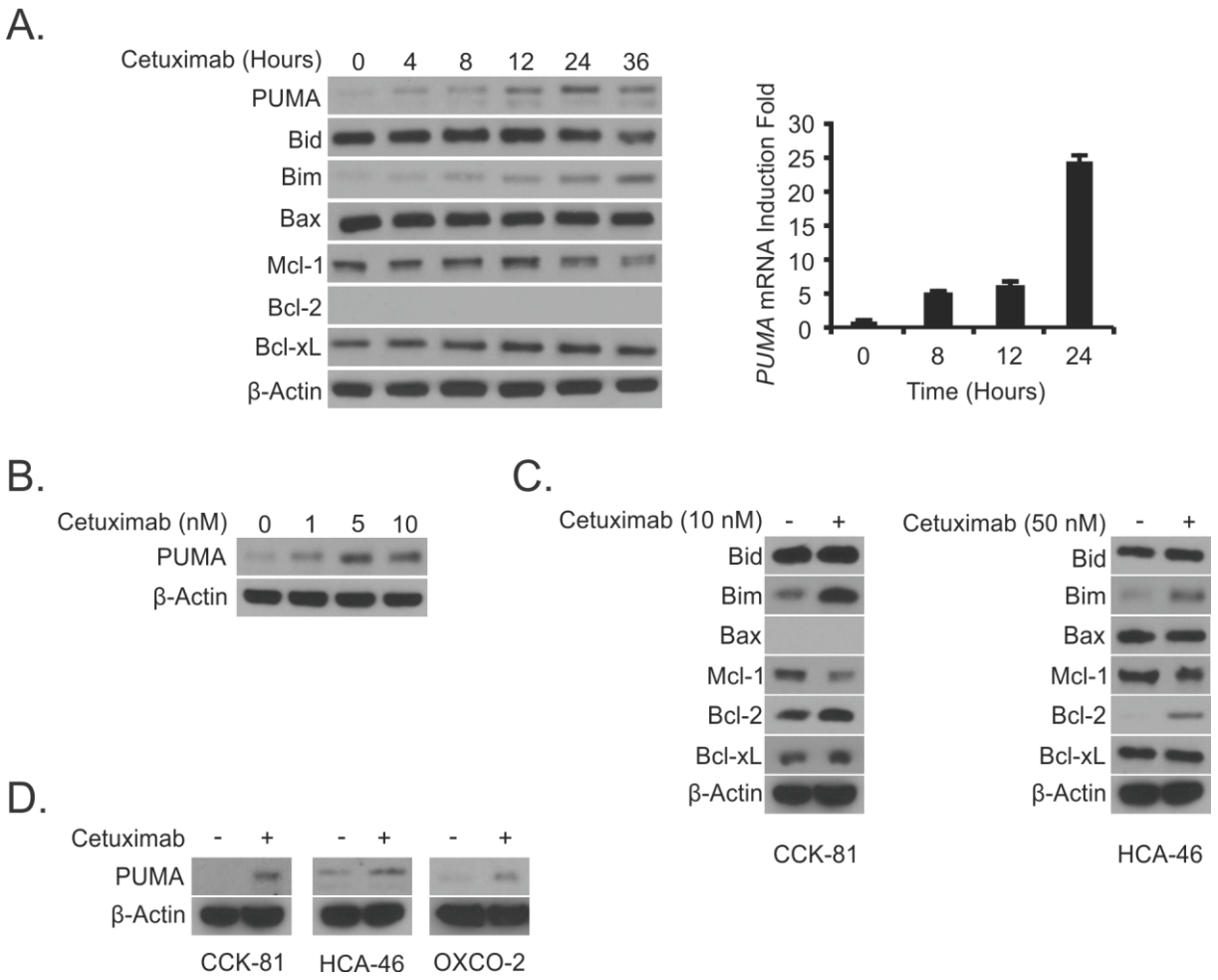

Figure 9. Anti-EGFR Antibodies Induce the Expression of PUMA in Colorectal Cancer Cell Lines. (A) *Left,* DiFi parental cells were treated with 10 nM cetuximab for the indicated time points. Bcl-2 family protein expression was analyzed by Western blot. *Right*, DiFi parental cells were treated for the indicated time points with 10 nM cetuximab. mRNA expression was determined by RT-PCR. **(B)** DiFi parental cells were treated for 24 hours with the indicated concentrations of cetuximab. PUMA expression was determined by Western blot. **(C)** CCK-81 and HCA-46 parental cells were treated for 24 hours with the indicated concentrations of cetuximab. Bcl-2 family protein expression was analyzed by Western blot. **(D)** CCK-81, HCA-46, and OXCO-2 parental cells were treated for 24 hours with 10 nM cetuximab (CCK-81) or 50 nM cetuximab (HCA-46 and OXCO-2). PUMA expression was analyzed by Western blot.

PUMA expression has been implicated in driving the apoptotic response to a number of cytotoxic stimuli in colorectal cancer cells [113, 114, 119]. To determine if PUMA is required for the apoptotic response to anti-EGFR antibodies, we depleted PUMA expression levels with siRNA and observed that the sensitivity to treatment was reduced as assessed by diminished amounts of fragmented nuclei and the abolishment of caspase-3 activation (Fig. 10A-B). To elucidate if suppression of PUMA expression can restore overall cellular viability, we performed crystal violet staining on DiFi cells treated with anti-EGFR antibodies following PUMA knockdown utilizing siRNA. Indeed, knockdown of PUMA was able to partially restore cellular viability after anti-EGFR antibody treatment when compared to scrambled siRNA transfection controls as assessed by crystal violet staining (Fig. 10C). Our results suggest that while the apoptotic effects of anti-EGFR antibodies due to PUMA knockdown are being mitigated, the cytostatic effects of antibody treatment are still inhibiting cell proliferation compared to untreated controls.

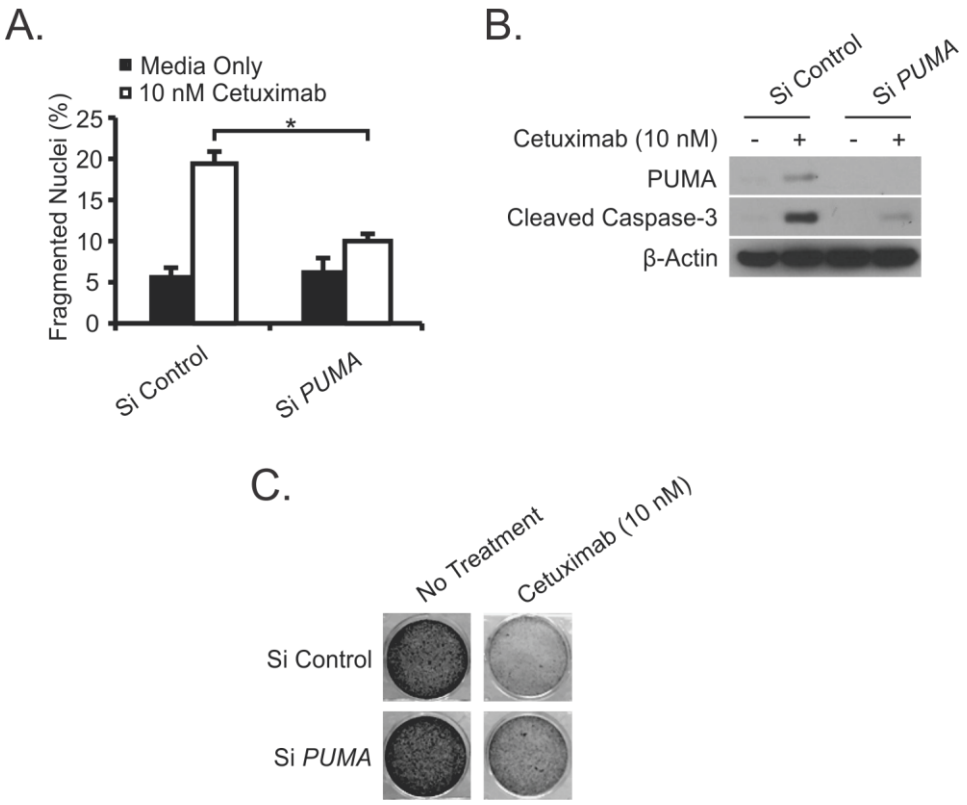

Figure 10. PUMA Knockdown Blocks Apoptosis and Restores Cell Viability. (A) DiFi parental cells were transfected with 200 pmol of either control or *PUMA* siRNA for 24 hours before treatment as indicated for 72 hours. Apoptotic cells were scored following staining with Hoechst 33258 by counting condensed and fragmented nuclei as a percentage of the total cells counted. *P<0.05. **(B)** DiFi parental cells were transfected with 200 pmol of either control siRNA or *PUMA* siRNA for 24 hours before treatment at the indicated concentration of cetuximab for another 24 hours. PUMA and cleaved caspase-3 expression were analyzed by Western blot. **(C)** DiFi parental cells were transfected with the equivalent of 200 pmol per well of a 12-well plate of either control or *PUMA* siRNA, re-plated 24 hours later, then treated 24 hours after the re-plating with the indicated dose of cetuximab. Staining by crystal violet was done 48 hours after treatment.

To test whether other anti-EGFR antibodies can also induce PUMA, we performed the same experiments in CRC cells utilizing the antibody panitumumab. We observed a strong induction of PUMA at both the protein and mRNA levels, and we also noted that PUMA was again required for the apoptotic response as analyzed by the nuclear fragmentation assay and executioner caspase activation following *PUMA* knockdown (Figs. 11A-C). Additionally, *PUMA* knockdown also partially restored cell viability (Fig. 11D).

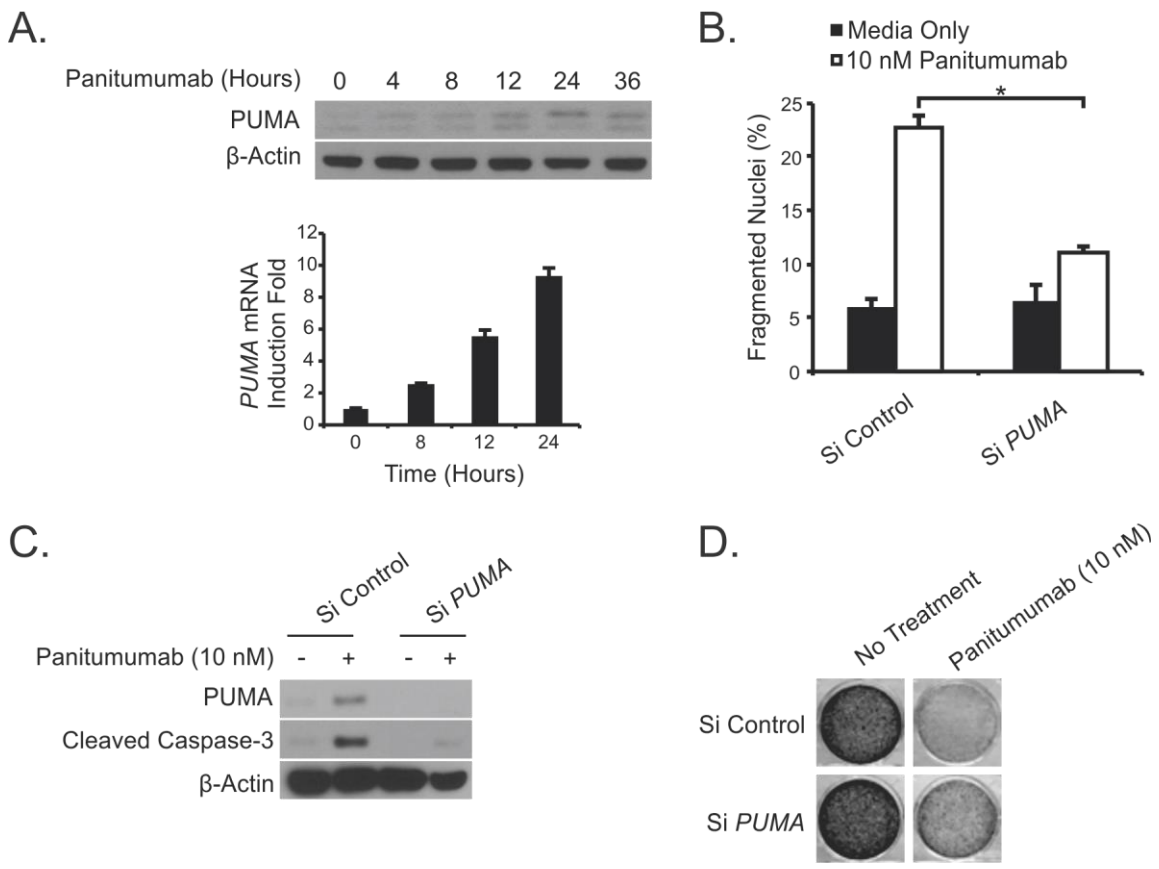

Figure 11. PUMA is Induced and is Required for Apoptosis Following Panitumumab Treatment. **(A)** *Top*, DiFi parental cells were treated for the indicated times with 10 nM panitumumab. PUMA protein expression was analyzed by Western blot. *Bottom*, mRNA was collected over the indicated time points following 10 nM panitumumab treatment in DiFi parental cells. PUMA mRNA expression was analyzed by RT-PCR. **(B)** DiFi parental cells were transfected with 200 pmol of either control siRNA or *PUMA* siRNA for 24 hours before treatment at the indicated dose for 72 hours. Apoptotic cells were quantified by counting condensed and fragmented nuclei following Hoechst 33258 staining. *P<0.05. **(C)** DiFi parental cells were transfected with 200 pmol of either control or *PUMA* siRNA for 24 hours before treatment at the indicated dose for 24 hours. Cleaved caspase-3 and PUMA expression were determined by Western blot. **(D)** DiFi parental cells were transfected with the equivalent of

200 pmol per well of a 12-well plate of control or *PUMA* siRNA, re-plated 24 hours later, and treated 24 hours after the re-plating with the indicated dose of panitumumab. Staining by crystal violet was done 48 hours after treatment.

2.3.3 PUMA Expression is Dependent on p73 and the Inactivation of AKT

The regulation of *PUMA* at the transcriptional level has been well studied, and PUMA expression has been shown to be dependent on transcription factors such as p53, the p65 subunit of NF-κB, the p53 homologue p73, and FoxO3A [113, 120-122]. To identify which transcription factors play a role in PUMA transcription, we performed siRNA knockdown experiments. While FoxO3A displayed an activating de-phosphorylation after cetuximab treatment, knockdown had no significant effect on PUMA expression (Fig. 12A). Similarly, knockdown of *p53* produced no change in PUMA expression following cetuximab treatment (Fig. 12B).

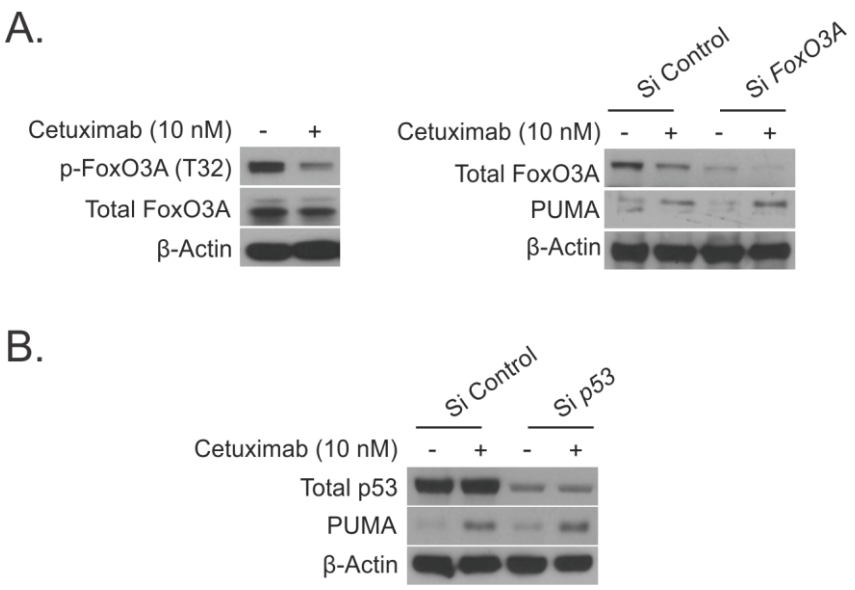

Figure 12. FoxO3A and p53 do not Regulate PUMA Expression. (A) *Left*, DiFi parental cells were treated for 24 hours at the indicated dose. Total and p-FoxO3A expression was determined by Western blot. *Right*, DiFi parental cells were transfected with 400 pmol of either control siRNA or *FOXO3A* siRNA for 24 hours followed by treatment at the indicated concentrations of drug for 24 hours. PUMA and total FoxO3A expression were determined by Western blot. **(B)** DiFi parental cells were transfected with 200 pmol of control siRNA or *p53* siRNA for 24 hours followed by treatment with 10 nM cetuximab for 24 hours. Total p53 and PUMA expression were determined by Western blot.

We next examined the expression of p73, and noted that there was a moderate increase, particularly at early time points (Fig. 13A). Additionally, we observed increased phosphorylation at Y99 following cetuximab treatment, indicative of an early activating phosphorylation of p73 (Fig. 13B) [123]. To further confirm that p73 can modulate *PUMA* expression directly, we performed ChIP which demonstrated direct p73 binding, and not p53

binding, to the *PUMA* promoter region (Fig. 13C). More significantly, knockdown of *p73* was able to block PUMA expression in addition to the activation of caspase-3 (Fig. 13D).

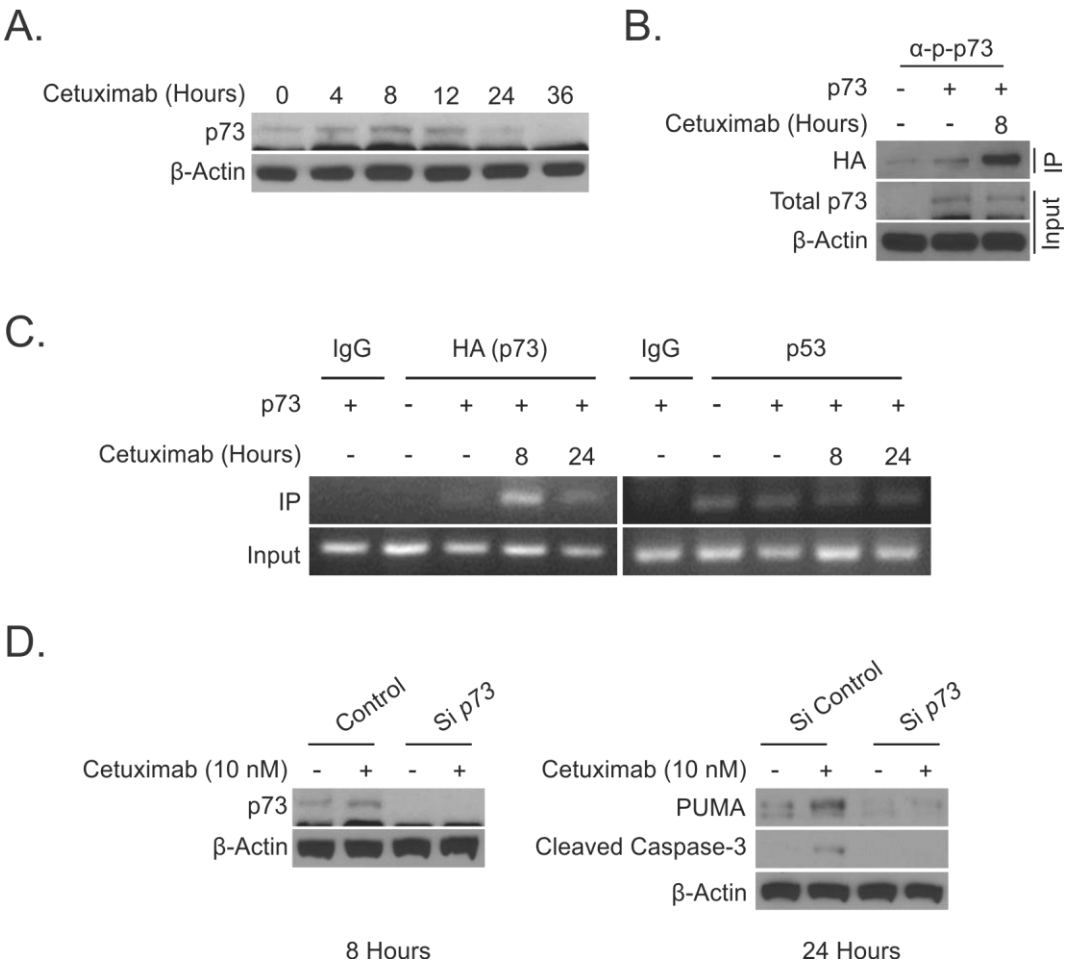

Figure 13. The Transcription Factor p73 Mediates PUMA Expression. (A) DiFi parental cells were treated 10 nM cetuximab for the indicated time points. p73 expression was analyzed by Western blot. **(B)** DiFi parental cells were transfected with either a control empty vector or an HA-tagged p73α construct and were treated with cetuximab for the indicated times. Immunoprecipitation was carried out by pulling down p-p73. Protein expression was determined by Western blot. **(C)** DiFi parental cells were transfected with either a control empty vector or an HA-tagged p73α construct and were treated with cetuximab for the indicated times. Immunoprecipitation was performed using antibodies against either HA for p73α or against endogenous p53. Products were amplified by PCR and run on an agarose gel. **(D)** DiFi parental cells were transfected with the equivalent of 200 pmol per well of a 12-well plate of either

control siRNA (24-hour condition only) or p73 siRNA (8 and 24-hour conditions) for 24 hours, were re-plated, and then treated 24 hours after plating for the indicated times. Control cells for the 8-hour condition were not transfected and were treated as indicated without re-plating. p73, PUMA, and cleaved caspase-3 expression were analyzed by Western blot.

EGFR inhibition is linked with suppression of key intracellular signaling pathways, notably AKT and ERK1/2 [47]. Treatment with cetuximab potently suppressed the activation of both AKT and ERK1/2 in DiFi cells (Fig. 14A). Our lab has previously shown that AKT can suppress p73 and subsequent PUMA protein levels in head and neck cancer cell lines [121]. Additionally, AKT is known to negatively regulate p73 activity via the transcriptional co-activator YAP [123]. We therefore hypothesized that AKT functioned to negatively regulate PUMA expression in colorectal cancer cells. Indeed, overexpression of constitutively-active AKT largely suppressed PUMA expression upon treatment with cetuximab (Fig. 14B).

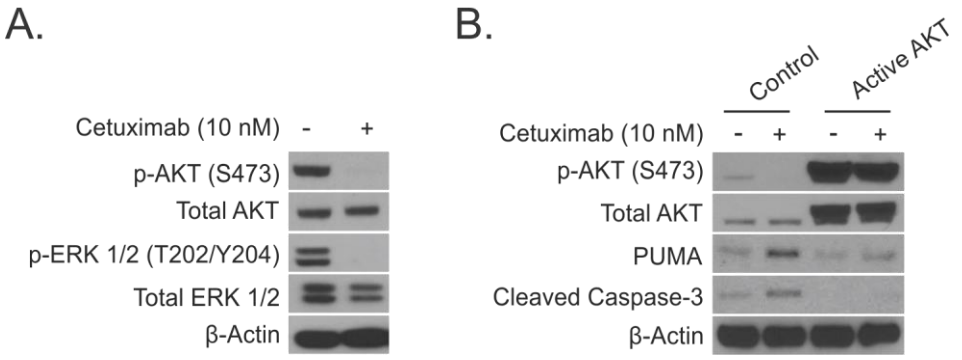

Figure 14. AKT Activation Suppresses PUMA Expression. (A) DiFi parental cells were treated for 24 hours with the indicated dose of cetuximab. Protein expression was determined by Western blot. **(B)** DiFi parental cells were transfected with a control empty vector or an active

AKT construct for 6 hours and then treated with the indicated dose of cetuximab for 24 hours. Protein expression was determined by Western blot.

2.3.4 Anti-EGFR Antibody Resistant Cells Circumvent Apoptosis and Suppress PUMA Expression

Resistance to anti-EGFR antibody therapy is a critical problem for colorectal cancer therapy and is in large part mediated through mutation or amplification of the *KRAS* oncogene [54, 67]. Several models of anti-EGFR antibody resistant cell lines have been previously developed by performing long-term exposure of colorectal cancer cell lines to antibody treatment [66]. Interestingly, analysis of the resistant cell lines shows that each harbors either a *KRAS* mutation or genetic amplification [66]. To elucidate the mechanisms of cell death suppression in anti-EGFR antibody resistant cells, we utilized DiFi cetuximab-resistant cells (R1 clone) which possess a *KRAS* gene amplification leading to protein overexpression [66, 67].

To verify that these cells are indeed resistant to anti-EGFR antibody treatment, we performed an MTS assay which measures cellular metabolism, and flow cytometry to analyze Annexin V binding. Compared to the parental DiFi cells, their resistant counterparts have little suppression of cell metabolism after anti-EGFR antibody treatment and display less Annexin V binding (Fig. 15A-C). Activation of caspase-3 also showed similar trends (Fig. 15D).

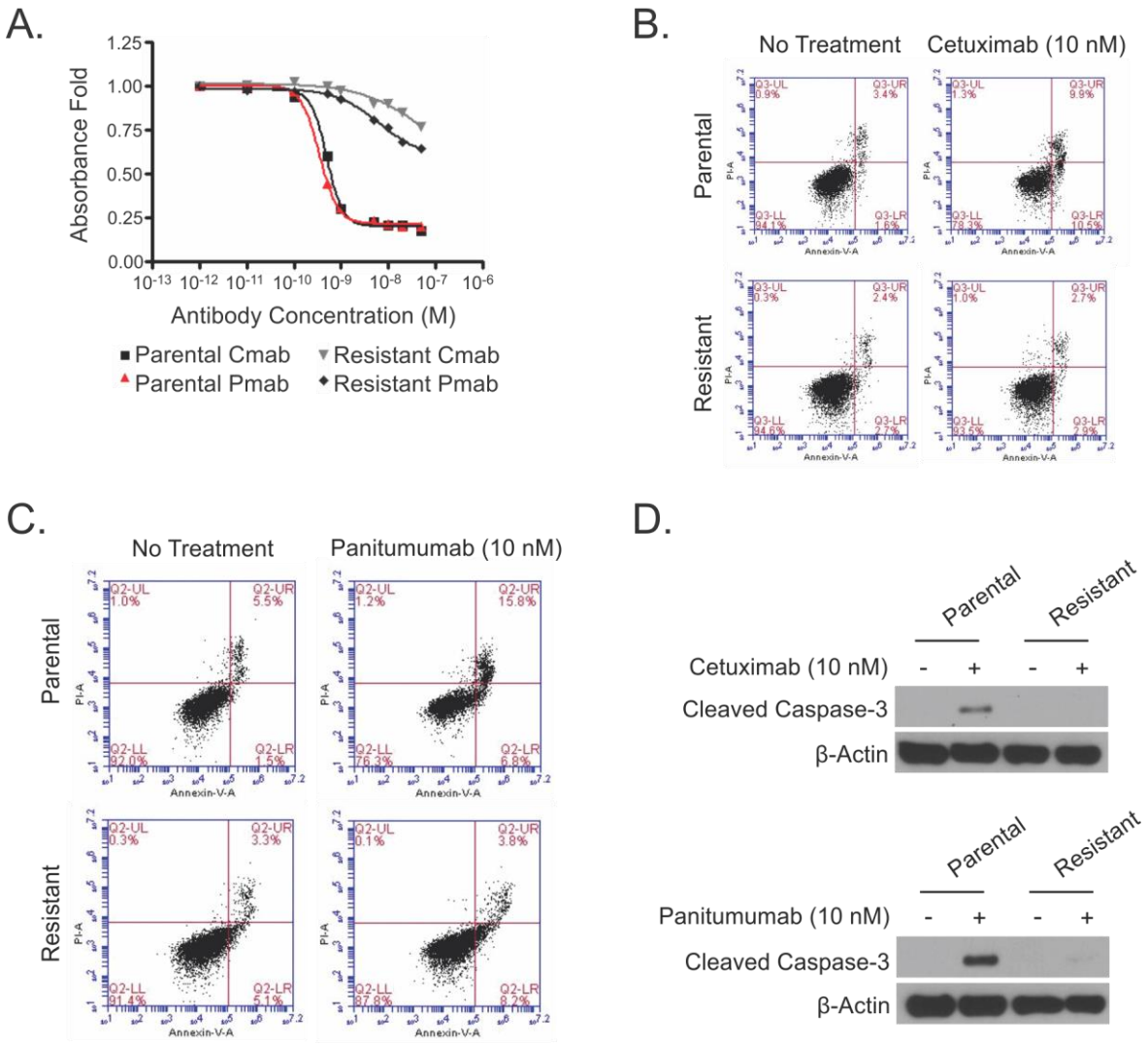

Figure 15. Cetuximab-Resistant Cells Suppress Apoptotic Induction Following Anti-EGFR Antibody Treatment. (A) DiFi parental and cetuximab-resistant cells were seeded at a density of 10,000 cells per well and were treated for 72 hours at the indicated doses of cetuximab and panitumumab. Cell metabolism was analyzed by MTS assay, and absorbances were normalized to the sample with the lowest treatment dose. DiFi cetuximab-resistant cells were maintained in their respective cell culture medium with the addition of 10 nM cetuximab prior to cell plating. **(B)** DiFi parental and cetuximab-resistant cells were treated for 72 hours at the indicated concentration of cetuximab. Cells were stained with Annexin V/PI, and apoptosis was analyzed

by flow cytometry. **(C)** DiFi parental and cetuximab-resistant cells were treated at the indicated dose of panitumumab for 72 hours before staining with Annexin V/PI followed by flow cytometry. **(D)** DiFi parental and cetuximab-resistant cells were treated for 24 hours at the indicated concentration of either cetuximab or panitumumab. Cleaved caspase-3 expression was assessed by Western blot.

We also confirmed key characteristics of these cells, including KRAS overexpression and the downregulation of total EGFR levels (Fig. 16A). Additionally, we noted less inhibition of both AKT and ERK1/2 in the resistant cells following anti-EGFR antibody treatment, suggesting that the pathways downstream of KRAS are incompletely inhibited compared to the parental cells (Fig. 16B). These results confirm the previously reported alterations of the resistant cells following acquired resistance to anti-EGFR antibodies [67]. Interestingly, total AKT levels were slightly elevated in resistant cells, possibly owing to a heightened dependence on downstream RAS effector proteins that suppress apoptosis.

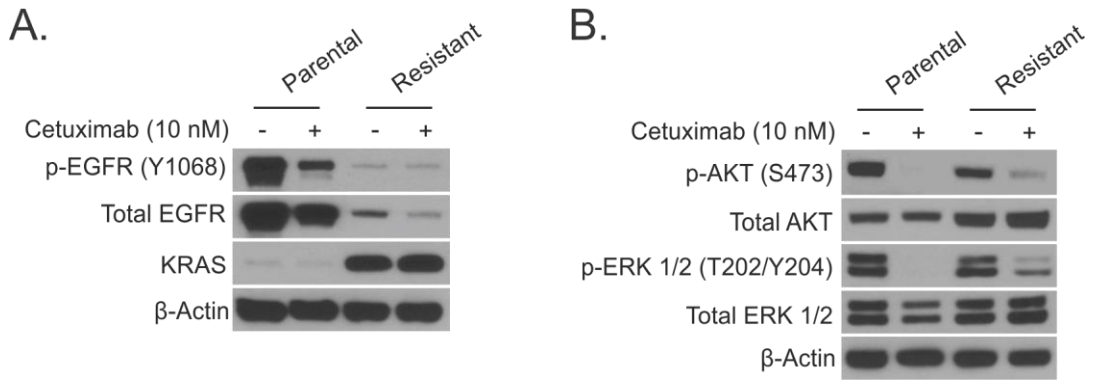

Figure 16. KRAS Signaling is Less Inhibited in Anti-EGFR Antibody Resistant Cells. (A) DiFi parental and cetuximab-resistant cells were treated for 24 hours at the indicated concentration of cetuximab. Protein expression was analyzed by Western blot. **(B)** DiFi parental

cells were treated 24 hours after plating. DiFi cetuximab-resistant cells were either maintained in normal medium with 10 nM cetuximab (treated), or maintained in medium without antibody (untreated) for 6 days prior to lysis of the cells for Western blot.

Due to the robust induction of apoptosis in DiFi parental cells and the lack of induction in resistant cells, we compared the profile of Bcl-2 family protein expression in each cell line. Interestingly, we noted that although PUMA was strongly expressed in the parental cells, the resistant cells lacked the same degree of expression (Fig. 17A). The same result was also observed in HCA-46 parental and panitumumab-resistant cells (Fig. 17B). Restoration of PUMA expression with an adenovirus restored sensitivity to cell death in resistant cells, indicating that they are not resistant to apoptosis (Fig. 17C). Additionally, treatment of DiFi resistant cells with the BH3 mimetic ABT-737 was able to synergize with cetuximab, further demonstrating that anti-EGFR antibody resistant cells can be re-sensitized to the induction of apoptosis (Fig. 17D-E).

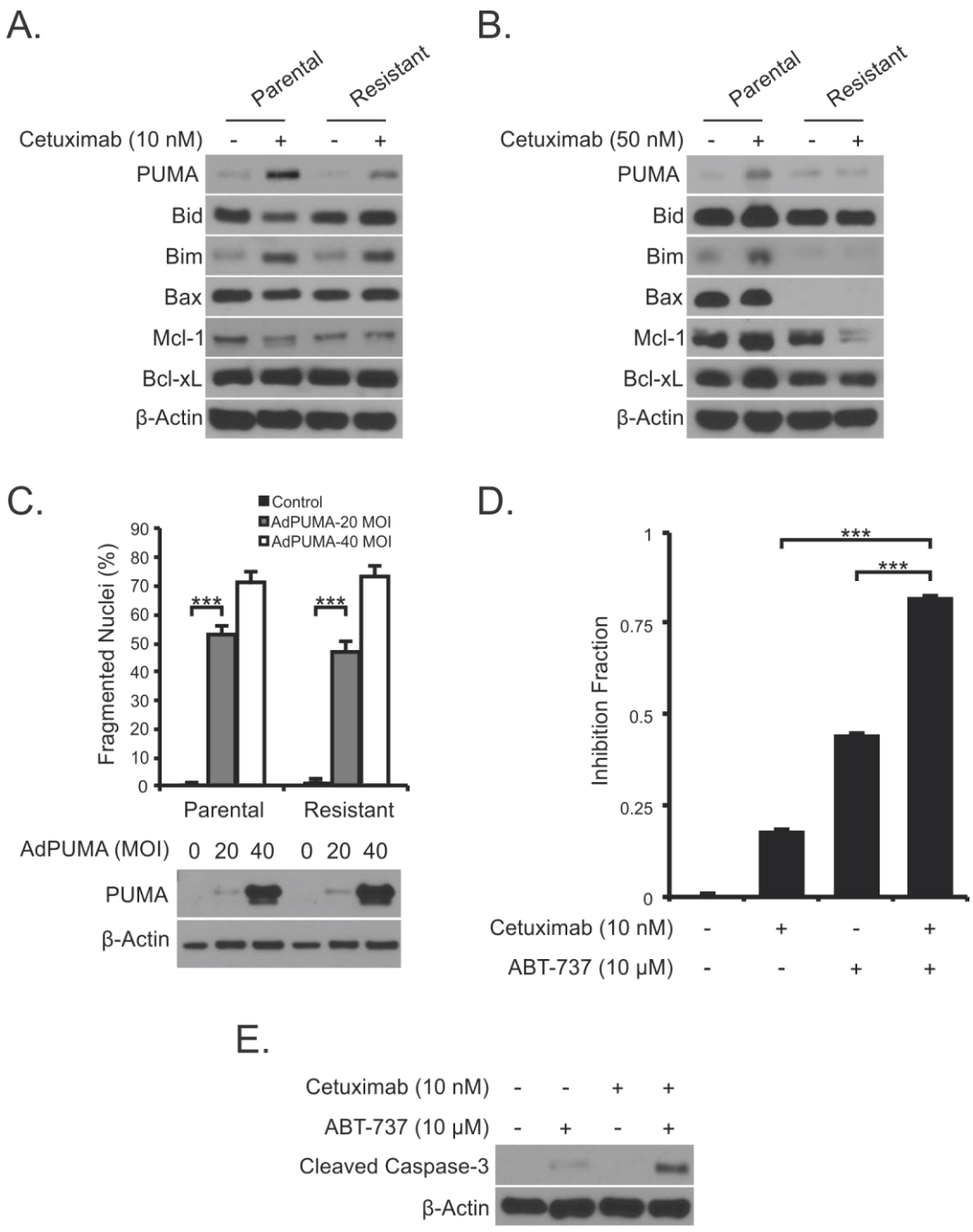

Figure 17. Anti-EGFR Antibody Resistant Cells Suppress PUMA Expression but Can Be Re-Sensitized to Apoptosis. (A) DiFi parental and cetuximab resistant cells were treated for 24 hours at the indicated concentration of cetuximab. Expression of the Bcl-2 family proteins was determined by Western blot. **(B)** HCA-46 parental and panitumumab-resistant cells were treated for 24 hours at the indicated dose of cetuximab. Bcl-2 family protein expression was analyzed

by Western blot. **(C)** *Top*, DiFi parental and cetuximab-resistant cells were infected for 24 hours with the indicated doses of AdPUMA-GFP. Condensed and fragmented nuclei were quantified following staining with Hoechst 33258. *Bottom*, PUMA protein expression was analyzed 24 hours after infection. ***P<0.001. **(D)** DiFi cetuximab-resistant cells were seeded at a density of 10,000 cells per well of a 96-well plate. Cells were treated for 48 hours at the indicated doses, and cell proliferation was assessed by the CellTiter-Glo assay. Results were normalized to untreated controls, and the inhibition fraction was determined by subtracting all normalized values from 1. Higher bars indicate greater proliferation inhibition. ***P<0.001. **(E)** DiFi cetuximab-resistant cells were treated with the indicated concentrations for 24 hours. Cleaved caspase-3 expression was determined by Western blot.

A further question we asked was whether the difference in PUMA expression was due to differences in p73 activity between the DiFi parental and resistant cells. To address this question, we first treated both cell lines with cetuximab and analyzed total p73 expression via Western blot. Interestingly, while there is a slight induction in the parental cells, there is a consistently high level of expression in the resistant cells (Fig. 18A). Phosphorylation of p73, such as at Y99, is an initial post-translational modification that promotes p73 activity [123]. Analysis of Y99 phosphorylation in p73 shows clear phosphorylation in the parental cells, but none in the resistant cells as assessed through a co-immunoprecipitation experiment (Fig. 18B). This result suggests that p73 is not being activated in the resistant cells. To further analyze p73 activity, we performed ChIP in both DiFi parental and resistant cells following cetuximab treatment. While p73 again showed binding to the *PUMA* promoter region in DiFi parental cells, this response was not observed in DiFi resistant cells (Fig. 18C). These data indicate that anti-

EGFR antibody resistant cells do not respond to antibody treatment in part by altering the upstream activation of p73.

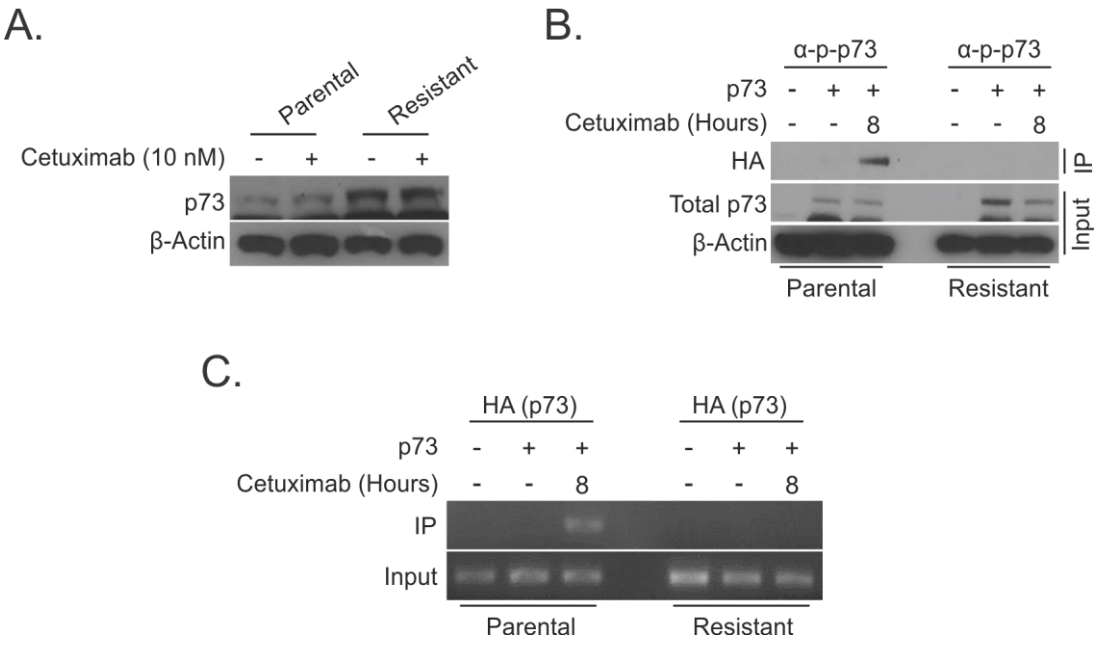

Figure 18. p73 is Upregulated but does not Promote PUMA Expression in Anti-EGFR Antibody Resistant Cells. (A) DiFi parental and cetuximab-resistant cells were treated for 8 hours with cetuximab. p73 expression was analyzed by Western blot. **(B)** DiFi parental and cetuximab-resistant cells were transfected with either a control empty vector or an HA-tagged p73α construct and were treated with cetuximab for the indicated times. Immunoprecipitation was carried out by pulling down p-p73. HA and p73 expression were assessed by Western blot. **(C)** DiFi parental and cetuximab-resistant cells were transfected with HA-tagged p73α or a control empty vector and were treated for the indicated times with cetuximab. ChIP was performed and products were PCR-amplified and run on an agarose gel.

2.4 DISCUSSION

Treatment for CRC typically involves the utilization of traditional chemotherapy, such as 5-fluorouracil (5-FU), irinotecan, and oxaliplatin, in addition to newer targeted therapies [41, 47]. The advent of EGFR antibody utilization saw increases in patient survival both alone and in combination with other therapies in several clinical trials [56, 124]. Although blocking growth signaling pathways can lead to a suppression of cell proliferation, anti-EGFR antibodies have also been shown to induce apoptosis in CRC cells [73, 125]. While the induction of apoptosis has been reported, much of the mechanism remains unclear as to how anti-EGFR antibodies lead to an apoptotic response.

Our data show that upon cetuximab treatment, the expression level of the p73 transcription factor is moderately increased, and its phosphorylation at Y99 is also elevated at early time points (Fig. 13A-B). This increase in expression appears to be sufficient to mediate PUMA expression, which is necessary for the apoptotic response to anti-EGFR antibodies. We also show that suppression of AKT signaling following antibody treatment correlates with the increased expression of PUMA, and that overexpression of active AKT can suppress this induction (Fig. 14B). Previous work has shown that the interaction between AKT and p73 is mediated by the transcriptional co-activator YAP1 [123, 126]. AKT functions to sequester YAP1 in the cytosol through phosphorylation, hindering its ability to promote p73 transcriptional activity. Therefore, inhibition of AKT can promote enhanced p73-mediated transcription through an increase in YAP1 activity; however, this remains to be tested in our CRC models.

Interestingly, p73 activation is associated with genotoxic stress, and phosphorylation at Y99 is mediated by the c-Abl kinase [127]. Our results therefore allow us to hypothesize that EGFR inhibition leads to c-Abl activation. This activation, however, must be independent of

direct activation by KRAS, such as through the RAS effector protein RIN1 [128], since EGFR inhibition silences KRAS signaling in DiFi parental cells. Further experiments will be needed to determine the regulation of c-Abl in both parental and resistant cells, specifically if c-Abl activity is heightened in parental cells, but strongly suppressed in resistant cells. Additionally, experiments will also be necessary to elucidate the involvement of upstream kinases involved in the DNA damage response, such as ATM, to determine a complete mechanistic picture leading to p73 activation. Taken together, our results suggest a model whereby both c-Abl activation and inhibition of AKT following antibody treatment both function to increase p73-mediated PUMA expression (Fig. 19).

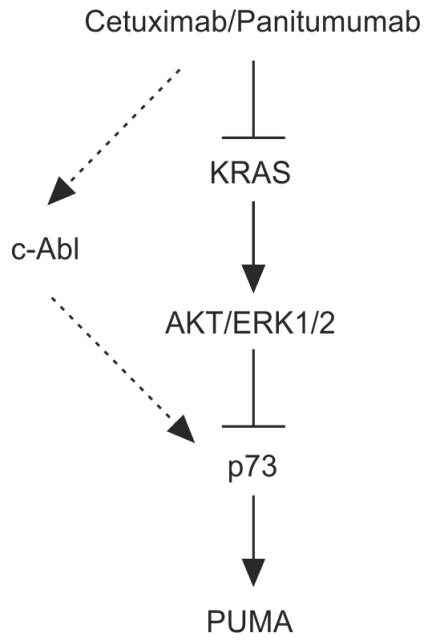

Figure 19. Model of Anti-EGFR Antibody-Mediated PUMA Expression. In this model, anti-EGFR antibodies block EGFR signaling resulting in a suppression of AKT activation. This could ultimately lead to an increased ability of YAP1 to promote the transcriptional activity of p73 that leads to *PUMA* expression. The left arm of the schematic shows that anti-EGFR

antibodies signal c-Abl to phosphorylate p73 at Y99, which further increases p73 transcriptional activity.

Resistance to anti-EGFR antibodies in the clinical setting remains a common occurrence. Retrospective analyses of clinical trial data and additional findings have shown that alterations in the *KRAS* oncogene are responsible for resistance to anti-EGFR antibodies [58, 62]. The anti-EGFR antibody resistant cell lines utilized in our study additionally contained either *KRAS* gene amplification or mutation, which mimics findings in the clinic [66]. Although these cell lines are resistant to antibody treatment, the mechanisms governing the suppression of cell death have not been uncovered.

We explored the signaling pathways upstream and downstream of KRAS in addition to the profile of the Bcl-2 family proteins to further elucidate the alterations suppressing the apoptotic response to antibody treatment. We noted that there exists a decreased expression of total EGFR and less inhibition of active AKT and ERK1/2 in resistant cell lines following treatment compared to parental cells as previously reported (Fig. 16A-B) [67]. Additionally, PUMA expression was suppressed, and the activity of p73 was attenuated (Figs. 17A, 18B-C). These results suggest that the resistant cells no longer rely as heavily on EGFR signaling due to its strongly decreased expression. This change in expression is likely a consequence of the highly increased expression of KRAS protein levels, which serve to bypass the EGFR signaling cascade [129]. Furthermore, the increased expression of KRAS promotes both AKT and ERK signaling, with the former suppressing PUMA protein expression based on our data. Additionally, sustained ERK signaling likely contributes to the continued cell proliferative effects following antibody treatment in resistant cells.

Our findings also show that anti-EGFR antibody resistant cells are not immune to apoptosis. Restoration of PUMA expression and chemical inhibition of anti-apoptotic Bcl-2 family proteins shows that the cells can indeed undergo apoptosis (Fig. 17C-E). This suggests that pharmacologic agents which shift the balance towards apoptosis at the level of the Bcl-2 family proteins can be an effective anti-cancer strategy once resistance has occurred. Further work remains to be done to uncover novel approaches to overcome KRAS-mediated resistance to antibody therapy. Uncovering signaling pathway dependencies in *KRAS*-mutant or amplified cells and exploiting the dependencies using pharmacologic agents represent one attractive therapeutic strategy.

3.0 OVERCOMING RESISTANCE TO ANTI-EGFR ANTIBODIES THROUGH AURORA KINASE INHIBITION

3.1 INTRODUCTION

Resistance to anti-EGFR antibodies in the clinic through the acquisition of alterations in the *KRAS* oncogene is a well-known phenomenon that has come to light within the past decade. *KRAS* mutations occur in approximately 40% of all CRC cases and account for at least 50% of metastatic CRC cases that do not respond to anti-EGFR antibody therapy [15, 68]. Recently, it has also been reported that *KRAS* mutation levels become elevated during anti-EGFR antibody treatment as detected by liquid biopsy utilizing circulating tumor DNA, and this elevation correlates with a decreased efficacy of antibody therapy [130]. These data indicate that alterations in the *KRAS* oncogene present a significant challenge in the clinic by limiting treatment options.

KRAS is a small GTPase which connects growth factor signaling with the PI3K/AKT and RAF/MEK/ERK signaling axes [5, 16, 22]. As a GTPase, KRAS cycles between two states: an active, or GTP-bound form, and an inactive, or GDP-bound form [5]. Mutations predominantly occur in codons 12 and 13 of *KRAS*, leading to a state of constitutive activation [5]. In light of the clinical challenge posed by *KRAS* mutations, much research has been devoted to targeting mutant KRAS directly and indirectly. One approach has been to exploit *KRAS*

mutations in shRNA or compound screens to identify a synthetic lethal interaction [97, 101]. Results from such attempts could uncover new targets or pharmacologic agents that selectively deplete *KRAS*-mutant cells while sparing *KRAS*-wild-type cells. Taken further, this approach could also be utilized to uncover novel combination therapies that enhance the tumor cell killing effect in cells that have acquired *KRAS* mutations after the initiation of anti-EGFR antibody therapy.

It has been reported that pharmacologic agents can be utilized to re-sensitize resistant cells that have acquired *KRAS* mutations to anti-EGFR therapy. In one study, MEK inhibition coupled with anti-EGFR antibodies was able to block resistant cell proliferation both *in vitro* and *in vivo* [66]. However, other novel combination therapies remain to be explored for their effectiveness in overcoming antibody resistance. In this study, we utilized a compound-based screening approach using isogenic cell lines that differ in their *KRAS* mutational status to uncover agents that reduced *KRAS*-mutant cell viability. Our results showed that *KRAS*-mutant cells were highly sensitive to Aurora kinase inhibition compared to their wild-type counterparts. More significantly, Aurora kinase inhibitors restored sensitivity to anti-EGFR therapy both *in vitro* and *in vivo*, indicating a potential therapeutic avenue to overcome *KRAS*-mediated resistance.

3.2 MATERIALS AND METHODS

3.2.1 Cell Culture and Drug Treatment

Human parental CRC cell lines, including DiFi and OXCO-2 along with the resistant derivatives DiFi cetuximab-resistant (R1 clone) and OXCO-2 cetuximab-resistant (R1 clone) cells were acquired from the laboratory of Dr. Alberto Bardelli at the University of Turin. DLD-1 and HCT116 WT cells were obtained from the American Type Culture Collection. HCT116 and DLD-1 *KRAS* isogenic cells were acquired from the laboratory of Dr. Bert Vogelstein. DLD-1 *PUMA*-KO cells have been previously described [131]. Cell lines were checked for the absence of mycoplasma approximately every 6 months. All CRC cell lines were maintained in McCoy's 5A modified media (Invitrogen, Carlsbad, CA). Cells were kept in a non-humidified incubator at 37°C with the addition of 5% CO_2. Cell culture media was supplemented with 10% FBS (HyClone, Logan, UT, USA) and 1% penicillin-streptomycin consisting of 100 units/mL penicillin and 100 µg/mL streptomycin (Invitrogen).

Unless otherwise specified, cells were plated at 20-30% density in 12-well plates for drug treatment. Chemicals utilized include: ZM-447439 (Selleck Chemicals, LLC), cetuximab (Eli Lilly and Company, NY/NJ), Sorafenib (LC Laboratories), Sunitinib (Cayman Chemical), 17-AAG (LC Laboratories), PF-02341066 (Crizotinib) (LC Laboratories), Vandetanib (LC Laboratories), Erlotinib, Hydrochloride Salt (LC Laboratories), Dasatinib, Free Base (LC Laboratories), MG-132 (Selleck Chemicals, LLC), Tozasertib, Free Base (LC Laboratories), and Volasertib (BI 6727) (Selleck Chemicals, LLC). All compounds except cetuximab were diluted first in DMSO (Sigma) to establish a stock solution prior to drug treatment.

3.2.2 Analysis of Cell Viability and Cell Death

To analyze cellular viability, CellTiter AQueous One Solution (MTS assay; Promega) was utilized according to the manufacturer's instructions with a minor modification in clear 96-well plates. Following aspiration of the existing media, a 1:5 mix of MTS solution and medium (120 μL total) were added to each well. Absorbance measurements were carried out at 490 nm using a Wallac Victor 1420 Multilabel Counter (PerkinElmer) following incubation at 37°C for approximately 2 hours.

To measure ATP levels, the CellTiter-Glo Luminescent Cell Viability Assay (Promega) was utilized in black clear-bottom 96-well plates (Corning). Existing cell culture medium was aspirated, followed by addition of 50 μL of a 1:1 mix of CellTiter-Glo and medium. Plates were placed in the dark on a rotary shaker for 3 minutes followed by a 20-minute incubation at room temperature away from light. Luminescence was measured on the Multilabel Counter.

Cell death was analyzed by staining floating and attached cells with Hoechst 33258 (Invitrogen) and by counting condensed and fragmented nuclei, which were divided by the total number of cells counted to obtain the final percentages. Each condition was analyzed at least in duplicate per experiment counting approximately 25-300 cells per sample. Conditions in which the rates of death were very high had the fewest cell counts due to sparse fields.

3.2.3 Western Blotting

For protein expression analysis, all samples were collected in 2X Laemmli buffer and were subsequently used for Western blotting. Briefly, samples were loaded onto 10% Bis-Tris gels and ran at approximately 175V for 45 minutes. Gels were transferred on a TransBlot SD semi-

dry transfer cell (Biorad) using PVDF membranes. Following the transfer, membranes were blocked in a 5% milk solution containing TBS and 0.05% Tween-20 (TBS-T) for 1 hour prior to overnight incubation in primary antibody at 4°C. After primary incubation, membranes were washed three times with TBS-T, followed by secondary antibody incubation for 1 hour at room temperature with either goat anti-mouse (Pierce #31432) or goat anti-rabbit (Pierce #31462). Membranes were washed again with TBS-T prior to developing by chemiluminescence detection using Western Lighting-Plus ECL according to the manufacturer's directions (Perkin-Elmer).

Antibodies utilized included: β-Actin (Sigma #A5441), cleaved caspase-3 (Cell Signaling #9661), Mcl-1 (BD #559027), Bax (BD #610983), Bid (Cell Signaling #2002), Bcl-xL (BD #610212), Bim (Cell Signaling #2819), Bcl-2 (DAKO #M0887), PUMA (QCB #3795), and Noxa (EMD Millipore #OP180).

3.2.4 Xenograft Experiments

Animal experiments for this study were permitted by the Institutional Animal Care and Use Committee (IACUC) at the University of Pittsburgh. Nu/Nu female mice (Charles River) aged 5-6 weeks were utilized for all xenograft experiments. Mice were maintained on-site in a sterile environment in micro-isolator cages and were given continuous access to water and chow. Following a one-week rest period, mice were injected subcutaneously with $5x10^6$ OXCO-2 parental and cetuximab-resistant cells (R1 clone) on two flanks. After one week of tumor growth, treatments were initiated by performing intraperitoneal (i.p.) injections with 40 mg/kg ZM-447439 in 10% DMSO every other day, 0.8 mg of cetuximab every 3 to 4 days, or their combination. Treatments were terminated either at day 5 (immunohistochemistry experiment) or at day 15 (tumor volume experiment). Control mice received 10% DMSO opposite ZM-443439

treatment and combination treatment or HBSS opposite cetuximab treatment. 10% DMSO and ZM-447439 preparations were diluted in a solution of filter-sterilized 50% HBSS/50% PEG300 to facilitate drug solubility.

Growth of tumors was measured every other day with calipers, and tumor volumes were calculated using the formula 0.5*(tumor length)*(tumor width)^2. For immunohistochemistry analysis, mice were sacrificed and tumors were excised and prepared by fixing in 10% formalin followed by paraffin embedding.

3.2.5 Immunohistochemistry

Following embedding in paraffin, 5 μm slices of tumor tissue were cut in preparation for staining. TUNEL staining (Millipore) was performed as indicated by the manufacturer's instructions. Active caspase-3 staining was completed by first removing residual paraffin with xylene followed by a decreasing gradient of ethanol washes. A pH 6.0 10 mM sodium citrate solution with 1 mM EDTA was utilized to perform antigen retrieval by boiling the tumor sections in solution for 10 minutes. Tumor sections were then quenched with 3% hydrogen peroxide for 5 minutes at room temperature. Blocking was performed with a 20% goat serum solution for an additional 30 minutes. Primary antibody incubations were done overnight at 4°C with a cleaved caspase-3 antibody (Cell Signaling #9661) at a 1:100 dilution in a humidified chamber kept away from light. A biotinylated goat anti-rabbit secondary antibody (Pierce #31822) was diluted in 5% goat serum and layered on the tumor sections for 1 hour at room temperature. Sections were then incubated with ABC reagents (Vector Laboratories #PK-6100) followed by DAB (Vector Laboratories #SK-4100) prior to counterstaining with Hematoxylin. Clarifier I and Bluing Reagent (Richard-Allan Scientific) washes were done following

counterstaining. Lastly, sections were dehydrated with an increasing ethanol gradient and were mounted (Fisher Scientific #SP15-500). Further details on the methods have been previously described [132].

3.2.6 Statistical Analysis

All statistical analyses were carried out with GraphPad Prism IV software. Two-sample Student's *t*-test analyses were performed to calculate all *P*-values and were considered statistically significant if *P* was found to be less than 0.05 in a two-tailed test. Bars representing the standard error of the means were reported with the means.

3.3 RESULTS

3.3.1 Aurora Kinase Inhibition Preferentially Kills *KRAS*-Mutant Colorectal Cancer Cells

Selectively targeting *KRAS*-mutant tumor cells is an attractive strategy to circumvent oncogene-mediated resistance. Several strategies have been employed to test preferential selectivity of pharmacological agents against *KRAS*-mutant cell lines compared to their wild-type counterparts [97, 99]. Inhibition of the mitotic kinase Polo-like Kinase 1 (PLK1) and treatment with the microtubule poison paclitaxel have both shown preferential killing of *KRAS*-mutant HCT116 and DLD-1 cells [97]. Due to the perceived heightened susceptibility of *KRAS*-mutant cells on the mitotic machinery, we hypothesized that additional targets can be uncovered through a drug

screening approach. Using isogenic HCT116 *KRAS* $^{+/-}$ and *KRAS* $^{G13D/-}$ cells, we screened a multitude of drug compounds, particularly kinase inhibitors with targets involved in cell proliferation and mitosis. From this screen, we identified inhibitors of the Aurora kinases as possessing preferential sensitivity in *KRAS*-mutant cells (Fig. 20A). Similar screening approaches in isogenic DLD-1 cells also revealed preferential sensitivity in *KRAS*-mutant cells (Fig. 20B).

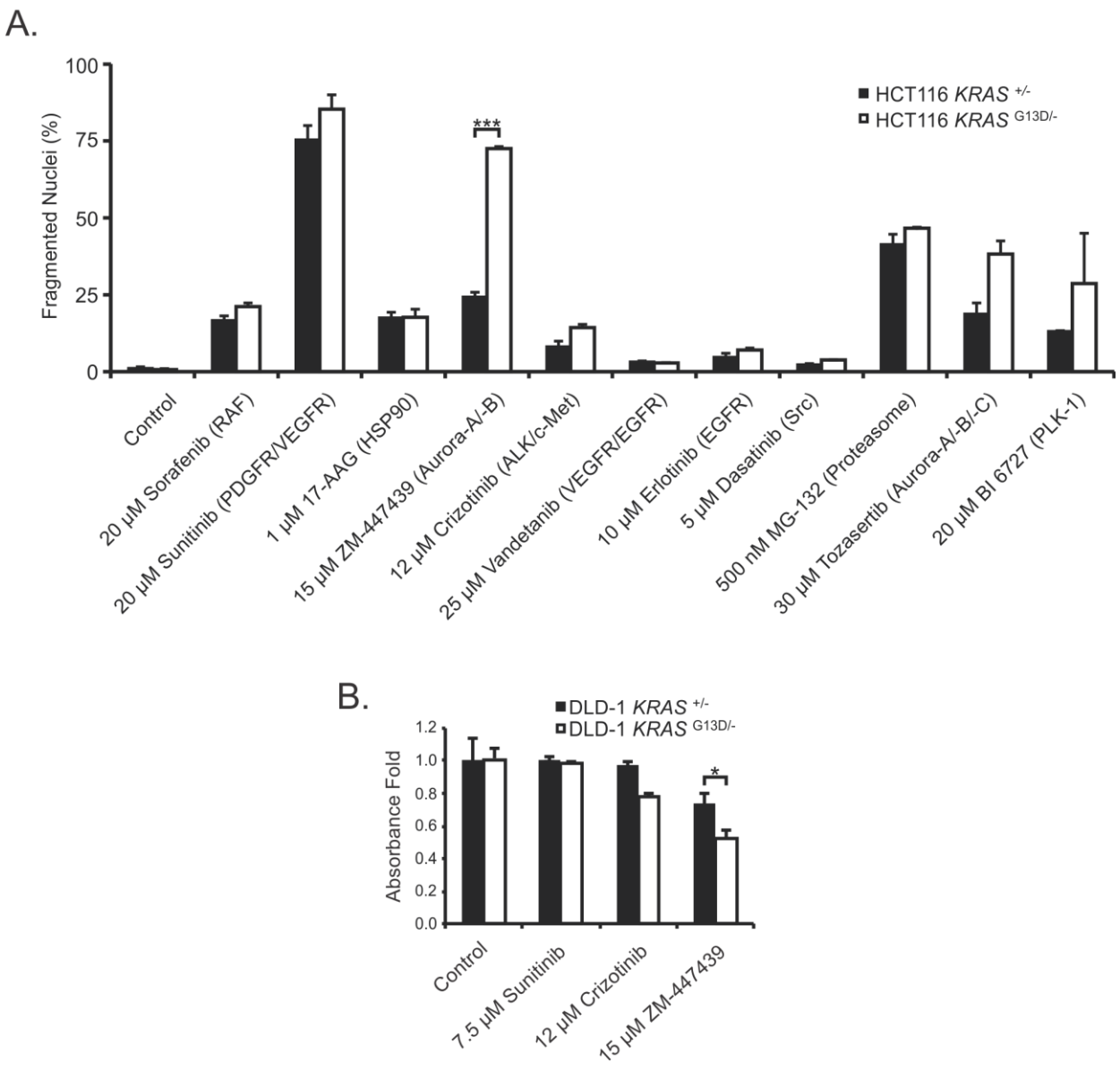

Figure 20. *KRAS*-Mutant Colorectal Cancer Cells are Sensitive to Aurora Kinase Inhibitors. (A) HCT116 isogenic cells were treated with the indicated concentrations of drugs for 48 hours. Cells were collected and stained with Hoechst 33258, and condensed and fragmented nuclei were quantified. At least two samples were quantified per condition, with 25-300 cells being counted per sample. Conditions that induced high amounts of fragmentation (>70%) had the lowest counts due to sparse fields. Otherwise, at least 100 counts per sample

were performed. ***P<0.001. **(B)** DLD-1 isogenic cells were seeded in 96-well plates at a density of 8,000 cells per well. Cells were treated with the indicated concentrations of drugs for 48 hours. Cell metabolism was assessed by the MTS assay. *P<0.05.

To determine if Aurora kinase inhibition induced apoptosis preferentially in *KRAS*-mutant cells, we treated isogenic DLD-1 cells with the Aurora kinase A/B/C inhibitor ZM-447439 (ZM) and analyzed cleaved caspase-3 expression. Note that DLD-1 parental cells harbor an endogenous *KRAS* G13D mutation on one allele [35]. Interestingly, we found increased expression in the mutant cells after ZM treatment (Fig. 21A). To further confirm a preferential induction of apoptosis in *KRAS*-mutant cells, we stained the cell nuclei of DLD-1 isogenic cells treated with ZM with Hoechst dye. Our results revealed higher amounts of fragmented and condensed nuclei in *KRAS*-mutant cells, indicating an increased fraction of apoptotic cells (Fig. 21B).

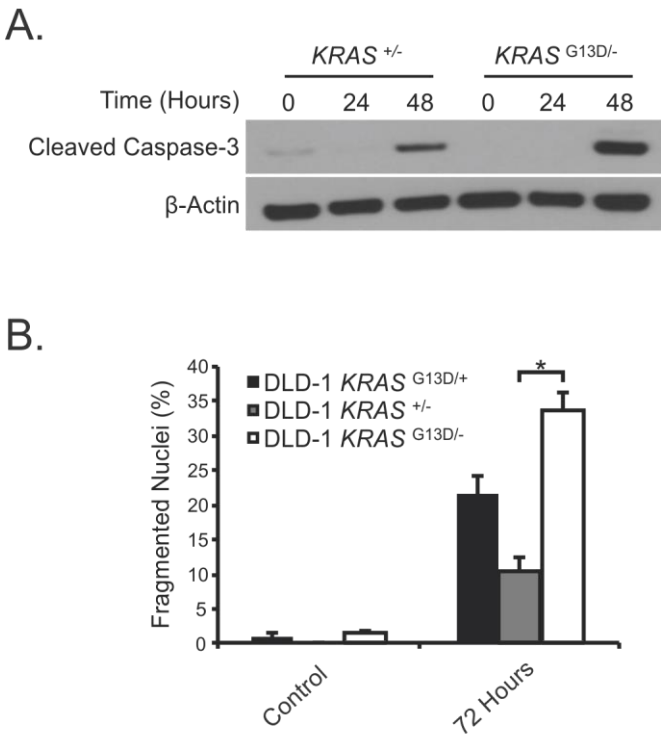

Figure 21. Aurora Kinase Inhibitors Preferentially Induce Apoptosis in *KRAS*-Mutant Cells. **(A)** DLD-1 cells were treated for the indicated time points with 15 μM ZM-447439. Cleaved caspase-3 expression was analyzed by Western blot. **(B)** The indicated DLD-1 cell lines were treated for 72 hours with 15 μM ZM-447439. After 72 hours of treatment, cells were stained with Hoechst 33258 and condensed and fragmented nuclei were quantified. *P<0.05.

To investigate the mechanism of cell death further, we detected the expression of several Bcl-2 family proteins. Interestingly, an increased expression of PUMA and another BH3-only protein Noxa were detected in *KRAS*-mutant DLD-1 cells (Fig. 22A). PUMA was found to be critical for this response, as DLD-1 *PUMA*-KO cells were resistant to Aurora kinase inhibition compared to DLD-1 parental cells (Fig. 22B). Our lab had previously reported that Aurora kinase inhibitors elicit an apoptotic response through increased PUMA expression in CRC cells that is mediated by p65 activation [113]. Together with our findings, this demonstrates that

KRAS mutations promote PUMA expression following Aurora kinase inhibition, possibly through an increased activation of p65.

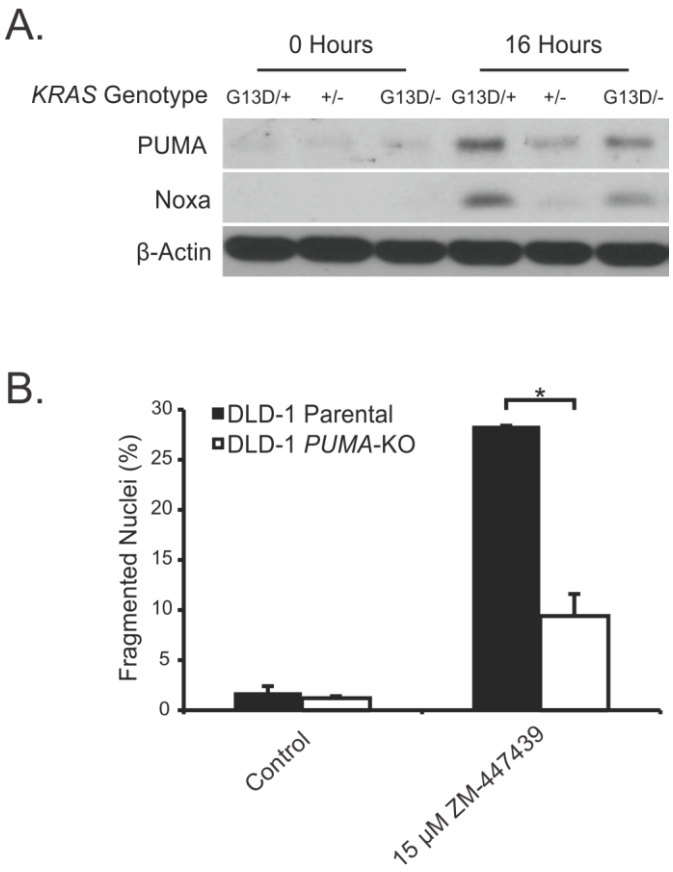

Figure 22. PUMA Mediates the Response to Aurora Kinase Inhibitors. (A) DLD-1 *KRAS* isogenic cells were treated for the indicated times with 15 μM ZM-447439. PUMA and Noxa expression were assessed by Western blot. **(B)** DLD-1 parental and *PUMA*-KO cells were treated with 15 μM ZM-447439 for 72 hours. Condensed and fragmented nuclei were quantified following staining with Hoechst 33258. This data is adapted from Sun et al. Molecular Cancer Therapeutics 2014 [113]. *P<0.05.

3.3.2 Anti-EGFR Antibody Resistant Cells are Sensitive to Aurora Kinase Inhibitor and Anti-EGFR Antibody Combination Treatment

KRAS mutations have previously been shown to be highly prevalent in CRC cells with acquired resistance to anti-EGFR therapy [66]. Attempts to overcome *KRAS*-mediated resistance to anti-EGFR antibodies have also been explored. One combinatorial treatment approach utilized dual MEK/EGFR inhibition, which inhibited CRC cell proliferation both *in vitro* and *in vivo* [66]. Due to the finding that resistant cells can be re-sensitized to anti-EGFR antibodies in combination treatments and that *KRAS*-mutant cells are more sensitive to Aurora kinase inhibition compared to their *KRAS*-wild-type counterparts, we hypothesized that resistant cells could be sensitized to an Aurora kinase and EGFR inhibition treatment scheme. We treated DiFi cetuximab-resistant cells with either ZM or cetuximab alone or in combination and found that the combination treatment strongly suppressed the growth of the resistant cells (Fig. 23). Although DiFi cetuximab-resistant cells harbor *KRAS* amplification and no detectable *KRAS* mutations, the resulting overexpression event is enough to cause significant resistance to anti-EGFR antibody treatment [67] (Fig. 23).

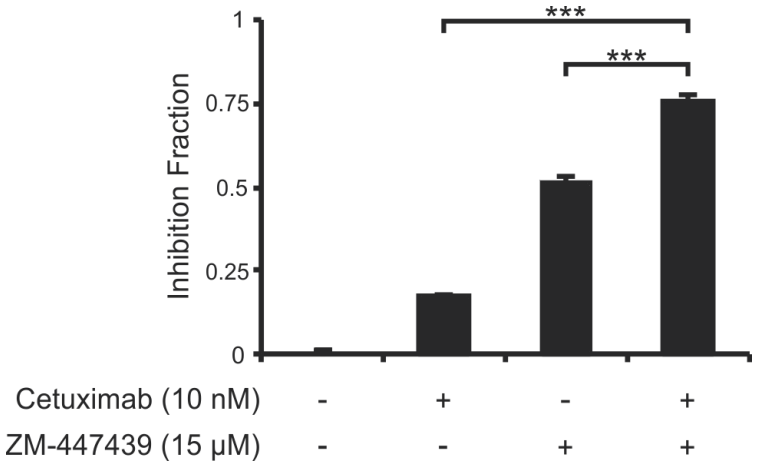

Figure 23. Aurora Kinase Inhibitor and Cetuximab Treatment Halts Anti-EGFR Antibody Resistant Cell Proliferation. DiFi cetuximab-resistant cells were plated at a density of 10,000 cells per well in 96-well plates and treated with the indicated doses of cetuximab and ZM-447439 for 48 hours. Cell proliferation was assessed using the CellTiter-Glo assay, and results were normalized to untreated controls. Inhibition fraction was determined by subtracting all normalized values from 1. Higher bars indicate greater proliferation inhibition. ***P<0.001.

We also asked whether the combination treatment was able to restore apoptosis in resistant cells. We probed for markers of cell death in the combination treatment and observed a marked increase in the expression of cleaved caspase-3 in the resistant cells (Fig. 24A). Additionally, we also detected an increase in the amounts of fragmented nuclei after the combination treatment, further indicating an apoptotic cell death (Fig. 24B).

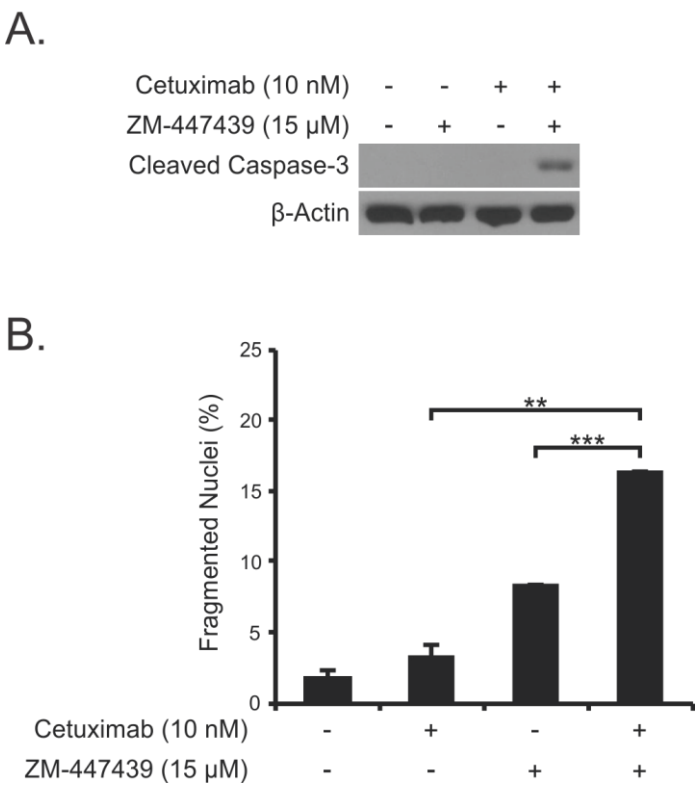

Figure 24. Aurora Kinase Inhibitor and Cetuximab Combination Restores Apoptosis. (A) DiFi cetuximab-resistant cells were treated with the indicated concentrations of cetuximab and ZM-447439 alone and in combination for 24 hours. Cleaved caspase-3 was detected by Western blot. **(B)** DiFi cetuximab-resistant cells were treated for 72 hours with the indicated concentrations of ZM-447439 and cetuximab alone and in combination. Apoptotic cells were quantified by counting condensed and fragmented nuclei following staining with Hoechst 33258. **P<0.01, ***P<0.001.

We next tested whether the combination of Aurora kinase inhibition and EGFR inhibition could lead to increased PUMA expression. Indeed, the combination treatment enhanced PUMA expression compared to each single treatment alone, whereas the expression of other Bcl-2 family proteins was not altered to the same degree (Fig. 25A). Additionally, we observed that combination treatment in OXCO-2 cetuximab-resistant cells, which harbor an endogenous *KRAS* G12D mutation, also resulted in increased PUMA expression and subsequent activation of caspase-3 (Fig. 25B). PUMA protein expression did not increase upon Aurora kinase inhibitor single treatment, likely from the dose being too low to significantly induce it alone in resistant cells.

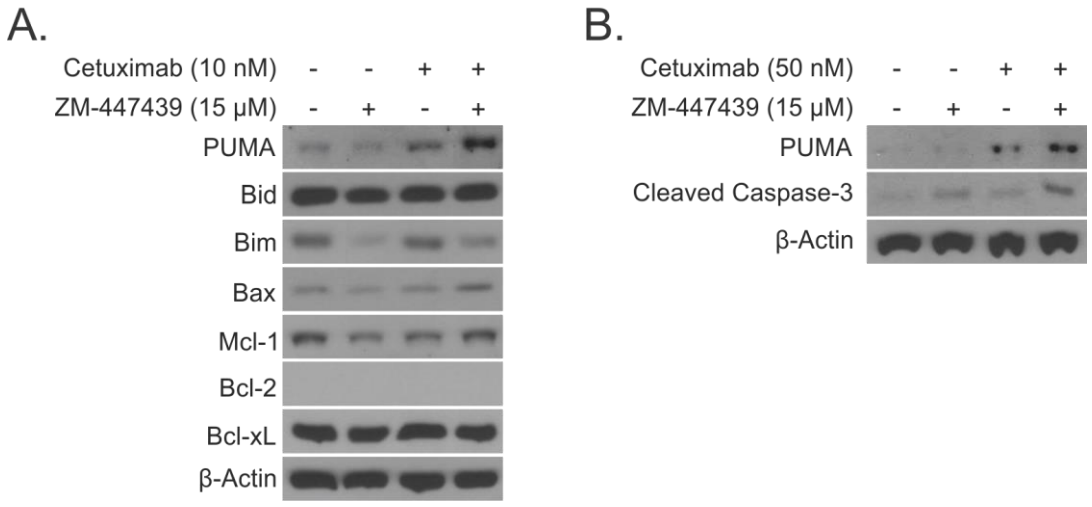

Figure 25. PUMA Expression is Restored upon Aurora Kinase Inhibitor and Cetuximab Treatment. (A) DiFi cetuximab-resistant cells were treated for 24 hours at the indicated concentrations of drugs. Bcl-2 family protein expression was analyzed by Western blot. **(B)** OXCO-2 resistant cells were treated for 24 hours at the indicated concentrations of cetuximab and ZM-447439 alone or in combination. PUMA and cleaved caspase-3 expression were analyzed by Western blot.

3.3.3 Anti-EGFR Antibody Resistant Cells are Sensitive to Aurora Kinase Inhibitor and Cetuximab Combination Therapy *in Vivo*

We next asked whether the Aurora kinase inhibitor and anti-EGFR antibody combination would be efficacious in arresting tumor growth *in vivo*. We established xenograft tumors utilizing parental OXCO-2 parental and cetuximab-resistant CRC cells, both of which formed robust and steady tumor growth in nude mice. We treated mice with ZM or cetuximab alone or in combination for approximately 2 weeks. Our results indicated a strong inhibition of resistant tumor cell proliferation in the combination treatment group, whereas the single treatments displayed little to moderate efficacy (Fig. 26A-B). Additionally, tumor cell lysates collected several days after the beginning of treatment showed a strong expression of PUMA in the resistant cells following the combination therapy, indicating a cell death response (Fig. 26C).

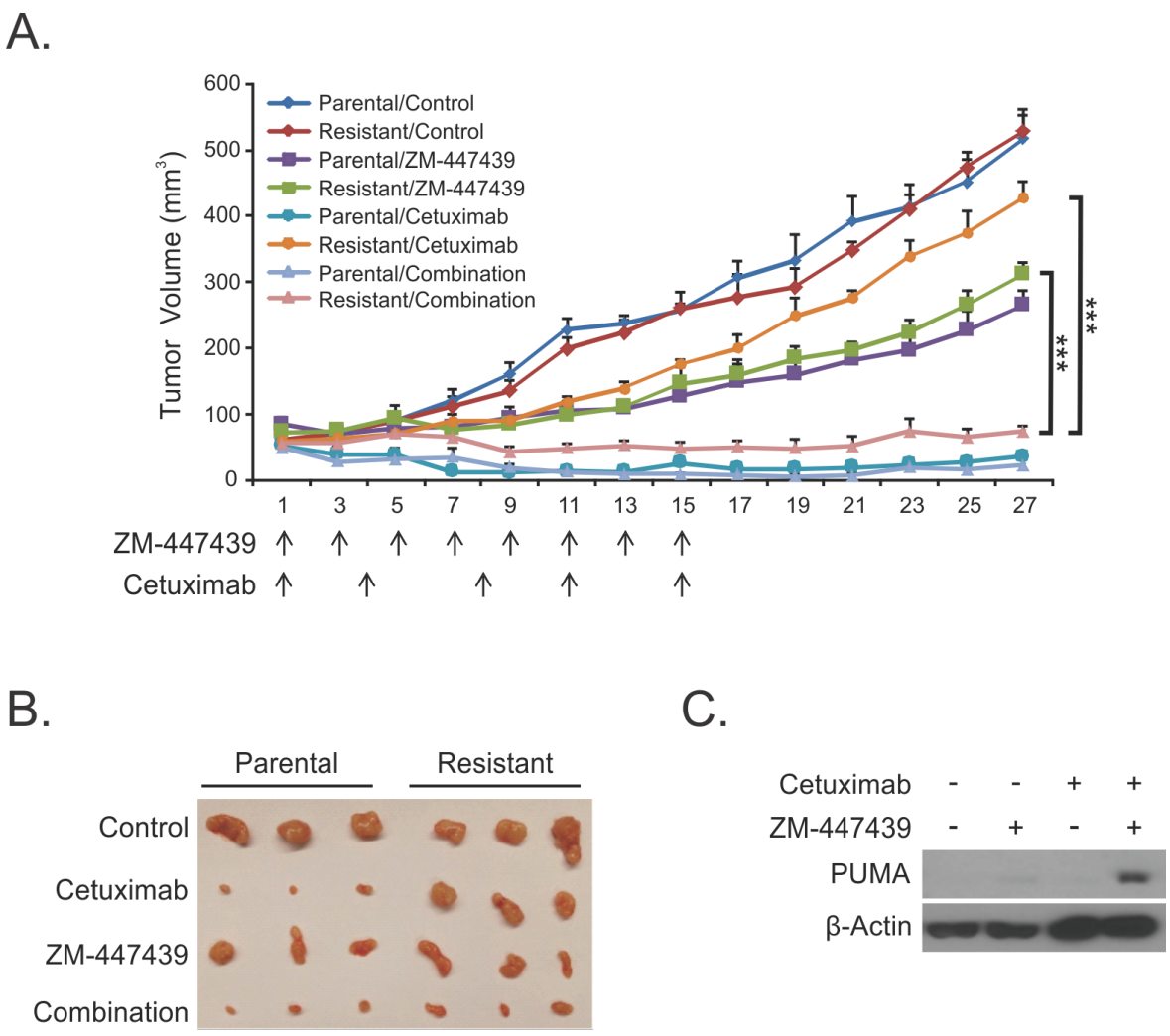

Figure 26. Aurora Kinase Inhibitor and Cetuximab Combination Treatment Inhibits Anti-EGFR Antibody-Resistant Cell Proliferation *in Vivo*. **(A)** $5x10^6$ OXCO-2 parental and resistant (R1 clone) cells were injected subcutaneously into female nude mice. Following 1 week of tumor growth, treatment was initiated with either 40 mg/kg ZM-447439 or 0.8 mg of cetuximab alone or in combination by intraperitoneal (i.p.) injection at the times indicated by the arrows. Tumor volumes were calculated every other day. Each treatment group contained six mice. ***P<0.001. **(B)** Representative tumors at the completion of the experiment in (A). **(C)** The initial 5 days of treatment as in (A) in nude mice were performed for each of the four

treatment groups, followed by harvesting tumor cell lysates to analyze PUMA expression levels by Western blot.

The strong increase in PUMA expression following the combination treatment suggested that there may be a robust apoptotic response in the anti-EGFR antibody resistant cells. To test this, we analyzed tumor sections following 5 days of treatment for markers of apoptosis. Our data indicated a strong increase in caspase-3 activity following the combination treatment (Fig. 27). To provide further evidence that apoptosis is being induced in response to the combination, we performed a TUNEL assay to detect DNA fragmentation in our treated tumor sections. We observed that TUNEL positive cells were most readily detectable in the combination group, correlating with our active caspase-3 staining data (Fig. 28). Our results indicate that a potent anti-tumor response is elicited in response to the ZM and cetuximab dual treatment *in vivo*, as evidenced by the strong anti-proliferative phenotype in the tumor growth curves and the apoptotic response as detected in the tumor sections.

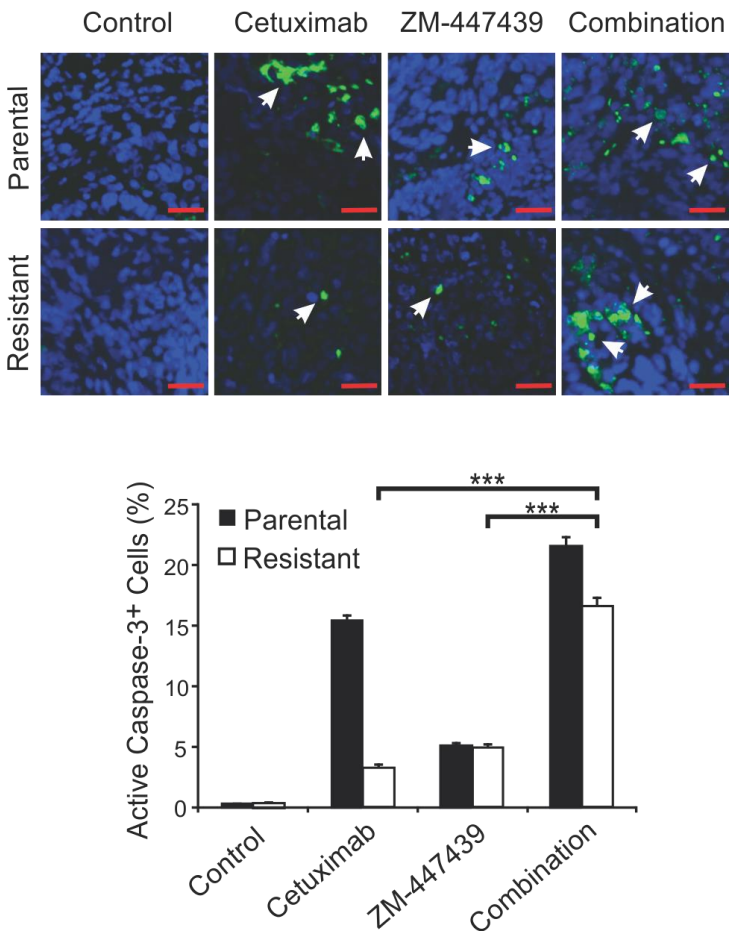

Figure 27. Caspase Activation is Induced in Response to Aurora Kinase Inhibitor and Cetuximab Treatment. Tumor sections from OXCO-2 parental and resistant cells treated as in Fig. 26C were embedded in paraffin and analyzed by active caspase-3 immunostaining. *Top*, representative images are shown following active caspase-3 staining of tumor sections with arrows pointing to cells with a positive signal. *Bottom*, image quantification of active caspase-3-positive cells from each of the four treatment groups. ***P<0.001. Scale bars, 25 μm.

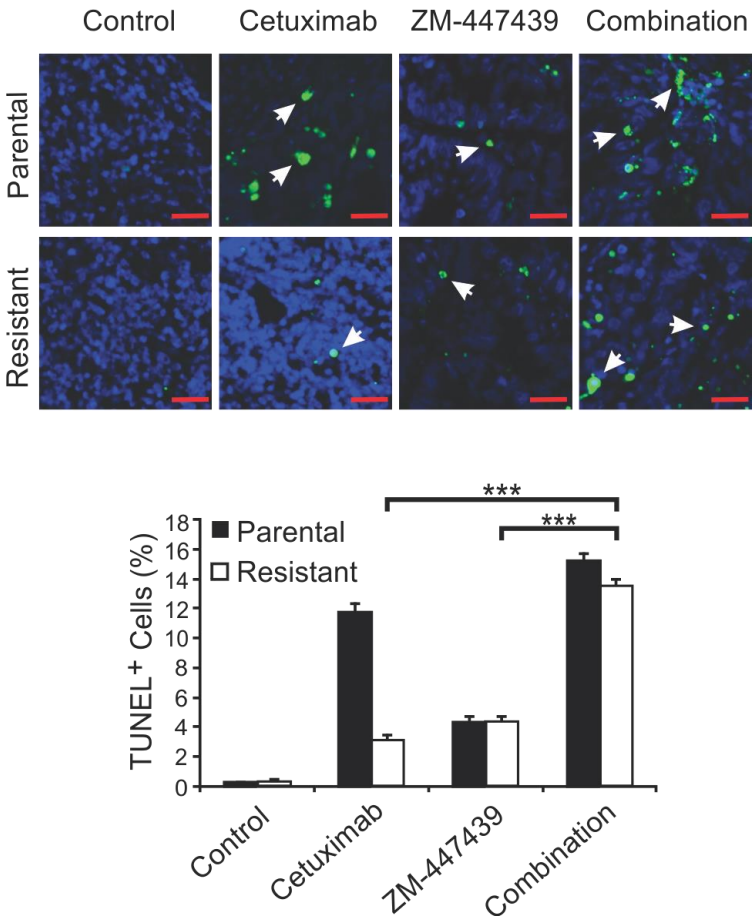

Figure 28. DNA Fragmentation is Increased Following Aurora Kinase Inhibitor and Cetuximab Treatment. Tumor sections from OXCO-2 parental and resistant cells treated as in Fig. 26C were embedded in paraffin and analyzed by TUNEL staining. *Top*, representative images are shown following TUNEL staining of tumor sections with arrows pointing to cells with a positive signal. *Bottom*, image quantification of TUNEL-positive cells from each of the four treatment groups. ***P<0.001. Scale bars, 25 μm.

3.4 DISCUSSION

Resistance to targeted therapy through alterations in the *KRAS* oncogene remains a significant clinical challenge. While direct and indirect methods of targeting mutant KRAS have been employed, they have either not met with clinical success or are still in the early stages of development [81, 84]. An additional method that has garnered much attention is the concept of synthetic lethality. In terms of cancer biology and therapeutics, this phenomenon posits that a cancer cell that has a specific mutation can have an intracellular target that when inhibited, selectively reduces or kills the cell compared to its wild-type counterpart [96]. Much research has been invested in identifying synthetic lethal interactions in various cancer models with specific mutations [97, 101, 103]. However, it is likely that combinatorial treatment strategies will be necessary to invoke a greater anti-tumor response and attack the cancer cells by inhibiting multiple targets that they require to survive. In the setting of targeted therapy resistance, combination therapies have recently garnered attention, such as the co-treatment of anti-EGFR antibody resistant cells with cetuximab and a MEK inhibitor [66].

Our approach therefore utilized a synthetic lethality-based screen with the ultimate goal of identifying compounds that had significant activity in *KRAS*-mutant CRC cells that could be utilized in combination with anti-EGFR antibodies. We initially conducted this screen using an isogenic pair of HCT116 cells that had a deletion of either the endogenous mutated *KRAS* allele or of the wild-type *KRAS* allele [35]. We first identified Aurora kinase inhibition as preferentially killing the *KRAS*-mutant cells, and we confirmed this result by employing the DLD-1 isogenic cell lines that possess the same *KRAS* genotypes (Fig. 20A-B).

In probing the mechanism, we were able to observe that Aurora kinase inhibition induced higher levels of PUMA in *KRAS*-mutant cells compared to their wild-type counterparts (Fig. 22A). This result correlates with the increased amounts of apoptosis observed in the *KRAS*-mutant cells, and these data suggest that *KRAS* mutations promote heightened sensitivity to apoptosis following Aurora kinase inhibition. While the mechanistic details of this increased sensitivity are not entirely known, it has recently been reported that Aurora-A and Aurora-B are targets of KRAS signaling mediated through KRAS' ability to upregulate the c-Myc oncoprotein, which in turn, can upregulate Aurora kinase expression [133]. As a result, it remains plausible that this represents a greater dependency on Aurora kinase activity in cells with deregulated KRAS signaling. Given that the Aurora kinases are crucial for mitosis and that *KRAS*-mutant cells have deregulated cell proliferation, Aurora kinase inhibition may promote apoptosis in a *KRAS*-mutant background due to the heightened cellular stress associated with the inability to complete mitosis. To elucidate the mechanism behind this, it will be necessary to test if p65 activation is further increased in *KRAS*-mutant cells compared to *KRAS*-wild-type cells following Aurora kinase inhibition. This could explain why cells that depend on Aurora kinase activity succumb to an apoptotic cell death.

We utilized the finding from our compound screening to hypothesize that *KRAS*-mutant or *KRAS*-amplified cells, which have been enriched as a result of establishing resistance to anti-EGFR antibody therapy, may also be susceptible to Aurora kinase inhibition as a unique strategy to re-sensitize these cells to anti-EGFR therapy. In treating DiFi cetuximab-resistant cells with this combination, we noted not only a restoration of PUMA expression, but a strong increase in caspase-3 activation and fragmented nuclei, as well as a significant decrease in cell viability (Figs. 23, 24A-B, and 25A). The basis for this re-sensitization is likely mediated specifically by

the p65 transcription factor, since p73 activity is strongly suppressed in resistant cells. This could be determined by assessing p65 phosphorylation and transcriptional activity following both single and combination treatments.

The re-sensitization effect was also noted in the OXCO-2 cetuximab-resistant CRC cell line (Fig. 25B). This cell line, along with its parental counterpart, was used to establish xenograft tumors in nude mice to further test the efficacy of the combination therapy *in vivo*. We utilized this pair of cell lines due to their ability to form steady tumor growth *in vivo* and due to the presence of a *KRAS* mutation, as opposed to *KRAS* amplification, within the resistant cell line [66]. This cell line was also reported to contain a *BRAF* mutation; however, it does not appear to have affected the response, as the results correlate with the data obtained from DiFi cetuximab-resistant cells (Figs. 24A, 25A). Most significantly, the combination therapy was able to induce apoptosis and PUMA expression in resistant cell tumors and was able to completely inhibit tumor growth (Figs. 26A, C, 27-28). These data suggest that Aurora kinase inhibition promotes PUMA expression when combined with cetuximab and that the dual therapy is an effective targeting strategy against anti-EGFR antibody resistant cells *in vivo*. Further work will focus on expanding this treatment strategy to test if other *KRAS*-mutant or *KRAS*-amplified cell lines that have acquired resistance to anti-EGFR antibodies respond similarly to strengthen our findings.

4.0 SUMMARY AND FUTURE DIRECTIONS

4.1 GENERAL SUMMARY

The importance of targeted therapy in the treatment of CRC cannot be disputed. Targeted therapies such as cetuximab and panitumumab are commonly utilized with both having roles in first-, second-, and third-line treatments [15, 48]. However, retrospective clinical trial analyses were implicated in uncovering the molecular basis governing resistance [62]. Since then, elucidating novel treatment schemes to overcome this resistance, discovered to be heavily influenced by alterations within the *KRAS* oncogene, has become an area of intense research. Our main aims were to investigate the mechanisms mediating resistance to anti-EGFR therapy, and to discover agents that possess activity against resistant cells that will assist in overcoming the resistance to targeted therapy.

In order to uncover the mechanisms of resistance, the initial steps of this project entailed studying the mechanisms of sensitivity to anti-EGFR antibody therapy to provide insight. A collaborating lab under the direction of Dr. Alberto Bardelli generously provided us with several CRC cell models, notably DiFi, OXCO-2, and CCK-81. These models display inherent susceptibility to anti-EGFR therapy [134]. We first were able to establish that apoptosis was induced to a high degree in these cell lines, and were able to further verify that regulation of the Bcl-2 family proteins, especially PUMA, was critical to the response to the antibody.

Ultimately, a connection was established between the transcription factor p73 and PUMA expression, as well as a link between AKT inhibition and PUMA expression. These regulations are illustrated in our proposed model (Fig. 19). The data generated from this segment of the project detailing the mechanisms of cell death in response to anti-EGFR antibody therapy comprises the first project aim.

The data we acquired from the first aim was then used to assemble predictions for the mechanistic basis behind resistance to antibody therapy. We additionally acquired anti-EGFR antibody resistant derivatives of the parental cells mentioned above from Dr. Bardelli's lab, which were generated through long-term anti-EGFR antibody exposure. These models serve primarily to study the mechanistic basis to antibody resistance. In comparing the parental and resistant cells side-by-side, we noted key differences that suggest that the mechanism we proposed in the first aim is being shut down in the resistant cells. This therefore enables the cells to express PUMA to a lesser degree and essentially evade apoptosis under anti-EGFR antibody treatment. While *KRAS* alterations are certainly assisting in evasion, as seen by the residual activity of major downstream RAS effectors like AKT and ERK1/2, other factors potentially independent of KRAS could be preventing the full activation of p73 in resistant cells as mentioned in the Chapter II Discussion. Nevertheless, the decreased sensitivity to apoptosis in resistant cells prompted us to explore combination treatments to restore cell death and provide a novel therapeutic avenue to overcome resistance. The data obtained in studying the mechanisms of resistance to anti-EGFR antibody therapy comprises our second major project aim.

The main focus of the last segment of the project entailed overcoming targeted therapy resistance. Our approach was based initially upon the concept of synthetic lethality, where we utilized several sets of isogenic cells that differed in *KRAS* status to observe which agents could

preferentially kill *KRAS*-mutant cells. As was previously noted, the goal of this screen was to discover compounds that ultimately had significant activity against *KRAS*-mutant cells. This would allow us to attempt combination therapies with anti-EGFR antibodies with the goal of re-sensitizing cells to the therapy. Due to the use of Aurora kinase inhibitors in clinical trials as well as the prevalent use of cetuximab, this treatment strategy represents a novel and reasonable therapeutic avenue that we have validated both *in vitro* and *in vivo* [135, 136].

In terms of the mechanism involving the significant anti-tumor activity against the resistant cells after combination treatment *in vivo*, our results correlate with a previous study from our lab where we reported that Aurora kinase inhibition upregulates PUMA expression to induce apoptosis in CRC cells [113]. In the resistant models utilized in this study that suppress PUMA expression, the use of Aurora kinase inhibitors to restore PUMA and subsequent apoptosis confirms that these cells can be re-sensitized to the induction of apoptosis by using an agent known to upregulate PUMA. Furthermore, our results validate our approach on taking advantage of compound screening to isolate various pharmacologic agents that possess activity against *KRAS*-mutant cells. Our third major project aim encompassed the drug screening assays as well as the *in vitro* and *in vivo* combination treatment data.

4.2 FUTURE DIRECTIONS

A question from the first project aim that warrants future investigation details the involvement of additional Bcl-2 family proteins. Bim, as well as the degradation of the anti-apoptotic Mcl-1 protein, may very likely play a contributing role to the sensitivity to anti-EGFR antibody therapy. Transfection experiments knocking down these Bcl-2 family proteins using siRNA can be used

to assess the induction of apoptosis and effect on cell survival following knockdown. This data could also point to further clues governing resistance in cells that have acquired resistance to antibody therapy.

Indeed, our data do suggest that some of these additional Bcl-2 family proteins are differentially regulated. We noted that at least in DiFi resistant cells, the protein level expression of Mcl-1 was unchanged after treatment (Fig. 17A). Given the role of Mcl-1 in promoting therapeutic resistance, it is possible that depleting Mcl-1 as an alternative to increasing the expression of PUMA may be a viable option [137, 138].

One critical question from our study of the resistance mechanism that remains is how the activation of p73 is ablated. Future investigation can explore if upstream kinases, such as c-Abl and ATM, are activated in response to anti-EGFR therapy in the sensitive CRC cell models, and if this regulation is not observed in resistant cells. Additionally, the role of the major KRAS effector pathways, notably AKT and ERK, need to be further delineated to determine how each affects p73 activity. This information would reveal a complete picture as to why p73 is not being activated in resistant cells, potentially giving additional insight into other therapeutic strategies to overcome resistance.

Another key segment of our third aim warrants further investigation, particularly in expanding our *in vivo* results. By utilizing several additional anti-EGFR antibody resistant cells with different *KRAS* mutations, it would be possible to test if there is a broad anti-tumor effect stemming from co-treatment of cetuximab or panitumumab with an Aurora kinase inhibitor. Even patient-derived xenograft (PDX) models could be utilized for such studies to provide even greater translational relevance. To observe if the anti-tumor effect is not only specific to ZM,

another experiment could test if other Aurora kinase inhibitors are just as effective in combination with anti-EGFR antibodies.

In terms of our compound screening approach, it is also possible to expand our efforts to test additional classes of agents using isogenic cell lines and parental and resistant cell pairs. This will help to determine if *KRAS*-mutant or resistant cells display higher sensitivity compared to their wild-type or parental counterparts, respectively. Other agents that can be tested include DNA damaging agents, such as 5-FU or oxaliplatin, which are heavily used in therapy for metastatic CRC in the clinic [15].

APPENDIX A

ABBREVIATIONS

Table 3. List of Useful Abbreviations

Abbreviated Name	Full Name
5-FU	5-fluorouracil
A1	Bcl-2-related protein A1
ACS	American Cancer Society
Ad	Adenovirus
AKT	Ak thymoma/Protein kinase B
ALK	Anaplastic lymphoma kinase
APC	Adenomatous polyposis coli
APC/C	Anaphase-promoting complex/cyclosome
ASCO	American Society of Clinical Oncology
ATM	Ataxia telangiectasia mutated
ATP	Adenosine triphosphate
Bad	Bcl-2-associated death promoter
Bak	Bcl-2 homologous antagonist/killer
Bax	Bcl-2-associated X protein
Bcl-2	B-cell lymphoma 2
Bcl-xL	B-cell lymphoma-extra large
BH	Bcl-2 homology domain
Bid	BH3-interacting domain death agonist
Bim	Bcl-2-like protein 11
BRAF	v-Raf murine sarcoma viral oncogene homolog B
BRCA1/2	Breast cancer type 1/2 susceptibility protein
c-Abl	Abelson murine leukemia viral oncogene homolog 1
c-Fos	Proto-oncogene c-Fos
ChIP	Chromatin immunoprecipitation

c-Jun	Transcription factor AP-1
Cmab	Cetuximab
c-Met	Hepatocyte growth factor receptor
c-Myc	Proto-oncogene c-Myc
CRC	Colorectal cancer
DAB	3, 3-diaminobenzidine
DCAI	4,6-dichloro-2-methyl-3-aminoethylindole
DMSO	Dimethyl sulfoxide
ECL	Enhanced chemiluminescence
EDTA	Ethylenediaminetetraacetic acid
EGFR	Epidermal growth factor receptor
ERBB	Avian erythroblastosis oncogene B
ERK	Extracellular signal–regulated kinase
Fas	Tumor necrosis factor receptor superfamily member 6
FBS	Fetal bovine serum
FDA	Food and Drug Administration
FOLFIRI	Folinic acid, 5-fluorouracil, and irinotecan
FOLFOX	Folinic acid, 5-fluorouracil, and oxaliplatin
FoxO3A	Forkhead box O3
FTase	Farnesyltransferase
FTI	Farnesyltransferase inhibitor
GAP	GTPase-activating protein
GATA-2	Endothelial transcription factor GATA-2
GDP	Guanosine diphosphate
GEF	Guanine nucleotide exchange factor
GFP	Green fluorescent protein
GGTase	Geranylgeranyltransferase
GMP	Guanosine monophosphate
GRB2	Growth factor receptor-bound protein 2
GTP	Guanosine triphosphate
HA	Human influenza hemagglutinin
HBSS	Hanks’ balanced salt solution
HEPES	4-(2-hydroxyethyl)-1-piperazineethanesulfonic acid
HRAS	Harvey rat sarcoma viral oncogene homolog
Hsp90	Heat shock protein 90
i.p.	Intraperitoneal
IgG1/2	Immunoglobulin G 1/2
IP	Immunoprecipitation
KRAS	V-Ki-ras2 Kirsten rat sarcoma viral oncogene homolog
Mcl-1	Myeloid cell leukemia-1
MEK	Mitogen-activated protein kinase kinase
MEM	Minimal essential medium

MOI	Multiplicity of infection
MOMP	Mitochondrial outer membrane permeabilization
MTS	3-(4,5-dimethylthiazol-2-yl)-5-(3-carboxymethoxyphenyl)-2-(4-sulfophenyl)-2H-tetrazolium
NCI	National Cancer Institute
NF-κB	Nuclear factor kappa-light-chain-enhancer of activated B cells
NMR	Nuclear magnetic resonance
Noxa	Phorbol-12-myristate-13-acetate-induced protein 1
NRAS	Neuroblastoma rat sarcoma viral oncogene homolog
p65	Nuclear factor NF kappa B p65 subunit
p73	Tumor protein 73
PARP	Poly (ADP-ribose) polymerase
PC8	Phenol-chloroform, pH 8.0
PDEδ	Phosphodiesterase delta
PDGFR	Platelet-derived growth factor receptor
PDX	Patient-derived xenograft
PEG	Polyethylene glycol
PI	Propidium iodide
PI3K	Phosphatidylinositol-4,5-bisphosphate 3-kinase
PLK1	Polo-like kinase 1
Pmab	Panitumumab
PUMA	p53-upregulated modulator of apoptosis
PVDF	Polyvinylidene fluoride
RAF	Rapidly accelerated fibrosarcoma
RAS	Rat sarcoma
RIN1	RAS and Rab interactor 1
RNAi	RNA interference
RTK	Receptor tyrosine kinase
RT-PCR	Reverse transcription polymerase chain reaction
shRNA	Small hairpin RNA
siRNA	Small interfering RNA
Snail2	Zinc finger protein SNAI2
SOS	Son of sevenless
Src	Proto-oncogene tyrosine-protein kinase Src
STK33	Serine/threonine kinase 33
TAK1	Transforming growth factor beta-activated kinase 1
tBid	Truncated BH3-interacting domain death agonist

TBK1	TANK-binding kinase 1
TBS-T	Tris-buffered saline-Tween 20
TE	Tris-EDTA
TNFα	Tumor necrosis factor alpha
TP53/p53	Tumor protein p53
TRAIL	TNF-related apoptosis-inducing ligand
TUNEL	Terminal deoxynucleotidyl transferase dUTP nick end labeling
UPCI	University of Pittsburgh Cancer Institute
VEGF	Vascular endothelial growth factor
VEGFR	Vascular endothelial growth factor receptor
WT	Wild-type
YAP1	Yes-associated protein 1
ZM	ZM-447439
zVAD-fmk/zVAD	carbobenzoxy-valyl-alanyl-aspartyl-[O-methyl]-fluoromethylketone

APPENDIX B

PRIMER AND SIRNA SEQUENCES

Table 4. List of Primer Sequences

Primer Name/Experiment	Sequence
PUMA/p73 binding by ChIP	Forward 5’ GTC GGT CTG TGT ACG CAT CG 3’ Reverse 5’ CCC GCG TGA CGC TAC GGC CC 3’
PUMA/RT-PCR	Forward 5’ CGA CCT CAA CGC ACA GTA CGA 3’ Reverse 5’ AGG CAC CTA ATT GGG CTC CAT 3’
β-Actin/RT-PCR	Forward 5’ GAC CTG ACA GAC TAC CTC AT 3’ Reverse 5’ AGA CAG CAC TGT GTT GGC TA 3’

Table 5. List of siRNA Sequences

siRNA Name/Experiment	Sequence
Luc-154 (Control)/All knockdown experiments	5’ AACGUACGCGGAAUACUUCGA 3’
PUMA-721/PUMA knockdowns, used with PUMA-1559	5’ ACCUCAACGCACAGUACGA 3’
PUMA-1559/PUMA knockdowns, used with PUMA-721	5’ ACGUGUGACCACUGGCAUU 3’
FoxO3A/FoxO3A knockdown experiment to assess the effect on PUMA expression	5’ GUACUCAACUAGUGCAAAC 3’
p53-946/p53 knockdown experiment to assess the effect on PUMA expression	5’ GUGAGCGCUUCGAGAUGUU 3’
p73-135/p73 knockdown experiment to assess the effect on PUMA expression	5’ GGAUUCCAGCAUGGACGUCUU 3’

APPENDIX C

PERMISSIONS REQUESTS

ELSEVIER LICENSE
TERMS AND CONDITIONS

Aug 04, 2016

This Agreement between Kyle Knickelbein ("You") and Elsevier ("Elsevier") consists of your license details and the terms and conditions provided by Elsevier and Copyright Clearance Center.

License Number	3922011419357
License date	Aug 04, 2016
Licensed Content Publisher	Elsevier
Licensed Content Publication	Cell
Licensed Content Title	A genetic model for colorectal tumorigenesis
Licensed Content Author	Eric R. Fearon,Bert Vogelstein
Licensed Content Date	1 June 1990
Licensed Content Volume Number	61
Licensed Content Issue Number	5
Licensed Content Pages	9
Start Page	759
End Page	767
Type of Use	reuse in a thesis/dissertation
Portion	figures/tables/illustrations
Number of figures/tables/illustrations	1
Format	both print and electronic
Are you the author of this Elsevier article?	No
Will you be translating?	No
Order reference number	
Original figure numbers	Figure 3
Title of your thesis/dissertation	Mechanisms and Novel Therapeutic Approaches for KRAS-Mediated Resistance to Anti-EGFR Therapy in Colorectal Cancer Cells
Expected completion date	Aug 2016
Estimated size (number of pages)	105
Elsevier VAT number	GB 494 6272 12
Requestor Location	Kyle Knickelbein 166 Freedom Lane SEWICKLEY, PA 15143 United States Attn: Kyle Knickelbein
Total	0.00 USD
Terms and Conditions	

This permissions processing is in reference to Figure 1.

BIBLIOGRAPHY

1. NCI. *What Is Cancer?* 2015 February 15, 2016]; Available from: http://www.cancer.gov/about-cancer/what-is-cancer.

2. NCI. *Cancer Statistics*. 2015 February 15, 2016]; Available from: http://www.cancer.gov/about-cancer/what-is-cancer/statistics.

3. Cunningham, D., et al., *Colorectal cancer.* Lancet, 2010. **375**(9719): p. 1030-47.

4. ACS. *Colorectal Cancer Facts & Figures*. 2014 September 15, 2014]; Available from: http://www.cancer.org/research/cancerfactsstatistics/colorectal-cancer-facts-figures.

5. Brand, T.M. and D.L. Wheeler, *KRAS mutant colorectal tumors: past and present.* Small GTPases, 2012. **3**(1): p. 34-9.

6. Fearon, E.R. and B. Vogelstein, *A genetic model for colorectal tumorigenesis.* Cell, 1990. **61**(5): p. 759-67.

7. Grady, W.M. and J.M. Carethers, *Genomic and epigenetic instability in colorectal cancer pathogenesis.* Gastroenterology, 2008. **135**(4): p. 1079-99.

8. Moran, A., et al., *Differential colorectal carcinogenesis: Molecular basis and clinical relevance.* World J Gastrointest Oncol, 2010. **2**(3): p. 151-8.

9. Fearnhead, N.S., M.P. Britton, and W.F. Bodmer, *The ABC of APC.* Hum Mol Genet, 2001. **10**(7): p. 721-33.

10. Markowitz, S.D. and M.M. Bertagnolli, *Molecular origins of cancer: Molecular basis of colorectal cancer.* N Engl J Med, 2009. **361**(25): p. 2449-60.

11. Naccarati, A., et al., *Mutations and polymorphisms in TP53 gene--an overview on the role in colorectal cancer.* Mutagenesis, 2012. **27**(2): p. 211-8.

12. Vogelstein, B. and K.W. Kinzler, *Cancer genes and the pathways they control.* Nat Med, 2004. **10**(8): p. 789-99.

13. Jancik, S., et al., *Clinical relevance of KRAS in human cancers.* J Biomed Biotechnol, 2010. **2010**: p. 150960.

14. Prenen, H., S. Tejpar, and E. Van Cutsem, *New strategies for treatment of KRAS mutant metastatic colorectal cancer.* Clin Cancer Res, 2010. **16**(11): p. 2921-6.

15. Sullivan, K.M. and P.S. Kozuch, *Impact of KRAS Mutations on Management of Colorectal Carcinoma.* Patholog Res Int, 2011. **2011**: p. 219309.

16. Pylayeva-Gupta, Y., E. Grabocka, and D. Bar-Sagi, *RAS oncogenes: weaving a tumorigenic web.* Nat Rev Cancer, 2011. **11**(11): p. 761-74.

17. Giehl, K., *Oncogenic Ras in tumour progression and metastasis.* Biol Chem, 2005. **386**(3): p. 193-205.

18. Lowy, D.R. and B.M. Willumsen, *Function and regulation of ras.* Annu Rev Biochem, 1993. **62**: p. 851-91.

19. Downward, J., *Targeting RAS signalling pathways in cancer therapy.* Nat Rev Cancer, 2003. **3**(1): p. 11-22.

20. Johnson, L., et al., *K-ras is an essential gene in the mouse with partial functional overlap with N-ras.* Genes & Development, 1997. **11**(19): p. 2468-2481.

21. Malumbres, M. and M. Barbacid, *RAS oncogenes: the first 30 years.* Nat Rev Cancer, 2003. **3**(6): p. 459-65.

22. Karnoub, A.E. and R.A. Weinberg, *Ras oncogenes: split personalities.* Nat Rev Mol Cell Biol, 2008. **9**(7): p. 517-31.

23. Reuther, G.W. and C.J. Der, *The Ras branch of small GTPases: Ras family members don't fall far from the tree.* Curr Opin Cell Biol, 2000. **12**(2): p. 157-65.

24. Knickelbein, K. and L. Zhang, *Mutant KRAS as a critical determinant of the therapeutic response of colorectal cancer.* Genes Dis, 2015. **2**(1): p. 4-12.

25. Cooper, G.M., *The cell: a molecular approach*. 2nd ed. 2000, Sunderland, MA: Sinauer Associates.

26. Buday, L. and J. Downward, *Epidermal growth factor regulates p21ras through the formation of a complex of receptor, Grb2 adapter protein, and Sos nucleotide exchange factor.* Cell, 1993. **73**(3): p. 611-20.

27. Shields, J.M., et al., *Understanding Ras: 'it ain't over 'til it's over'.* Trends Cell Biol, 2000. **10**(4): p. 147-54.

28. Pruitt, K. and C.J. Der, *Ras and Rho regulation of the cell cycle and oncogenesis.* Cancer Lett, 2001. **171**(1): p. 1-10.

29. Cox, A.D. and C.J. Der, *The dark side of Ras: regulation of apoptosis.* Oncogene, 2003. **22**(56): p. 8999-9006.

30. Lambert, J.M., et al., *Tiam1 mediates Ras activation of Rac by a PI(3)K-independent mechanism.* Nat Cell Biol, 2002. **4**(8): p. 621-5.

31. Downward, J., *Ras signalling and apoptosis.* Curr Opin Genet Dev, 1998. **8**(1): p. 49-54.

32. Matallanas, D., et al., *Mutant K-Ras activation of the proapoptotic MST2 pathway is antagonized by wild-type K-Ras.* Mol Cell, 2011. **44**(6): p. 893-906.

33. Wang, H.L., et al., *KRAS mutation testing in human cancers: The pathologist's role in the era of personalized medicine.* Adv Anat Pathol, 2010. **17**(1): p. 23-32.

34. Perkins, G., et al., *Beyond KRAS status and response to anti-EGFR therapy in metastatic colorectal cancer.* Pharmacogenomics, 2014. **15**(7): p. 1043-52.

35. Shirasawa, S., et al., *Altered growth of human colon cancer cell lines disrupted at activated Ki-ras.* Science, 1993. **260**(5104): p. 85-8.

36. Yun, J., et al., *Glucose deprivation contributes to the development of KRAS pathway mutations in tumor cells.* Science, 2009. **325**(5947): p. 1555-9.

37. Kim, J.S., et al., *B-Raf is dispensable for K-Ras-mediated oncogenesis in human cancer cells.* Cancer Res, 2004. **64**(6): p. 1932-7.

38. Arena, S., et al., *Knock-in of oncogenic Kras does not transform mouse somatic cells but triggers a transcriptional response that classifies human cancers.* Cancer Res, 2007. **67**(18): p. 8468-76.

39. Shao, D.D., et al., *KRAS and YAP1 converge to regulate EMT and tumor survival.* Cell, 2014. **158**(1): p. 171-84.

40. Kapoor, A., et al., *Yap1 activation enables bypass of oncogenic Kras addiction in pancreatic cancer.* Cell, 2014. **158**(1): p. 185-97.

41. Viale, P.H., A. Fung, and L. Zitella, *Advanced colorectal cancer: current treatment and nursing management with economic considerations.* Clin J Oncol Nurs, 2005. **9**(5): p. 541-52.

42. Meyerhardt, J.A. and R.J. Mayer, *Systemic therapy for colorectal cancer.* N Engl J Med, 2005. **352**(5): p. 476-87.

43. Venook, A., *Critical evaluation of current treatments in metastatic colorectal cancer.* Oncologist, 2005. **10**(4): p. 250-61.

44. DeLap, R.J., *The effect of leucovorin on the therapeutic index of fluorouracil in cancer patients.* Yale J Biol Med, 1988. **61**(1): p. 23-34.

45. NCI. *Colon Cancer Treatment*. 2014 September 15, 2014]; Available from: http://www.cancer.gov/cancertopics/pdq/treatment/colon/Patient/page4.

46. Grothey, A., et al., *Regorafenib monotherapy for previously treated metastatic colorectal cancer (CORRECT): an international, multicentre, randomised, placebo-controlled, phase 3 trial.* The Lancet, 2013. **381**(9863): p. 303-312.

47. El Zouhairi, M., A. Charabaty, and M.J. Pishvaian, *Molecularly targeted therapy for metastatic colon cancer: proven treatments and promising new agents.* Gastrointest Cancer Res, 2011. **4**(1): p. 15-21.

48. Abrams, T.A., et al., *Chemotherapy usage patterns in a US-wide cohort of patients with metastatic colorectal cancer.* J Natl Cancer Inst, 2014. **106**(2): p. djt371.

49. Saif, M.W., *Colorectal cancer in review: the role of the EGFR pathway.* Expert Opin Investig Drugs, 2010. **19**(3): p. 357-69.

50. Singh, A., et al., *A gene expression signature associated with "K-Ras addiction" reveals regulators of EMT and tumor cell survival.* Cancer Cell, 2009. **15**(6): p. 489-500.

51. Mendelsohn, J. and J. Baselga, *The EGF receptor family as targets for cancer therapy.* Oncogene, 2000. **19**(56): p. 6550-65.

52. Hagan, S., M.C. Orr, and B. Doyle, *Targeted therapies in colorectal cancer-an integrative view by PPPM.* EPMA J, 2013. **4**(1): p. 3.

53. Messersmith, W.A. and M. Hidalgo, *Panitumumab, a monoclonal anti epidermal growth factor receptor antibody in colorectal cancer: another one or the one?* Clin Cancer Res, 2007. **13**(16): p. 4664-6.

54. Heinemann, V., et al., *Targeted therapy in metastatic colorectal cancer -- an example of personalised medicine in action.* Cancer Treat Rev, 2013. **39**(6): p. 592-601.

55. Cunningham, D., et al., *Cetuximab monotherapy and cetuximab plus irinotecan in irinotecan-refractory metastatic colorectal cancer.* N Engl J Med, 2004. **351**(4): p. 337-45.

56. Jonker, D.J., et al., *Cetuximab for the treatment of colorectal cancer.* N Engl J Med, 2007. **357**(20): p. 2040-8.

57. Douillard, J.Y., et al., *Final results from PRIME: randomized phase III study of panitumumab with FOLFOX4 for first-line treatment of metastatic colorectal cancer.* Ann Oncol, 2014. **25**(7): p. 1346-55.

58. Lievre, A., et al., *KRAS mutation status is predictive of response to cetuximab therapy in colorectal cancer.* Cancer Res, 2006. **66**(8): p. 3992-5.

59. Benvenuti, S., et al., *Oncogenic activation of the RAS/RAF signaling pathway impairs the response of metastatic colorectal cancers to anti-epidermal growth factor receptor antibody therapies.* Cancer Res, 2007. **67**(6): p. 2643-8.

60. Banck, M.S. and A. Grothey, *Biomarkers of Resistance to Epidermal Growth Factor Receptor Monoclonal Antibodies in Patients with Metastatic Colorectal Cancer.* Clin Cancer Res, 2009. **15**(24): p. 7492-7501.

61. De Roock, W., et al., *Effects of KRAS, BRAF, NRAS, and PIK3CA mutations on the efficacy of cetuximab plus chemotherapy in chemotherapy-refractory metastatic colorectal cancer: a retrospective consortium analysis.* Lancet Oncol, 2010. **11**(8): p. 753-62.

62. Karapetis, C.S., et al., *K-ras mutations and benefit from cetuximab in advanced colorectal cancer.* N Engl J Med, 2008. **359**(17): p. 1757-65.

63. Amado, R.G., et al., *Wild-type KRAS is required for panitumumab efficacy in patients with metastatic colorectal cancer.* J Clin Oncol, 2008. **26**(10): p. 1626-34.

64. Allegra, C.J., et al., *American Society of Clinical Oncology provisional clinical opinion: testing for KRAS gene mutations in patients with metastatic colorectal carcinoma to predict response to anti-epidermal growth factor receptor monoclonal antibody therapy.* J Clin Oncol, 2009. **27**(12): p. 2091-6.

65. Bardelli, A. and S. Siena, *Molecular mechanisms of resistance to cetuximab and panitumumab in colorectal cancer.* J Clin Oncol, 2010. **28**(7): p. 1254-61.

66. Misale, S., et al., *Blockade of EGFR and MEK intercepts heterogeneous mechanisms of acquired resistance to anti-EGFR therapies in colorectal cancer.* Sci Transl Med, 2014. **6**(224): p. 224ra26.

67. Misale, S., et al., *Emergence of KRAS mutations and acquired resistance to anti-EGFR therapy in colorectal cancer.* Nature, 2012. **486**(7404): p. 532-6.

68. Misale, S., et al., *Resistance to anti-EGFR therapy in colorectal cancer: from heterogeneity to convergent evolution.* Cancer Discov, 2014. **4**(11): p. 1269-80.

69. Bettegowda, C., et al., *Detection of circulating tumor DNA in early- and late-stage human malignancies.* Sci Transl Med, 2014. **6**(224): p. 224ra24.

70. Diaz, L.A., Jr., et al., *The molecular evolution of acquired resistance to targeted EGFR blockade in colorectal cancers.* Nature, 2012. **486**(7404): p. 537-40.

71. Valtorta, E., et al., *KRAS gene amplification in colorectal cancer and impact on response to EGFR-targeted therapy.* Int J Cancer, 2013. **133**(5): p. 1259-65.

72. Martini, M., et al., *Targeted therapies: how personal should we go?* Nat Rev Clin Oncol, 2012. **9**(2): p. 87-97.

73. Kasper, S., et al., *Oncogenic RAS simultaneously protects against anti-EGFR antibody-dependent cellular cytotoxicity and EGFR signaling blockade.* Oncogene, 2013. **32**(23): p. 2873-81.

74. Fisher, G.H., et al., *Induction and apoptotic regression of lung adenocarcinomas by regulation of a K-Ras transgene in the presence and absence of tumor suppressor genes.* Genes Dev, 2001. **15**(24): p. 3249-62.

75. Vigil, D., et al., *Ras superfamily GEFs and GAPs: validated and tractable targets for cancer therapy?* Nat Rev Cancer, 2010. **10**(12): p. 842-57.

76. Wang, Y., et al., *Targeting mutant KRAS for anticancer therapeutics: a review of novel small molecule modulators.* J Med Chem, 2013. **56**(13): p. 5219-30.

77. Shima, F., et al., *In silico discovery of small-molecule Ras inhibitors that display antitumor activity by blocking the Ras-effector interaction.* Proc Natl Acad Sci U S A, 2013. **110**(20): p. 8182-7.

78. Sun, Q., et al., *Discovery of small molecules that bind to K-Ras and inhibit Sos-mediated activation.* Angew Chem Int Ed Engl, 2012. **51**(25): p. 6140-3.

79. Maurer, T., et al., *Small-molecule ligands bind to a distinct pocket in Ras and inhibit SOS-mediated nucleotide exchange activity.* Proc Natl Acad Sci U S A, 2012. **109**(14): p. 5299-304.

80. Ostrem, J.M., et al., *K-Ras(G12C) inhibitors allosterically control GTP affinity and effector interactions.* Nature, 2013. **503**(7477): p. 548-51.

81. Lim, S.M., et al., *Therapeutic targeting of oncogenic K-Ras by a covalent catalytic site inhibitor.* Angew Chem Int Ed Engl, 2014. **53**(1): p. 199-204.

82. Haluska, P., G.K. Dy, and A.A. Adjei, *Farnesyl transferase inhibitors as anticancer agents.* Eur J Cancer, 2002. **38**(13): p. 1685-700.

83. Gysin, S., et al., *Therapeutic strategies for targeting ras proteins.* Genes Cancer, 2011. **2**(3): p. 359-72.

84. Berndt, N., A.D. Hamilton, and S.M. Sebti, *Targeting protein prenylation for cancer therapy.* Nat Rev Cancer, 2011. **11**(11): p. 775-91.

85. Cox, A.D. and C.J. Der, *Farnesyltransferase inhibitors and cancer treatment: targeting simply Ras?* Biochim Biophys Acta, 1997. **1333**(1): p. F51-71.

86. Friday, B.B. and A.A. Adjei, *K-ras as a target for cancer therapy.* Biochim Biophys Acta, 2005. **1756**(2): p. 127-44.

87. Zimmermann, G., et al., *Small molecule inhibition of the KRAS-PDEdelta interaction impairs oncogenic KRAS signalling.* Nature, 2013. **497**(7451): p. 638-42.

88. Fruman, D.A. and C. Rommel, *PI3K and cancer: lessons, challenges and opportunities.* Nat Rev Drug Discov, 2014. **13**(2): p. 140-56.

89. Neuzillet, C., et al., *MEK in cancer and cancer therapy.* Pharmacol Ther, 2014. **141**(2): p. 160-71.

90. Engelman, J.A., et al., *Effective use of PI3K and MEK inhibitors to treat mutant Kras G12D and PIK3CA H1047R murine lung cancers.* Nat Med, 2008. **14**(12): p. 1351-6.

91. Yuan, T.L., et al., *Development of siRNA Payloads to Target KRAS-Mutant Cancer.* Cancer Discov, 2014.

92. Lamba, S., et al., *RAF Suppression Synergizes with MEK Inhibition in KRAS Mutant Cancer Cells.* Cell Rep, 2014. **8**(5): p. 1475-83.

93. Stephen, A.G., et al., *Dragging ras back in the ring.* Cancer Cell, 2014. **25**(3): p. 272-81.

94. Ferrari, E., C. Lucca, and M. Foiani, *A lethal combination for cancer cells: synthetic lethality screenings for drug discovery.* Eur J Cancer, 2010. **46**(16): p. 2889-95.

95. Chan, D.A. and A.J. Giaccia, *Harnessing synthetic lethal interactions in anticancer drug discovery.* Nat Rev Drug Discov, 2011. **10**(5): p. 351-64.

96. Kaelin, W.G., Jr., *Synthetic lethality: a framework for the development of wiser cancer therapeutics.* Genome Med, 2009. **1**(10): p. 99.

97. Luo, J., et al., *A genome-wide RNAi screen identifies multiple synthetic lethal interactions with the Ras oncogene.* Cell, 2009. **137**(5): p. 835-48.

98. Barbie, D.A., et al., *Systematic RNA interference reveals that oncogenic KRAS-driven cancers require TBK1.* Nature, 2009. **462**(7269): p. 108-12.

99. Scholl, C., et al., *Synthetic lethal interaction between oncogenic KRAS dependency and STK33 suppression in human cancer cells.* Cell, 2009. **137**(5): p. 821-34.

100. Wang, Y., et al., *Critical role for transcriptional repressor Snail2 in transformation by oncogenic RAS in colorectal carcinoma cells.* Oncogene, 2010. **29**(33): p. 4658-70.

101. Singh, A., et al., *TAK1 inhibition promotes apoptosis in KRAS-dependent colon cancers.* Cell, 2012. **148**(4): p. 639-50.

102. Kumar, M.S., et al., *The GATA2 transcriptional network is requisite for RAS oncogene-driven non-small cell lung cancer.* Cell, 2012. **149**(3): p. 642-55.

103. Corcoran, R.B., et al., *Synthetic lethal interaction of combined BCL-XL and MEK inhibition promotes tumor regressions in KRAS mutant cancer models.* Cancer Cell, 2013. **23**(1): p. 121-8.

104. Koehler, B.C., D. Jager, and H. Schulze-Bergkamen, *Targeting cell death signaling in colorectal cancer: current strategies and future perspectives.* World J Gastroenterol, 2014. **20**(8): p. 1923-34.

105. Chen, D., J. Yu, and L. Zhang, *Necroptosis: an alternative cell death program defending against cancer.* Biochim Biophys Acta, 2016. **1865**(2): p. 228-36.

106. Zhang, L., L. Ming, and J. Yu, *BH3 mimetics to improve cancer therapy; mechanisms and examples.* Drug Resist Updat, 2007. **10**(6): p. 207-17.

107. Elmore, S., *Apoptosis: a review of programmed cell death.* Toxicol Pathol, 2007. **35**(4): p. 495-516.

108. Tait, S.W. and D.R. Green, *Mitochondria and cell signalling.* J Cell Sci, 2012. **125**(Pt 4): p. 807-15.

109. Chipuk, J.E., et al., *The BCL-2 family reunion.* Mol Cell, 2010. **37**(3): p. 299-310.

110. Li, H., et al., *Cleavage of BID by caspase 8 mediates the mitochondrial damage in the Fas pathway of apoptosis.* Cell, 1998. **94**(4): p. 491-501.

111. Chen, L., et al., *Differential targeting of prosurvival Bcl-2 proteins by their BH3-only ligands allows complementary apoptotic function.* Mol Cell, 2005. **17**(3): p. 393-403.

112. Yu, J., et al., *PUMA induces the rapid apoptosis of colorectal cancer cells.* Mol Cell, 2001. **7**(3): p. 673-82.

113. Sun, J., et al., *Aurora kinase inhibition induces PUMA via NF-kappaB to kill colon cancer cells.* Mol Cancer Ther, 2014. **13**(5): p. 1298-308.

114. Chen, D., et al., *Regorafenib inhibits colorectal tumor growth through PUMA-mediated apoptosis.* Clin Cancer Res, 2014. **20**(13): p. 3472-84.

115. Liu, B., et al., *Induction of apoptosis and activation of the caspase cascade by anti-EGF receptor monoclonal antibodies in DiFi human colon cancer cells do not involve the c-jun N-terminal kinase activity.* Br J Cancer, 2000. **82**(12): p. 1991-9.

116. Chen, D., et al., *TAp73 promotes cell survival upon genotoxic stress by inhibiting p53 activity.* Oncotarget, 2014. **5**(18): p. 8107-22.

117. Ming, L., et al., *PUMA Dissociates Bax and Bcl-X(L) to induce apoptosis in colon cancer cells.* J Biol Chem, 2006. **281**(23): p. 16034-42.

118. Czabotar, P.E., et al., *Control of apoptosis by the BCL-2 protein family: implications for physiology and therapy.* Nat Rev Mol Cell Biol, 2014. **15**(1): p. 49-63.

119. Zheng, X., et al., *Crizotinib induces PUMA-dependent apoptosis in colon cancer cells.* Mol Cancer Ther, 2013. **12**(5): p. 777-86.

120. He, K., et al., *Hsp90 inhibitors promote p53-dependent apoptosis through PUMA and Bax.* Mol Cancer Ther, 2013. **12**(11): p. 2559-68.

121. Sun, Q., et al., *PUMA mediates EGFR tyrosine kinase inhibitor-induced apoptosis in head and neck cancer cells.* Oncogene, 2009. **28**(24): p. 2348-57.

122. Dudgeon, C., et al., *PUMA induction by FoxO3a mediates the anticancer activities of the broad-range kinase inhibitor UCN-01.* Mol Cancer Ther, 2010. **9**(11): p. 2893-902.

123. Conforti, F., et al., *Regulation of p73 activity by post-translational modifications.* Cell Death Dis, 2012. **3**: p. e285.

124. Wolpin, B.M. and A.J. Bass, *Managing advanced colorectal cancer: have we reached the PEAK with current therapies?* J Clin Oncol, 2014. **32**(21): p. 2200-2.

125. Lu, Y., et al., *Epidermal growth factor receptor (EGFR) ubiquitination as a mechanism of acquired resistance escaping treatment by the anti-EGFR monoclonal antibody cetuximab.* Cancer Res, 2007. **67**(17): p. 8240-7.

126. Strano, S., et al., *Physical interaction with Yes-associated protein enhances p73 transcriptional activity.* J Biol Chem, 2001. **276**(18): p. 15164-73.

127. Tsai, K.K. and Z.M. Yuan, *c-Abl stabilizes p73 by a phosphorylation-augmented interaction.* Cancer Res, 2003. **63**(12): p. 3418-24.

128. Hu, H., et al., *RIN1 is an ABL tyrosine kinase activator and a regulator of epithelial-cell adhesion and migration.* Curr Biol, 2005. **15**(9): p. 815-23.

129. van Houdt, W.J., et al., *Oncogenic KRAS desensitizes colorectal tumor cells to epidermal growth factor receptor inhibition and activation.* Neoplasia, 2010. **12**(6): p. 443-52.

130. Siravegna, G., et al., *Clonal evolution and resistance to EGFR blockade in the blood of colorectal cancer patients.* Nat Med, 2015. **21**(7): p. 795-801.

131. Wang, P., J. Yu, and L. Zhang, *The nuclear function of p53 is required for PUMA-mediated apoptosis induced by DNA damage.* Proc Natl Acad Sci U S A, 2007. **104**(10): p. 4054-9.

132. Leibowitz, B.J., et al., *Uncoupling p53 functions in radiation-induced intestinal damage via PUMA and p21.* Mol Cancer Res, 2011. **9**(5): p. 616-25.

133. Dos Santos, E.O., et al., *Aurora kinase targeting in lung cancer reduces KRAS-induced transformation.* Mol Cancer, 2016. **15**: p. 12.

134. Medico, E., et al., *The molecular landscape of colorectal cancer cell lines unveils clinically actionable kinase targets.* Nat Commun, 2015. **6**: p. 7002.

135. Bavetsias, V. and S. Linardopoulos, *Aurora Kinase Inhibitors: Current Status and Outlook.* Front Oncol, 2015. **5**: p. 278.

136. Umene, K., et al., *Aurora kinase inhibitors: Potential molecular-targeted drugs for gynecologic malignant tumors.* Biomed Rep, 2013. **1**(3): p. 335-340.

137. He, K., et al., *BRAFV600E-dependent Mcl-1 stabilization leads to everolimus resistance in colon cancer cells.* Oncotarget, 2016.

138. Tong, J., et al., *FBW7 mutations mediate resistance of colorectal cancer to targeted therapies by blocking Mcl-1 degradation.* Oncogene, 2016.